UNIVERSIDAD NACIONAL AUTÓNOMA DE MÉXICO

POSGRADO EN CIENCIAS BIOLÓGICAS

FACULTAD DE CIENCIAS

BIOLOGÍA EVOLUTIVA

ESTRUCTURACIÓN Y FLUJO GÉNICO ENTRE LAS POBLACIONES DEL MURCIÉLAGO FRUGÍVORO *STURNIRA PARVIDENS* (CHIROPTERA: PHYLLOSTOMIDAE)

TESIS

(**POR ARTÍCULO CIENTÍFICO**)

Mito-nuclear genetic discordance in the Little Yellow-shouldered Mesoamerican bat, *Sturnira parvidens* (Chiroptera: Phyllostomidae)

QUE PARA OPTAR POR EL GRADO DE:

MAESTRO EN CIENCIAS BIOLÓGICAS

PRESENTA:

MARTÍN YAIR CABRERA GARRIDO

TUTORA PRINCIPAL DE TESIS: DRA. LIVIA S. LEÓN-PANIAGUA
Facultad de Ciencias, UNAM
COMITÉ TUTOR: DR. LUIS E. EGUIARTE FRUNS
Instituto de Ecología, UNAM
DR. JORGE ORTEGA REYES
Escuela Nacional de Ciencias Biológicas, IPN

CIUDAD UNIVERSITARIA, CD. MX., SEPTIEMBRE 2020

Universidad Nacional Autónoma de México
UNAM
Biblioteca Central
Dirección General de Bibliotecas de la UNAM

UNAM – Dirección General de Bibliotecas
Tesis Digitales
Restricciones de uso

DERECHOS RESERVADOS ©
PROHIBIDA SU REPRODUCCIÓN TOTAL O PARCIAL

Todo el material contenido en esta tesis esta protegido por la Ley Federal del Derecho de Autor (LFDA) de los Estados Unidos Mexicanos (México).

El uso de imágenes, fragmentos de videos, y demás material que sea objeto de protección de los derechos de autor, será exclusivamente para fines educativos e informativos y deberá citar la fuente donde la obtuvo mencionando el autor o autores. Cualquier uso distinto como el lucro, reproducción, edición o modificación, será perseguido y sancionado por el respectivo titular de los Derechos de Autor.

UNIVERSIDAD NACIONAL AUTÓNOMA DE MÉXICO

POSGRADO EN CIENCIAS BIOLÓGICAS

FACULTAD DE CIENCIAS

BIOLOGÍA EVOLUTIVA

ESTRUCTURACIÓN Y FLUJO GÉNICO ENTRE LAS POBLACIONES DEL MURCIÉLAGO FRUGÍVORO *STURNIRA PARVIDENS* (CHIROPTERA: PHYLLOSTOMIDAE)

TESIS

(**POR ARTÍCULO CIENTÍFICO**)

Mito-nuclear genetic discordance in the Little Yellow-shouldered Mesoamerican bat, *Sturnira parvidens* (Chiroptera: Phyllostomidae)

QUE PARA OPTAR POR EL GRADO DE:

MAESTRO EN CIENCIAS BIOLÓGICAS

PRESENTA:

MARTÍN YAIR CABRERA GARRIDO

TUTORA PRINCIPAL DE TESIS: DRA. LIVIA S. LEÓN-PANIAGUA
Facultad de Ciencias, UNAM
COMITÉ TUTOR: DR. LUIS E. EGUIARTE FRUNS
Instituto de Ecología, UNAM
DR. JORGE ORTEGA REYES
Escuela Nacional de Ciencias Biológicas, IPN

CIUDAD UNIVERSITARIA, CD. MX. **2020**

POSGRADO
CIENCIAS
BIOLÓGICAS

UNAM
POSGRADO

COORDINACIÓN DEL POSGRADO EN CIENCIAS BIOLÓGICAS

FACULTAD DE CIENCIAS
DIVISIÓN ACADÉMICA DE INVESTIGACIÓN Y POSGRADO
OFICIO FCIE/DAIP/325/2020

ASUNTO: Oficio de Jurado

M. en C. Ivonne Ramírez Wence
Directora General de Administración Escolar, UNAM
P r e s e n t e.

Me permito informar a usted que en la reunión ordinaria del Comité Académico del Posgrado en Ciencias Biológicas, celebrada el día **20 del mes de enero de 2020** se aprobó el siguiente jurado para el examen de grado de **MAESTRO EN CIENCIAS BIOLÓGICAS** en el campo de conocimiento de **Biología Evolutiva** del alumno **CABRERA GARRIDO MARTÍN YAIR** con número de cuenta **410038365** por la modalidad de graduación de **tesis por artículo científico** titulado: **"Mito-nuclear genetic discordance in the Mesoamerican lowland shouldered bat *Sturnira parvidens* (Chiroptera: Phyllostomidae)"**, que es producto del proyecto realizado en la maestría que lleva por título **"Estructuración y flujo génico entre las poblaciones del murciélago frugívoro *Sturnira parvidens* (Chiroptera: Phyllostomidae)"** ambos realizados bajo la dirección del **DRA. LIVIA SOCORRO LEON PANIAGUA**, quedando integrado de la siguiente manera:

Presidente:	DRA. ELLA GLORIA VÁZQUEZ DOMÍNGUEZ
Vocal:	DRA. GABRIELA CASTELLANOS MORALES
Secretario:	DR. LUIS ENRIQUE EGUIARTE FRUNS
Suplente:	DR. GIOVANI HERNÁNDEZ CANCHOLA
Suplente:	DR. LUIS ANTONIO SÁNCHEZ GONZÁLEZ

Sin otro particular, me es grato enviarle un cordial saludo.

A T E N T A M E N T E
"POR MI RAZA HABLARÁ EL ESPÍRITU"
Cd. Universitaria, Cd. Mx., a 11 de agosto de 2020

COORDINADOR DEL PROGRAMA

POSGRADO EN CIENCIAS BIOLOGICAS
COORDINACIÓN

DR. ADOLFO GERARDO NAVARRO SIGÜENZA

Agradecimientos institucionales

Agradezco al Posgrado en Ciencias Biológicas de la Universidad Nacional Autónoma de México.

Al Consejo Nacional de Ciencia y Tecnología (CONACYT) por el apoyo económico no. 778388 otorgado para realizar los estudios de maestría. Y por el financiamiento de la investigación a través del proyecto CONACYT (239482).

De forma muy especial agradezco a mi tutora Dra. Livia S. León Paniagua y a los miembros de mi comité tutor Dr. Luis E. Eguiarte Fruns y Dr. Jorge Ortega Reyes, por todo su apoyo y sus valiosas aportaciones a este trabajo.

Agradecimientos personales

A mi jurado Dr. Giovani Hernández, Dra. Gabriela Castellanos, Dr. Luis Antonio Sánchez y Dra. Ella Vázquez, por aceptar formar parte de este sínodo, por su tiempo, compromiso y contribuciones para mejorar el trabajo.

A mis padres y hermanos por su presencia constante y por brindarme siempre su apoyo y amor sin condición. Gracias porque gran parte de lo que soy se lo debo a ustedes.

A mis tíos Columba, Gloria y Alejandro, Aidé y René, Eloísa y Carlos, por estar siempre al pendiente de mí y expresarme su cariño en muy diversas situaciones.

A todos los que pertenecen y pertenecieron al Cubil, y con los que durante el desarrollo de este proyecto compartí momentos cotidianos y eventos importantes, trabajo de campo y de laboratorio, reflexiones disparatadas y bases teóricas, colecciones de chistes y charlas constructivas, situaciones fáciles y difíciles. La tendencia de ayudarse unos a otros es una tradición reforzada en este lugar y un lema que busca ser heredado por cualquiera que decida formar parte de sus filas. Por su gran amistad, apoyo y cariño, gracias a: Livia, Giovani, Yire, Tania, Darcy, Alina, Pablito, Lázaro, Sara, Alfredo, Iván, Adriana, Juan, Lorena, Josué, Marco, Melissa, Rodolfo y Brenda.

A mis amigos del 1202, porque vivir juntos fue toda una aventura. Sin duda un gran sitio dónde compartir el día a día en una gran ciudad. Gracias por apoyar los días de Mercado del trueque, soportar sismos en las alturas, y formar una amena colectividad: Giovani, Grabiel y Gabriel.

A mis amigos de la vida y la universidad, con quienes los lazos de amistad siguen perdurando a través de la distancia y los fenómenos naturales y sociales de actualidad. Gracias por acompañarme, aconsejarme y hacer divertida nada menos que la vida: Gerardo, Miguel, Carlos, Manuel, Daniel e Irai; Odette, Tonichi, Inari, Pau, Danielini, Freddy, Gabo, Fer, Jessie y Arturo.

A la Universidad Nacional Autónoma de México por las motivaciones, oportunidades y satisfacciones que brinda a la comunidad. Siempre serás un gran orgullo para mí y nunca dejaré de agradecer lo tan nutrido que has dejado mi corazón con tus experiencias.

Índice

Resumen

La variación genética se refiere a la diversidad en la composición de los genes que se manifiesta entre los individuos de una misma especie y entre especies. El flujo génico es una fuerza evolutiva que influye en la variación genética, cuyo efecto tiende a homogenizar las poblaciones. El uso de herramientas genéticas moleculares permite obtener aproximaciones sobre los procesos históricos y contemporáneos que afectan la variación y estructura genética de las poblaciones. Diversos estudios han demostrado que al combinar la información genética de diferentes marcadores moleculares, incluyendo ADN nuclear y ADN mitocondrial, es posible desarrollar inferencias más precisas sobre la historia evolutiva de los taxa. Sin embargo, no siempre se encuentran patrones concordantes entre el ADN mitocondrial y el ADN nuclear, por ejemplo debido a inconsistencias geográficas (discordancia biogeográfica mito-nuclear). *Sturnira parvidens*, el murciélago de charreteras de tierras bajas mesoamericanas, pertenece al género más diverso de murciélagos frugívoros neotropicales y presenta la distribución más norteña dentro de éste. En este trabajo describimos la variación genética de *S. parvidens* a lo largo de Mesoamérica (*n* = 134) usando ocho loci nucleares (*gen activador de la recombinación I* y 7 microsatélites) y dos regiones mitocondriales (*citocromo b* y *región control* o *D-loop*). Comparamos la estructura poblacional detectada por herencia materna y biparental (loci mitocondriales y nucleares, respectivamente), y evaluamos el flujo génico entre poblaciones. Los resultados mostraron una alta diversidad genética y dos grupos genéticos bien diferenciados (Oeste y Este). Asimismo, se observa un patrón de discordancia biogeográfica mito-nuclear significativo entre los dos grupos, con un límite geográfico mitocondrial en la depresión del río Balsas y un límite geográfico nuclear en el valle de Tehuacán-Cuicatlán y los valles Centrales de Oaxaca. Se determinó que el ADN nuclear del grupo del Oeste se sobrepone con el área de distribución del linaje del Este, sugiriendo que aunque los linajes genéticos de *S. parvidens* pudieron haberse separado completamente en el pasado y formado dos grupos bien estructurados durante las oscilaciones climáticas de la segunda mitad del Pleistoceno, probablemente volvieron a entrar en contacto más recientemente, generando el patrón de discordancia biogeográfica mito-nuclear que hoy observamos. Nuestro estudio apoya la idea de que las hembras de *S. parvidens* son filopátricas, y que el flujo génico a larga distancia lo realizan los machos. Es importante conocer la dinámica evolutiva poblacional de especies comunes como *S. parvidens* en áreas biológicamente diversas como Mesoamérica, para determinar los patrones biogeográficos de la región.

Abstract

Genetic variation is the diversity in the gene composition found among individuals of the same species and between species. Gene flow is an evolutionary force that influences genetic variation, the effect of which tends to homogenize populations. Molecular genetic tools can clarify the historical and contemporary processes that affect the genetic variation and genetic structure of populations. Several studies have shown that by combining the genetic information from different molecular markers, including nuclear DNA and mitochondrial DNA, it is possible to develop accurate inferences about the evolutionary history of taxa. However, genetic patterns are not always consistent between mitochondrial DNA and nuclear DNA, for example, due to geographic inconsistencies between their differentiation patterns (mito-nuclear biogeographic discordance). *Sturnira parvidens*, the little yellow-shouldered Mesoamerican bat, belongs to the most diverse genus of Neotropical fruit bats and has the northernmost distribution of the genus. We describe the genetic variation of *S. parvidens* throughout Mesoamerica (*n* = 134) using eight nuclear loci (*recombination activating gene I* and 7 microsatellite loci) and two mitochondrial regions (cytochrome *b* and *hypervariable region I* or *D-loop*). We compared the population structure detected by maternal and biparental inheritance (mitochondrial and nuclear loci, respectively), and evaluated gene flow among populations. The results showed a high genetic diversity and two well-differentiated genetic groups (West and East). Likewise, a significant mito-nuclear biogeographic discordance pattern was observed between the two groups, with a mitochondrial geographic limit in the Balsas River Basin and a nuclear geographic limit in the Tehuacán-Cuicatlán Valley and the Central Valleys of Oaxaca. It was determined that the nuclear DNA of the West group overlaps with the distribution range of the East lineage, suggesting that although the genetic lineages of *S. parvidens* may have been completely separated and formed two well-structured genetic groups in the past, during the climatic oscillations of the second half of the Pleistocene, they likely came back into contact more recently, generating the pattern of mito-nuclear biogeographic discordance that we observe today. Our study supports the idea that *S. parvidens* females are philopatric, and that long-distance gene flow is carried out by males. It is important to know the evolutionary population dynamic of common species such as *S. parvidens* in biologically diverse areas such as Mesoamerica, to determine the biogeographic patterns of the region.

Introducción general

Los individuos de una misma especie no son idénticos entre sí. Gran parte de la disparidad entre ellos proviene de su material genético, es decir, se trata de variación genética. La variación genética se refiere a las diferencias en el ADN que existen entre los individuos de una población, y debido a que en cada generación únicamente una fracción de la población sobrevive y se reproduce transmitiendo rasgos particulares a su descendencia, la variación genética permite la evolución de las especies (Frankham 2005, Nielsen & Slatkin 2013).

Los niveles de variación genética que existen dentro y entre las poblaciones que constituyen a las especies son estudiados por la genética de poblaciones, y esta disciplina busca explicar sus patrones en términos de diversas fuerzas evolutivas (Eguiarte *et al.* 2013). De esta manera, es posible investigar los factores del pasado que han determinado la composición genética actual de las poblaciones y también, bajo una perspectiva predictiva, modelar escenarios futuros en los que su composición genética podría verse comprometida (Nielsen & Slatkin 2013). Ambas bases teóricas son necesarias para comprender los mecanismos del cambio evolutivo de las poblaciones a través del tiempo y el espacio.

El flujo genético es una de las fuerzas evolutivas que influencian la variación genética, y es definido como el movimiento de individuos entre grupos o poblaciones que tiene como resultado el intercambio genético (Endler 1977). Sin embargo, la dispersión no siempre produce flujo genético, y se piensa que la dispersión es consecuencia del balance de una serie de factores que pueden favorecer o repercutir sobre ésta, tales como la disponibilidad de recursos, la evasión de la endogamia y los costos de la mortalidad (Lawson Handley & Perrin 2007). Debido a que estos factores suelen ser diferentes entre hembras y machos, la dispersión suele variar según el sexo de los organismos (Greenwood 1980). En el caso general de los mamíferos, ha sido bien estudiado que los machos tienden a dispersarse más que las hembras, y que las hembras tienden a desarrollar un comportamiento de filopatría, es decir, a permanecer en un mismo territorio por cuestiones reproductivas, y por lo tanto, a dispersarse menos (Fabiani *et al.* 2003, González-Suárez *et al.* 2009).

El uso de herramientas genéticas moleculares (p. ej., marcadores de ADN mitocondrial y ADN nuclear, microsatélites, SNPs, AFLPs, RAPDs, etc.) permite obtener aproximaciones sobre los procesos históricos (p. ej., eventos de aislamiento en refugios

geográficos, expansión de la distribución geográfica, colonización, cuellos de botella) y contemporáneos (p. ej., flujo genético, estructura y éxito reproductivos) que afectan la variación genética y la estructura genética de las poblaciones (Neubaum *et al.* 2007). Esto es especialmente relevante para aquellas especies difíciles de observar directamente debido a sus hábitos nocturnos, alta vagilidad, tamaño corporal pequeño y/o que viven en ambientes hostiles o inaccesibles, como es el caso de muchos mamíferos, donde las herramientas genéticas moleculares adquieren importancia crucial para inferir aspectos de su historia natural y eventos evolutivos (Castañeda-Rico *et al.* 2011, Cegelski *et al.* 2003, Marshall *et al.* 2011, Moussy *et al.* 2015, Uphyrkina *et al.* 2001).

Los microsatélites (*simple sequence repeats*, SSRs) son secuencias de ADN constituidas por repeticiones de nucleótidos de 1 a 6 pares de bases (Hancock 1999). Se distribuyen en regiones codificantes y no codificantes del ADN y se caracterizan por ser altamente polimórficos en cuanto a su longitud. De esta manera, son regiones genéticas adecuadas para usarse como marcadores moleculares a nivel poblacional (Zane *et al.* 2002). Su alto grado de polimorfismo es consecuencia de una elevada tasa de mutación (desde 10^{-6} hasta 10^{-2} mutaciones por sitio por generación; Schlötterer 2000), que se atribuye a eventos de inserción y deleción durante la replicación del ADN (Vázquez & García 2014).

Los microsatélites nucleares han sido extensamente usados en el estudio de mamíferos silvestres, incluyendo murciélagos, con propósitos muy diversos, por ejemplo: estudiar los efectos de las barreras geográficas y los eventos post-glaciales (Bilgin *et al.* 2009, Jadwiszczak *et al.* 2006), evaluar la estructura genética de especies en alguna categoría de riesgo para ayudar en su conservación (Castellanos-Morales *et al.* 2015), y determinar los patrones de dispersión y flujo génico en especies que realizan grandes desplazamientos (Proctor *et al.* 2004, Bryja *et al.* 2009), entre otros.

Utilizar información de marcadores moleculares con distintas formas de herencia y tasas de mutación – por ejemplo el uso conjunto de genes (mitocondriales y nucleares) y de diversos *loci* de microsatélites – suele ayudar a identificar procesos evolutivos que no pueden visualizarse con cualquiera de dichos marcadores de manera independiente. Asimismo, la interpretación de los eventos históricos y contemporáneos que han afectado la diversidad y estructura genética de las poblaciones resulta más confiable (Brito 2007, Flanders *et al.* 2009, You *et al.* 2010). En diversos estudios con un considerable esfuerzo de muestreo, se ha observado que los distintos marcadores moleculares regularmente producen patrones congruentes entre ellos (Avise 2004, Kerr *et al.* 2007). Sin embargo, no siempre se observan patrones concordantes entre el ADN mitocondrial y el ADN

nuclear (Funk & Omland 2003). De hecho, el número de estudios que reportan variación entre los patrones de estos marcadores se ha incrementado en las últimas dos décadas (Castella *et al.* 2001, Martins *et al.* 2009, Naidoo *et al.* 2016, Roca *et al.* 2005).

La discordancia entre el ADN mitocondrial (mtADN) y el ADN nuclear (nuADN) puede definirse más ampliamente como una diferencia significativa entre los patrones de diferenciación de ambos tipos de marcadores (Toews & Brelsford 2012). Más comúnmente, ello resulta de la cantidad total de diferenciación o de cómo dichos marcadores reconstruyen las relaciones entre grupos. De cierta forma, se espera que exista este tipo de discordancia, ya que el genoma mitocondrial es haploide y de herencia uniparental en la mayoría de los animales y, por lo tanto, tiene un tamaño efectivo cuatro veces menor (Hudson & Turelli 2003). Esto significa que el mtADN completaría el proceso de "sorteo de linajes" o *lineage sorting*, donde los polimorfismos ancestrales son perdidos a través del tiempo, más rápido que el nuADN, ya que esta tasa es inversamente proporcional al tamaño efectivo poblacional (Funk & Omland 2003). La prevalencia de la clasificación incompleta de linajes en la contribución a los patrones de discordancia entre el mtADN y el nuADN ha sido extensamente discutida (McKay & Zink 2010, Zink & Barrowclough 2008), y la principal respuesta a esto ha sido la inclusión de múltiples *loci* independientes en los trabajos de investigación para generar relaciones filogenéticas más robustas entre los taxa (Edwards & Bensch 2009).

Es difícil distinguir entre el sorteo incompleto de linajes y otras formas de discordancia. Sin embargo, una diferencia importante es que no se espera que la discordancia causada por sorteo incompleto de linajes deje un patrón biogeográfico predecible (Funk & Omland 2003). Por lo tanto, en los casos donde existan fuertes inconsistencias geográficas entre los patrones de diferenciación del mtADN y el nuADN, se puede descartar el sorteo incompleto de linajes. La discordancia de este último tipo – mejor conocida como discordancia biogeográfica – puede resultar de clinas en el mtADN que son desplazadas por el nuADN ya sea en su ubicación y/o en su amplitud (Toews & Brelsford 2012). La mayoría de los taxa que muestran patrones de discordancia biogeográfica mito-nuclear son grupos que estuvieron aislados por largos períodos de tiempo y que actualmente presentan contacto secundario o que han sido simpátricos en algún punto de su pasado (Hudson & Turelli 2003, Toews & Brelsford 2012). La discordancia biogeográfica puede ser extensa, hasta producir un reemplazamiento completo del mtADN de una especie por otra (captura mitocondrial), o más limitada, donde los haplotipos mitocondriales muestran una frecuencia más alta en una población dada de lo que se esperaría de los marcadores nucleares (Toews & Brelsford 2012).

Los patrones de discordancia biogeográfica, en muchos casos, se han usado para inferir los potenciales conductores de este fenómeno. Para las situaciones donde el centro de la clina del mtADN es desplazado y/o es más amplio comparado con el nuADN, se han mencionado una serie de procesos conductores de la discordancia, p. ej., introgresión adaptativa del mtADN (Currat *et al.* 2008), disparidades demográficas, asimetrías sesgadas por el sexo, movimiento de la zona de hibridación (Rohwer *et al.* 2001), infección por *Wolbachia* en insectos (Jiggins 2003, Sun *et al.* 2015) e introducciones humanas (Perry *et al.* 2001). Las disparidades demográficas pueden generar discordancia si existen grandes diferencias en el tamaño de las poblaciones o del área de distribución entre los dos taxa, en especial si se trata de tamaños poblaciones muy pequeños que influencian la frecuencia del mtADN por efectos de muestreo (deriva génica), promoviendo la introgresión asimétrica (Currat *et al.* 2008). Diferencias demográficas más generales, sistemas de dispersión sesgados por algún sexo, diferencias de comportamiento en la probabilidad de apareamiento y la producción diferencial de descendencia pueden promover la introgresión de mtADN (Toews & Brelsford 2012). El movimiento de una zona de hibridación también puede crear discordancia cuando la mayoría de los marcadores nucleares (junto con rasgos fenotípicos) cambian su localización geográfica (Rohwer *et al.* 2001). Las acciones humanas pueden facilitar contactos secundarios entre taxa y generar asimetrías demográficas al desplazar o trasladar individuos, o generar discordancia al facilitar su interacción debido a la alteración de los ecosistemas (Perry *et al.* 2001).

Los murciélagos son uno de los grupos de mamíferos más diversos en el mundo, en los cuales se han desarrollado diversos estudios moleculares. Por ejemplo, trabajos genéticos en diferentes especies han sido útiles para describir patrones de estructura genética que a su vez reflejan diferencias en sus sistemas de apareamiento (Furmankiewicz & Altringham 2007), en sus patrones de dispersión y migración, que se encuentran sesgados por el sexo (Moussy *et al.* 2013), en su demografía e historia de las poblaciones (Flanders *et al.* 2009), y en aspectos de diversidad críptica y para el descubrimiento de nuevas especies (Goodman *et al.* 2010, Racey *et al.* 2007).

Las especies de murciélagos del género *Sturnira* son un modelo de estudio excelente para analizar procesos y patrones de diversificación genética en Mesoamérica. *Sturnira* es el género con mayor número de especies dentro de la familia Phyllostomidae y, tan sólo en las últimas dos décadas, se ha generado una notable cantidad de información sobre sus relaciones evolutivas (Contreras Vega & Cadena 2000; Hernández-Canchola & León-Paniagua 2017; Iudica 2000; Jarrín- V & Kunz 2011; Jarrín & Clare

2013; McCarthy *et al.* 2006; Molinari *et al.* 2017; Sánchez- Hernández *et al.* 2005; Velazco & Patterson 2019, 2013, 2014).

Este género comprende 24 especies descritas distribuidas en dos clados filogenéticos de acuerdo con diferencias morfológicas y genéticas y con su asociación con bosques de tierras altas o bajas desde México hasta Sudamérica (Velazco & Patterson 2013). Para el clado asociado con bosques de tierras bajas, se ha propuesto que las oscilaciones climáticas del Pleistoceno y las altas tasas de diversificación al interior del linaje a través del tiempo, pueden explicar la actual diversidad de especies (Hernández-Canchola & León-Paniagua 2017, Rojas *et al.* 2016).

Sturnira parvidens es una especie de murciélago frugívoro relativamente común y abundante en los bosques de tierras bajas de Mesoamérica, y posee la distribución geográfica más norteña de los murciélagos de charreteras, la cual va desde Sonora y Tamaulipas en el norte de México hasta la Cordillera de Talamanca en Costa Rica (Hernández-Canchola & León-Paniagua 2017). Usando datos de loci mitocondriales y nucleares, Hernández-Canchola & León-Paniagua (2017) encontraron que existen dos haplogrupos bien diferenciados dentro de *S. parvidens* (Oeste y Este), los cuales divergieron hace cerca de 0.423 millones de años (Ma; 95% CI: 0.586-0.268), en el Pleistoceno Medio, al final del intenso período glacial MIS-12 (0.424 Ma; Lisiecki & Raymo 2005). Sin embargo, actualmente dichos haplogrupos están en contacto y sin barreras geográficas aparentes. El límite entre los dos haplogrupos se encuentra cerca de la Sierra Madre del Sur, en la vertiente del Pacífico Mexicano, sin embargo dicho límite no está bien definido a una escala fina. Aunque se han realizado considerables e importantes esfuerzos, son necesarios estudios adicionales que incluyan un mayor número de loci con marcadores moleculares de diferentes tipos, como el presente trabajo, para describir nuevos aspectos de la historia evolutiva, diversificación y biología de *S. parvidens*.

El objetivo de este estudio fue examinar y comparar los patrones de variación genética, estructura genética y flujo génico en *S. parvidens* usando microsatélites y diferentes genes como marcadores moleculares. De manera puntual, (1) describimos la variación genética actual dentro de las poblaciones de *S. parvidens* usando loci de microsatélites nucleares, (2) comparamos la estructura genética poblacional con base en loci de herencia materna (genes mitocondriales *citocromo b* [*cyt-b*] y *región control o D-loop* [*D-loop*]) con la obtenida usando loci nucleares de herencia biparental (microsatélites y *gen activador de la recombinación I* [*RAG1*]), y (3) analizamos si existe flujo génico entre las poblaciones de esta especie de murciélago.

OXFORD UNIVERSITY PRESS | Journal of Heredity

Mito-nuclear genetic discordance in the Little Yellow-shouldered Mesoamerican bat, *Sturnira parvidens* (Chiroptera: Phyllostomidae)

Journal:	*Journal of Heredity*
Manuscript ID	JOH-2020-003.R1
Manuscript Type:	Original Article
Date Submitted by the Author:	n/a
Complete List of Authors:	Cabrera, Martín; Universidad Nacional Autónoma de México Facultad de Ciencias, Biología Evolutiva Hernández-Canchola, Giovani; LSU Museum of Natural Science Eguiarte, Luis; Instituto de Ecologia, Universidad Nacional Autonoma de Mexico, Evolutionary Ecology Ortega, Jorge; Intituto Politecnico Nacional, Zoologia León-Paniagua, Livia; Universidad Nacional Autónoma de México Facultad de Ciencias, Biología Evolutiva
Keywords:	gene flow, genetic structure, microsatellites, philopatry, Tehuacán-Cuicatlán and Oaxacan Central Valleys

SCHOLARONE™
Manuscripts

Mito-nuclear genetic discordance in the Little Yellow-shouldered Mesoamerican bat, *Sturnira parvidens* (Chiroptera: Phyllostomidae)

Running title: Mito-nuclear discordance in *S. parvidens*

Martín Y. Cabrera-Garrido[a, b], Giovani Hernández-Canchola[a, c], Luis E. Eguiarte[d], Jorge Ortega[e], and Livia León-Paniagua[a]

[a] Colección de Mamíferos – Museo de Zoología "Alfonso L. Herrera", Departamento de Biología Evolutiva, Facultad de Ciencias, Universidad Nacional Autónoma de México, Circuito Exterior s/n, Ciudad Universitaria, 04510, CDMX, Mexico

[b] Posgrado en Ciencias Biológicas, Universidad Nacional Autónoma de México, Circuito de los Posgrados s/n, Ciudad Universitaria, 04510, CDMX, Mexico

[c] Museum of Natural Science, 119 Foster Hall, Louisiana State University, Baton Rouge, LA 70803, USA

[d] Laboratorio de Evolución Molecular y Experimental, Departamento de Ecología Evolutiva, Instituto de Ecología, Universidad Nacional Autónoma de México, Circuito Zona Deportiva s/n Anexo al Jardín Botánico, Ciudad Universitaria, 04510, CDMX, Mexico

[e] Laboratorio de Bioconservación y Manejo, Posgrado en Ciencias Químicobiológicas, Departamento de Zoología, Escuela Nacional de Ciencias Biológicas, Instituto Politécnico Nacional, Prolongación de Carpio y Plan de Ayala s/n, Col. Sto. Tomás, 11340, CDMX, Mexico

Cabrera-Garrido: mcabrera@ciencias.unam.mx

Hernández-Canchola: canchola@lsu.edu

Eguiarte: fruns@unam.mx

Ortega: artibeus2@aol.com

*León-Paniagua (corresponding author): llp@ciencias.unam.mx

ABSTRACT

One of the most important processes influencing genetic variation is gene flow, but genetic patterns are not always consistent between mitochondrial and nuclear markers for a variety of reasons. *Sturnira parvidens* is the lowland shouldered bat with the most northern distribution in the most diverse genus of Neotropical fruit bats. We described its genetic variation throughout Mesoamerica (*n*= 134) using eight nuclear loci (recombination activating gene I and 7 microsatellite loci) and two mitochondrial regions (cytochrome *b* and hypervariable region I). We compared the population structure revealed by mitochondrial (maternally inherited) loci with structure revealed by nuclear (biparentally inherited) loci and analysed whether there is gene flow among populations. We observed high genetic diversity in this species and both types of markers recovered two genetically well-differentiated groups. However, there was biogeographic mito-nuclear discordance in the boundary between the two groups; mitochondrial analysis showed a geographic boundary at the Balsas River Basin, while the nuclear geographic limit was at the Tehuacán-Cuicatlán and Oaxacan Central Valleys. Our results support the idea that females are philopatric and that long-distance gene flow is due to male dispersal. Understanding the evolutionary population dynamics of common species like *S. parvidens* in biologically diverse areas such as Mesoamerica is an important first step for maintaining the health of global ecosystems into the future.

Keywords: gene flow, genetic structure, microsatellites, philopatry, Tehuacán-Cuicatlán and Oaxacan Central Valleys.

INTRODUCTION

Molecular genetic tools can clarify the historical and contemporary processes that affect the genetic variation and genetic structure of populations (Neubaum et al. 2007, Hedrick 2011). This is especially true for species that are difficult to observe directly due to nocturnal habits, high vagility, small body size, and harsh or inaccessible habitats, as is the case of many mammals (Eizirik et al. 2001, Marshall et al. 2011, Castañeda-Rico et al. 2011). Molecular genetic tools thus acquire an unparalleled importance to infer evolutionary events and aspects of species' natural history (Uphyrkina et al. 2001, Cegelski et al. 2003, Moussy et al. 2015, Gariboldi et al. 2016). Nuclear microsatellite markers are known for their high mutation rates and high degree of polymorphism (Schlötterer 2000, Eguiarte et al. 2013), so they have been extensively used to address a wide variety of research questions in wild mammals, such as determining dispersal and gene flow patterns (Proctor et al. 2004, Bryja et al. 2009), testing philopatry (Kerth & Van Schaik 2012), evaluating the effects of geographic barriers (Bilgin et al. 2009, García-Mudarra et al. 2009), and studying genetic structure of endangered species (Ritland et al. 2001, Loew et al. 2005, Castellanos-Morales et al. 2015).

One of the most important contemporary processes influencing genetic variation is gene flow – the movement of individuals between groups or populations that results in genetic exchange (Endler 1977). However, dispersal does not always results in gene flow, and dispersal is thought to be a balance of factors selecting for and against it, including mortality costs, resource availability, and inbreeding avoidance (Lawson Handley & Perrin 2007). Because these factors often differ between females and males, dispersal often differs between sexes (Greenwood 1980, Hedrick 2011). In general among mammals, males tend to disperse, while females tend to be philopatric and defend resources near where they were born (Lyrholm et al. 1999, Fabiani et al. 2003, Lawson Handley & Perrin 2007, González-Suárez et al. 2009).

In many studies with a considerable sampling effort and a diverse array of genetic markers that vary in their types of inheritance and evolution rates, distinct genetic markers

usually yield congruent patterns (e.g., Avise 2004, Kerr et al. 2007, Zink & Barrowclough 2008). However, this is not always the case; in some cases mtDNA and nuDNA show different patterns (Funk & Omland 2003), and the number of studies that report such incongruence between marker types – known as mito-nuclear discordance – has increased in recent years (Toews & Brelsford 2012, Naidoo et al. 2016).

There are two common patterns of mito-nuclear discordance: (1) a lack of a discernible geographic pattern in the distribution of mtDNA clades among clearly defined nuclear groups, which suggests incomplete lineage sorting (Funk & Omland 2003), and (2) strong differences in the geographic distribution of mtDNA and nuDNA groups (usually called biogeographic discordance), with mtDNA and nuDNA clines that differ in their location or their width, a pattern thought to be due to long periods of isolation of taxa with past or current instances of secondary contact (Hudson & Turelli 2003, Toews & Brelsford 2012). When a mtDNA cline centre is displaced and/or wider than the nuDNA cline, there are several explanations, including introgression of mtDNA (Currat et al. 2008), sex-biased asymmetries and demographic disparities, hybrid zone movement (Rohwer et al. 2001), *Wolbachia* infection in insects (Sun et al. 2015), and human introductions (Perry et al. 2001).

Recent research has analysed the evolutionary relationships within *Sturnira*, the most speciose genus of New World leaf-nosed bats (Contreras Vega & Cadena 2000; Hernández-Canchola & León-Paniagua 2017; Iudica 2000; Jarrín-V & Kunz 2011; Jarrín & Clare 2013; McCarthy et al. 2006; Molinari et al. 2017; Sánchez-Hernández et al. 2005; Velazco & Patterson 2019, 2013, 2014). Pleistocene climatic oscillations and high diversification rates within the *Sturnira* lineage (Rojas et al. 2016) have been proposed to explain their high current species diversity (Hernández-Canchola & León-Paniagua 2017).

Sturnira parvidens, a relatively common and abundant bat species in the Mesoamerica lowlands, has the most northern distribution among shouldered bats, ranging from Sonora and Tamaulipas in northern Mexico to the Talamanca Mountain Range in Costa Rica (Hernández-

Canchola & León-Paniagua, 2017; Figure 1). Using data from mitochondrial and nuclear loci, Hernández-Canchola & León-Paniagua (2017) found two well-defined haplogroups within *S. parvidens* (West and East), which diverged *c.* 0.423Ma (95% CI: 0.586–0.268) in the Middle Pleistocene at the end of MIS-12 intense glacial period (0.424 Ma; Lisiecki & Raymo 2005), but currently the haplogroups are in contact and lack apparent geographic barriers. The boundary between the two haplogroups is near the Sierra Madre del Sur, on the Mexican Pacific Slope, but that limit is not well defined at a fine scale. While considerable and important efforts have been made, further studies are necessary to describe aspects of the evolutionary history, diversification and biology of *S. parvidens*.

To recover accurate inferences, with more reliable and complete evidence about the evolutionary history of this taxon, the aim of this study was to examine and compare patterns of genetic variation, genetic structure, and gene flow in *S. parvidens* using microsatellite and gene markers. Here, we (1) describe the current genetic variation within the *S. parvidens* populations using microsatellite loci, (2) compare the population structure revealed by maternally inherited mitochondrial loci (*cytochrome b* [*cyt-b*] and the *hypervariable D-loop region I* [*D-loop*]) with that of biparentally inherited nuclear loci (microsatellite markers and *recombination activating gene 1* [*RAG1*]), and (3) analyse whether there is current gene flow between the populations of this bat species.

MATERIALS AND METHODS

Samples and DNA extraction. We obtained tissue samples from 134 individuals of *S. parvidens* from 50 different localities along its full distributional range in Mexico and Central America. Several localities were combined to form larger populations based on their proximity to each other, the biogeographic regions for Mexican mammals proposed by Ramírez-Pulido & Castro-Campillo (1990), and the similarity of environmental conditions between different areas, yielding a total of 21 populations (Figure 1).

Figure 1. Locations of the 21 populations of *Sturnira parvidens* analysed in this work, throughout its full distributional range in Mexico and Central America (grey shaded area). SMW: Sierra Madre Occidental; NAY: Nayarit; JNP: Pacific coasts of Nayarit and Jalisco; JAL: Los Naranjitos, Jalisco; JAB: El Jabalí, Colima; YER: La Yerbabuena, Colima; MAG: Arteaga, Michoacán; MBR: Michoacán lowlands of the Balsas River; BAL: Balsas River Basin; OXT: Tehuacán-Cuicatlán and Oaxaca Valleys; SMS: Sierra Madre del Sur; TAM: Tamaulipas; SME: Sierra Madre Oriental; VEP: Puebla-Veracruz; NIZ: Nizanda, Oaxaca; ISN: North of the Tehuantepec Isthmus; CHI: Chiapas; YAX: Yaxchilán, Chiapas; PYU: Yucatan Peninsula; HND: Honduras; CRN: Nicaragua and Costa Rica lowlands. At the bottom left, a close-up of the main physiographic regions of south-central Mexico is shown. Highlands (in medium grey and dark grey): 1. Trans-Mexican Volcanic Belt; 2. Sierra Madre del Sur. Lowlands (in light grey): 3. Balsas River Basin; 4. Tehuacán-Cuicatlán Valley; 5. Central Valleys of Oaxaca.

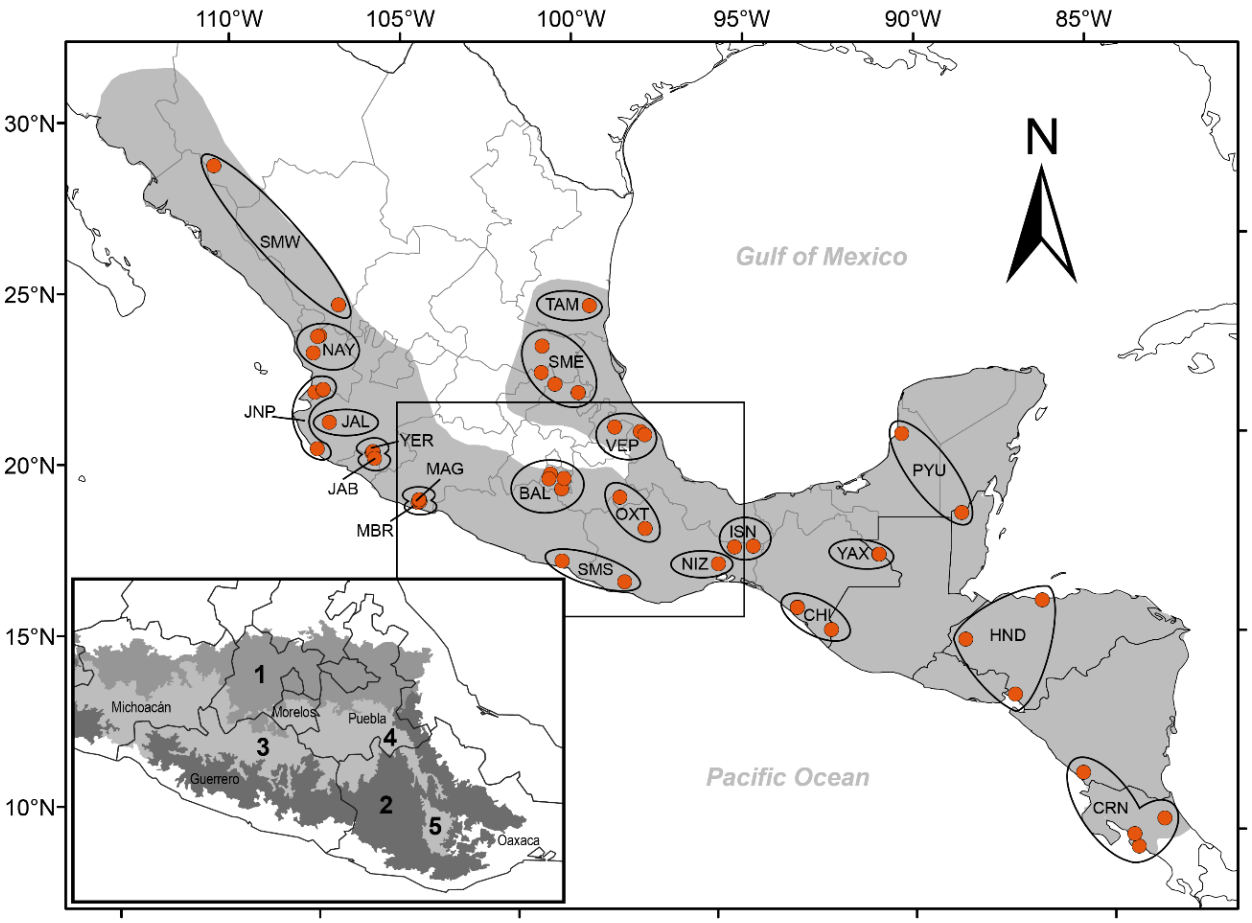

Specimens were provided by several scientific collections: Universidad Nacional Autónoma de México – Museo de Zoología ‘‘Alfonso L. Herrera’’, Facultad de Ciencias (MZFC-M); Instituto Politécnico Nacional – Centro Interdisciplinario de Investigación para el Desarrollo Integral Regional, Durango, México (CIIDIR-IPN); Louisiana State University, Museum of Natural Science, Baton Rouge (LSUMZ); Museo Nacional de Costa Rica, San José, Costa Rica (MNCR-

M); Museum of Texas Tech University, Lubbock (TTU); and the Royal Ontario Museum, Toronto, Canada (ROM). Tissue samples were extracted following a modified protocol using NaCl and chloroform: isoamyl alcohol (Mullenbach et al. 1989).

Microsatellite typing. We tested 12 fluorescently labelled microsatellite primers (Spar01, Spar02, Spar05, Spar07, Spar08, Spar09, Spar010, Spar011, Spar012, Spar013, Spar030, and Spar040) designed for *Sturnira parvidens* (Gutiérrez et al. 2017). We amplified by PCR the nuclear microsatellite loci using the following conditions: 5 min of initial denaturation at 94°C, 30 cycles of 40 s of denaturation at 94°C, 1 min of annealing at 55–64°C, and 2 min for extension at 72°C; we included a 10 min step for final extension at 72°C. The DNA was amplified in a 7.5 μL reaction volume containing the following: 4.23 μL of H_2O, 0.75 μL Buffer [10x], 0.36 μL of dNTP's Mix [2 mM], 0.75 μL of $MgCl_2$ [25 mM], 0.375 μL of forward primer labelled with 6-FAM fluorescence [10 μM], 0.375 μL of reverse primer [10 μM], 0.06 μL of Taq polimerase [5u/μL] (Vivantis Technologies Sdn. Bhd., Selangor, Malaysia), and 0.6 μL of DNA. With 1 μL of each PCR, we visualized these products by electrophoresis in 2% agarose gels with TAE [1x], stained with GelRed (Biotium Inc., Fremont, CA, USA).

We sent PCR products for genotyping with an ABI 3730xl sequencer (Applied Biosystems) to the UIUC Core Sequencing Facility at the University of Illinois (unicorn.biotec. illinois.edu). Every sample was genotyped at least twice to assure reproducibility and correct readings. We visualized the fragments in PEAK SCANNER software v1.0 (Applied Biosystems) and followed the recommendations in Arif et al. (2010) for correct interpretations of alleles.

Mitochondrial and nuclear sequences. We downloaded sequences for the mitochondrial loci *cyt-b* (1,140 bp) and *D-loop* (388 bp), and for the nuclear locus *RAG1* (1,072 bp); from GenBank for 172, 173, and 161 individuals of *S. parvidens* respectively, reported in Velazco & Patterson (2013) and Hernández-Canchola & León-Paniagua (2017). The corresponding accession numbers are as

follows: *cyt-b* (KC753857- KC753875, MF441774- MF441776, MF441778- MF441927), *D-loop* (KC754085- KC754103, MF441954- MF442107), and *RAG1* (KC754204- KC754222, MF442118- MF442259). Although it would have been ideal to genotyped all of the 173 specimens analysed by Hernández-Canchola & León-Paniagua (2017), we could only obtained microsatellite data for 134 of those individuals (see below).

Tests of assumptions and genetic diversity estimates. For the microsatellites, we tested for scoring inconsistencies, null alleles, large allele dropout and stuttering with MICRO-CHECKER 2.2.3 (Van Oosterhout et al. 2004) using both a 95% and Bonferroni confidence intervals and 1,000 randomizations. We tested possible departures from Hardy–Weinberg equilibrium for each locus using 1,000 permutations with GENALEX v6.503 (Peakall & Smouse, 2006, 2012) and poppr v2.7.1 (Kamvar et al. 2014). The latter is an R package (R Core Team 2016) for genetic analysis of populations.

Linkage disequilibrium (LD) was tested using the index of association (I_A) originally proposed by Brown et al. (1980) and implemented in the poppr v2.7.1 R package using a permutation approach to assess whether loci are linked; the $\bar{r}_d$ index also accounts for the number of loci sampled that is lesast biased; we used 999 permutations of the data in order to calculate *p*-values.

Genetic variation estimates (number of alleles [N_a], effective number of alleles[N_e], observed [H_o] and expected heterozygosity [H_e]), a fixation index (F) to evaluate heterozygote deficit or excess (Weir & Cockerham 1984), and plots of allele length frequencies for each population were generated with GENALEX v6.503. We also performed rarefaction to determine allelic and private allelic richness per population (R and R_P, respectively) while compensating for sampling bias using HP-RARE (Kalinowski 2004, 2005). We followed the HP-RARE sample size analysis from our samples, which suggested a minimum sample size of 6 (n = 6) to perform the rarefaction calculations.

For the nuclear gene *RAG1*, we obtained the allelic phases using the phase algorithm and the method implemented by Hernández-Canchola & León-Paniagua (2017).

For mitochondrial and nuclear genes we calculated the following genetic measures for each locus with the software DNASP v5.10 (Librado & Rozas 2009): number of segregating sites (*S*), number of haplotypes (*h*), haplotype diversity (*Hd*), and nucleotide diversity (π).

Based on the results of the analyses of genetic structure described below, we also calculated the genetic diversity within the clusters obtained.

Genetic structure. To recover and compare the mitochondrial haplogroups detected by Hernández-Canchola & León-Paniagua (2017), we generated mitochondrial haplotype networks in pegas v0.10 R package (R Core Team 2016) using the individuals from which we obtained the microsatellite data (n = 133 for *cyt-b*, and n = 134 for *D-loop*). We also compared the genetic-geographic structure for each of the genes and for microsatellites in GENELAND (Guillot et al. 2005, 2012). This Bayesian method considers genetic data and their geographic coordinates to identify genetic discontinuities between populations, and includes models to calculate genetic structuring in both mitochondrial and nuclear loci. We tested the occurrence 1 to 10 populations using $1x10^6$ iterations with a thinning of 100, a true spatial model, an uncorrelated model of genetic frequencies, a value of 0.03° as coordinate uncertainty (equivalent to the largest distance travelled by *S. parvidens*; Fenton et al. 2000), and the presence of null alleles (in the case of microsatellites). We did a burn-in of $1x10^3$ and the run with the highest likelihood value was chosen based on the convergence of the results over 15 independent runs.

To validate the genetic structuring of microsatellite data, we used a discriminant analysis of principal components (DAPC, Jombart et al. 2010), implemented in the adegenet v2.1.1 (Jombart 2008) R package(R Core Team, 2016). The strength of this multivariate method lies in its independence from population genetic models and, therefore, inferences are based only on allelic similarity (Jombart et al. 2009). DAPC was developed to summarise the overall genetic variability

of individuals within groups while optimising discrimination between groups. The first 50 principal components (PC) from a principal components analysis were retained during the data transformation step, covering 88.53% of genetic variance.

We also used the Bayesian clustering software STRUCTURE v2.3.4 (Pritchard et al. 2000) to assess genetic structure of the microsatellite information. We evaluated the number of assumed clusters *K* from 1 to 10 using a burn-in of $1x10^5$ iterations followed by $9x10^5$ Markov Chain Monte Carlo iterations. The admixture model with correlated allele frequencies was run without sampling location information as a prior. Each *K* value was run 15 times to ensure stability and convergence of chains. We obtained the optimal number of clusters *K* from ΔK, based on the rate of change in the log probability of data in successive *K* values (Evanno et al. 2005) as performed in STRUCTURE HARVESTER (Earl & VonHoldt 2012).

Based on results from the multivariate and Bayesian analyses, we tested the population structure obtained from microsatellite loci with an analysis of molecular variance (AMOVA) in ARLEQUIN v3.5 (Excoffier et al. 1992, 2010) with $1x10^4$ permutations. Genetic subdivision among populations was also calculated in ARLEQUIN v3.5 using pairwise estimates of F_{ST}, where the significance of F_{ST} values was tested with $1x10^4$ permutations for each pairwise comparison.

Matrices of geographic and genetic distances by pairwise comparisons of populations were generated with GENALEX v6.503 and ARLEQUIN v3.5. The correlation between geographic and genetic distances for each genetic marker was evaluated by a Mantel test using 9,999 permutations with GENALEX. For the Mantel tests, $F_{ST} / (1-F_{ST})$ was used as the measure of population distance, following Rousset (1997).

Gene flow. In order to strengthen gene flow analyses, we used a coalescent analysis of the eight nuclear (*RAG1* gene and 7 microsatellites) and two mitochondrial (*cyt-b* and *D-loop* genes) unlinked loci to infer the history of geographic groups detected in previous analyses. The Isolation with Migration Analytical computer program (IMA2; Hey & Nielsen 2007) jointly estimates

demographic parameters to obtain posterior probability distributions from unlinked genes and for multiple populations (Hey 2010a, 2010b, 2011). We used IMa2 to estimate the migration rates (m), and the time of population splitting (t). These parameters offer the opportunity to capture the dynamics of a population during the early stages of differentiation (Hey 2005); it is therefore important that they are scaled to the per-locus mutation rate. To convert the parameter estimates into biologically informative values, we assumed an average generation time of 7.5 months, and substitution rates of *cyt-b* = 0.0147 s/s/Ma (95% CI [confidence interval]: 0.0106–0.0233); *D-loop* = 0.0434 s/s/Ma (95% CI: 0.0313–0.0685); and *RAG1* = 0.0060 s/s/Ma (95% CI: 0.0043–0.0094), reported in *S. parvidens* (Hernández-Canchola & León-Paniagua 2017). Time units of these biological values were transformed to years and the substitution rates were adjusted considering only the proportion of variable sites. Inherited scalars were defined depending on the mode of inheritance for each locus (nuclear = 1, mitochondrial = 0.25). Mutation models were defined considering the best fit of each locus to the available models (microsatellites = Stepwise – SSM, *genes* = Hasegawa-Kishino-Yano – HKY). Mutational rates, mutation models, and inherited scalars were provided in the IMa2 input file. To improve mixing of the Markov chains (to facilitate convergence), we ran multiple heated chains and monitored the autocorrelation and ESS (effective sample sizes) estimates. To verify the convergence of results, we ran the analysis twice using the same priors but different seeds in each one. The runs included $1x10^6$ generations, a burn-in of $6x10^5$, using 10 heated chains by the geometric heating model, and sampling every 50 generations. In addition, we used IMFIG (Hey 2010b) to visualize the phylogenetic history as a figure.

RESULTS

Sample size and tests of assumptions from microsatellites. We discarded 5 loci for different reasons. Two loci never amplified (Spar05 and Spar07). The presence of null alleles was detected for two loci in different populations (Spar011 and Spar013; Supplementary Figure S1). One more locus

(Spar040, trinucleotide) had an excess of homozygote individuals (more than 80%) and a limited range of allele variation (174-183, only four alleles).

Of the remaining 7 loci, three deviated from Hardy-Weinberg equilibrium in one or two populations out of 21, five showed very low levels of estimated null alleles, and only one population had a significant (≤ 0.05) *p*-value of I_A and $\bar{r}_d$ for the locus set (Supplementary Figures S2-S4). Deviation from Hardy–Weinberg expectation was due to heterozygote deficiency in one locus ($F = 0.247$ of Spar02 for JAB; Supplementary Table S1), and it was observed in only two more populations (SMS and OXT; Supplementary Figure S3), so it could be the result of factors other than selection on the markers. Thus, the genotypes of these 7 microsatellite loci were used for subsequent analyses of 134 *S. parvidens* individuals.

Genetic diversity. In microsatellites, a total of 155 alleles were observed with 10-54 alleles per locus (Table 1; Figure 2; Supplementary Table S1). The highest values of number of alleles (N_a = 11.143), effective number of alleles (n_e = 7.676), Shannon's information index (I = 2.127), and expected heterozygosity (H_e = 0.852 [0.764-0.930]) were found in JAB. The highest value of observed heterozygosity (H_o = 0.914 [0.800-1.000]) was found in CHI. In general, heterozygosity values for all populations were high. For 14 of the 21 populations, H_o values were higher than H_e, whereas for six populations (JAB, YER, TAM, VEP, YAX, and CRN) H_o values were smaller than H_e; in JAL the H_o and H_e values were equal (Table 1; Supplementary Table S1). For the population size of 6, the allelic richness found by rarefaction was the highest for TAM (R = 4.84), followed by VEP (R = 4.79) and CHI (R = 4.78). The private allelic richness was highest for HND (R_P = 0.71), followed by ISN (R_P = 0.57) and CHI (R_P = 0.45; Table 1; Figure 2; Supplementary Table S1).

In the mitochondrial and nuclear sequences, we found 115, 135, and 111 haplotypes in *cyt-b*, *D-loop*, and *RAG1*, respectively. The percentage of variable sites in *cyt-b* was 10.35%, in *D-loop* was 18.56%, and in RAG1 was 5.22%. In all loci and populations, we detected high levels of haplotype diversity (*Hd*) and low levels of nucleotide diversity (π; Table 2; Supplementary Tab S1).

Table 1. Allelic patterns of *Sturnira parvidens* throughout 21 populations of its geographic distribution. Sample size (*n*), number of different alleles (N_a), number of common alleles with a frequency ≥ 5% (*CA*), effective number of alleles (N_e), Shannon's information index (*I*), allelic richness (*n* = 6; *R*), private allelic richness (*n* = 6; R_P), observed heterozygosity (H_o), expected heterozygosity (H_e), and heterozygote deficit or excess (fixation index, *F*; Weir & Cockerham 1984). The highest value in each column is indicated by superscript a.

Population	*n*	N_a	*CA*	N_e	*I*	*R*	R_P	H_o	H_e	*F*
SMW	6	6.143	6.143	4.668	1.599	4.080	0.040	0.810	0.750	-0.066
NAY	4	4.429	4.429	3.370	1.299	3.750	0.020	0.750	0.670	-0.114
JNP	4	5.143	5.143	4.379	1.496	4.280	0.130	0.821	0.737	-0.110
JAL	7	7.286	7.286	5.561	1.684	4.150	0.060	0.735	0.735	-0.005
JAB	21	11.143[a]	6.143	7.676[a]	2.127[a]	4.470	0.270	0.776	0.852[a]	0.089
YER	7	7.286	7.286	5.813	1.820	4.450	0.240	0.776	0.812	0.047
MAG	9	7.857	7.857	5.314	1.743	4.080	0.080	0.825	0.757	-0.091
MBR	5	5.857	5.857	4.664	1.602	4.270	0.060	0.857	0.760	-0.122
BAL	9	8.571	8.571	6.178	1.898	4.380	0.150	0.825	0.810	-0.021
OXT	4	5.000	5.000	4.319	1.463	4.200	0.270	0.786	0.723	-0.094
SMS	7	6.571	6.571	5.222	1.725	4.260	0.190	0.816	0.794	-0.019
TAM	5	7.000	7.000	5.905	1.832	4.840[a]	0.420	0.800	0.817	0.023
SME	6	7.000	7.000	5.741	1.820	4.600	0.310	0.857	0.817	-0.050
VEP	8	9.286	9.286[a]	7.110	2.058	4.790	0.210	0.821	0.848	0.031
NIZ	5	5.714	5.714	4.761	1.596	4.240	0.360	0.829	0.766	-0.085
ISN	6	6.857	6.857	5.228	1.697	4.290	0.570	0.857	0.766	-0.107
CHI	5	6.857	6.857	6.003	1.810	4.780	0.450	0.914[a]	0.814	-0.130
YAX	4	5.000	5.000	4.396	1.516	4.290	0.320	0.714	0.759	0.050
PYU	3	4.714	4.714	4.329	1.495	4.710	0.030	0.810	0.762	-0.057
HND	5	6.571	6.571	5.578	1.745	4.610	0.710[a]	0.886	0.797	-0.114
CRN	4	4.857	4.857	4.131	1.488	4.190	0.210	0.750	0.754	0.006

Figure 2. Allelic patterns across populations in the geographic distribution of *Sturnira parvidens*. N_a is the number of different alleles; *CA* is the number of common alleles with a frequency ≥ 5%; N_e is the effective number of alleles; *I* is the Shannon's information index; *R* is the allelic richness (*n* = 6); R_P is the private allelic richness (*n* = 6); and H_e, which is depicted by the line, is the expected heterozygosity.

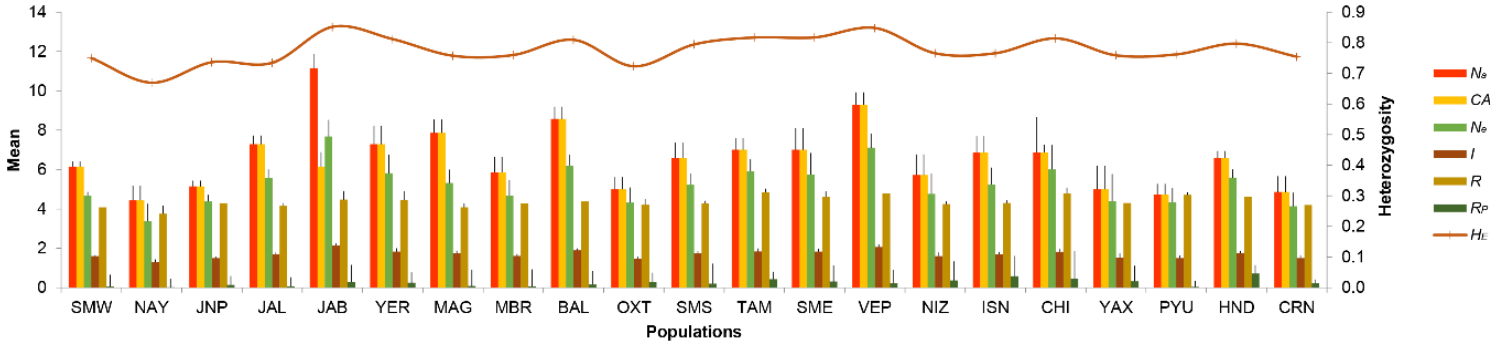

Table2. Genetic diversity obtained from 7 nuclear microsatellite loci and mtDNA and nuDNA sequences for *Sturnira parvidens*. Group (clusters obtained by GENELAND analysis), number of individuals genotyped (*n*), number of alleles (N_a), effective number of alleles (N_e), Shannon's information index (*I*), allelic richness (*n* = 6; *R*), private allelic richness (*n* = 6; R_P), observed heterozygosity (H_o), expected heterozygosity (H_e), and heterozygote deficit or excess (fixation index, *F*; Weir & Cockerham 1984) for microsatellite data. Bold numbers indicate the highest *F* values. Number of sequences per group (*n*), number of segregating sites (*S*), number of haplotypes (*h*), haplotype diversity (*Hd*) and their standard deviation [*Hd* (sd)], and nucleotide diversity (π) and their standard deviation [π (sd)] for mtDNA and nuDNA sequences.

		Nuclear Microsatellites									mtDNA and nuDNA sequences		
Group		**Spar01**	**Spar02**	**Spar08**	**Spar09**	**Spar010**	**Spar012**	**Spar030**	**Average**		***cyt-b*** (1140 bp)	***D-loop*** (388 bp)	***RAG1*** (1072 bp)
West-nu *n* = 83	N_a	40	24	9	13	15	9	12	17.429	*n*	91	91	166
	N_e	21.905	7.600	4.848	9.662	8.177	5.596	6.478	9.181	*S*	78	62	31
	I	3.344	2.517	1.777	2.381	2.320	1.894	2.092	2.332	*h*	59	68	46
	R	5.444	4.545	3.805	4.728	4.555	4.016	4.258	4.480	*Hd*	0.979	0.984	0.938
	R_P	4.647	3.036	1.865	3.044	2.832	2.035	2.345	2.830	*Hd* (sd)	0.007	0.007	0.009
	H_o	0.928	0.759	0.699	0.855	0.904	0.687	0.735	0.795	π	0.00848	0.02922	0.00342
	H_e	0.954	0.868	0.794	0.897	0.878	0.821	0.846	0.865	π (sd)	0.00038	0.00086	0.00020
	F	0.028	**0.126**	**0.120**	0.046	-0.030	**0.164**	**0.131**	0.083				
East-nu *n* = 51	N_a	46	27	9	16	15	14	12	19.857	*n*	81	82	156
	N_e	26.010	9.306	7.410	10.552	10.616	8.363	9.563	11.689	*S*	65	49	47
	I	3.536	2.768	2.062	2.522	2.484	2.311	2.336	2.574	*h*	56	68	73
	R	5.592	4.859	4.397	4.874	4.870	4.605	4.740	4.850	*Hd*	0.975	0.995	0.976
	R_P	4.794	3.350	2.457	3.189	3.147	2.623	2.827	3.200	*Hd* (sd)	0.009	0.003	0.005
	H_o	0.922	0.804	0.882	0.843	0.882	0.627	0.843	0.829	π	0.00309	0.1630	0.00581
	H_e	0.962	0.893	0.865	0.905	0.906	0.880	0.895	0.901	π (sd)	0.00023	0.00083	0.00016
	F	0.042	0.099	-0.020	0.069	0.026	**0.287**	0.058	0.080				
Total *n* = 134	N_a	54	31	10	17	17	14	12	22.143	*n*	172	173	322
	N_e	27.991	8.763	6.429	11.339	10.028	7.243	8.313	11.444	*S*	118	72	56
	I	3.580	2.727	2.010	2.545	2.486	2.162	2.268	2.540	*h*	115	135	111
	R	5.544	4.707	4.202	4.876	4.765	4.354	4.541	4.710	*Hd*	0.989	0.995	0.976
	H_o	0.925	0.776	0.769	0.851	0.896	0.664	0.776	0.808	*Hd* (sd)	0.003	0.002	0.003
	H_e	0.964	0.886	0.844	0.912	0.900	0.862	0.880	0.893	π	0.00836	0.02811	0.00496
	F	0.040	0.124	0.090	0.067	0.005	**0.229**	0.118	0.096	π (sd)	0.00026	0.00076	0.00013

Genetic differentiation analyses defined two main groups (West-nu and East-nu) (see below). The highest number of alleles (N_a = 19.857) and effective number of alleles (N_e = 11.689) were found in East-nu. H_o values were 0.795 (0.687-0.928) for West-nu and 0.829 (0.627-0.922) for East-nu. H_e values were higher than H_o in both groups (H_e = 0.865 [0.794-0.954] and 0.901 [0.865-0.962], in West-nu and East-nu respectively; Table 2).

For the genes, we found in West-nu and East-nu respectively: 59 and 56 haplotypes in *cyt-b*, 68 and 68 in *D-loop*, and 46 and 73 in the nuclear *RAG1* (Table 2). The percentages of variable sites, in West-nu and East-nu respectively, were: 6.84% and 5.70% in *cyt-b*, 15.98% and 12.63% in *D-loop*, and 2.89% and 4.38% in *RAG1*. In all loci and both groups, we detected high levels of haplotype diversity (*Hd*) and low levels of nucleotide diversity (π; Table 2).

Genetic Structure. The mitochondrial networks recovered the West and East haplogroups previously reported by Hernández-Canchola & León-Paniagua (2017). These mitochondrial haplotype networks coloured with the mitochondrial genetic structure results, showed well-defined West and East groups for both *cyt-b* (88 haplotypes in total: 44 for West, and 44 for East; Figure 3A) and *D-loop* (107 haplotypes in total: 54 for West, and 53 for East; Figure 3B). The mitochondrial haplotype networks coloured with the nuclear genetic structure results obtained by GENELAND (see below; Figures 3C and 3D) showed almost no mixing between the West-nu and East-nu groups, with few West-nu haplotypes scattered among East-nu haplotypes and few shared haplotypes, for both *cyt-b* (52 haplotypes for West-nu, 35 for East-nu, and 1 shared haplotype; Figure 3C) and *D-loop* (61 haplotypes for West-nu, 45 for East-nu, and 1 shared haplotype; Figure 3D). Additionally, the mitochondrial networks coloured with the genetic structure information obtained by STRUCTURE (see below; Figure 5A and 5B) showed less definition between the West-nu and East-nu groups, with more haplotypes shared between both groups.

Figure 3. Haplotype networks for two mitochondrial loci in *Sturnira parvidens*: *cyt-b* (A) and *D-loop* (B). (A) and (B) are coloured according to West (orange) and East (yellow) groups (Hernández-Canchola & León-Paniagua 2017). (C) and (D) are coloured according to West-nu (orange) and East-nu (yellow) groups detected by GENELAND. Each haplotype is represented by a circle. Relative sizes of the circles indicate haplotype frequency, and the length of the branches is proportional to the number of mutations.

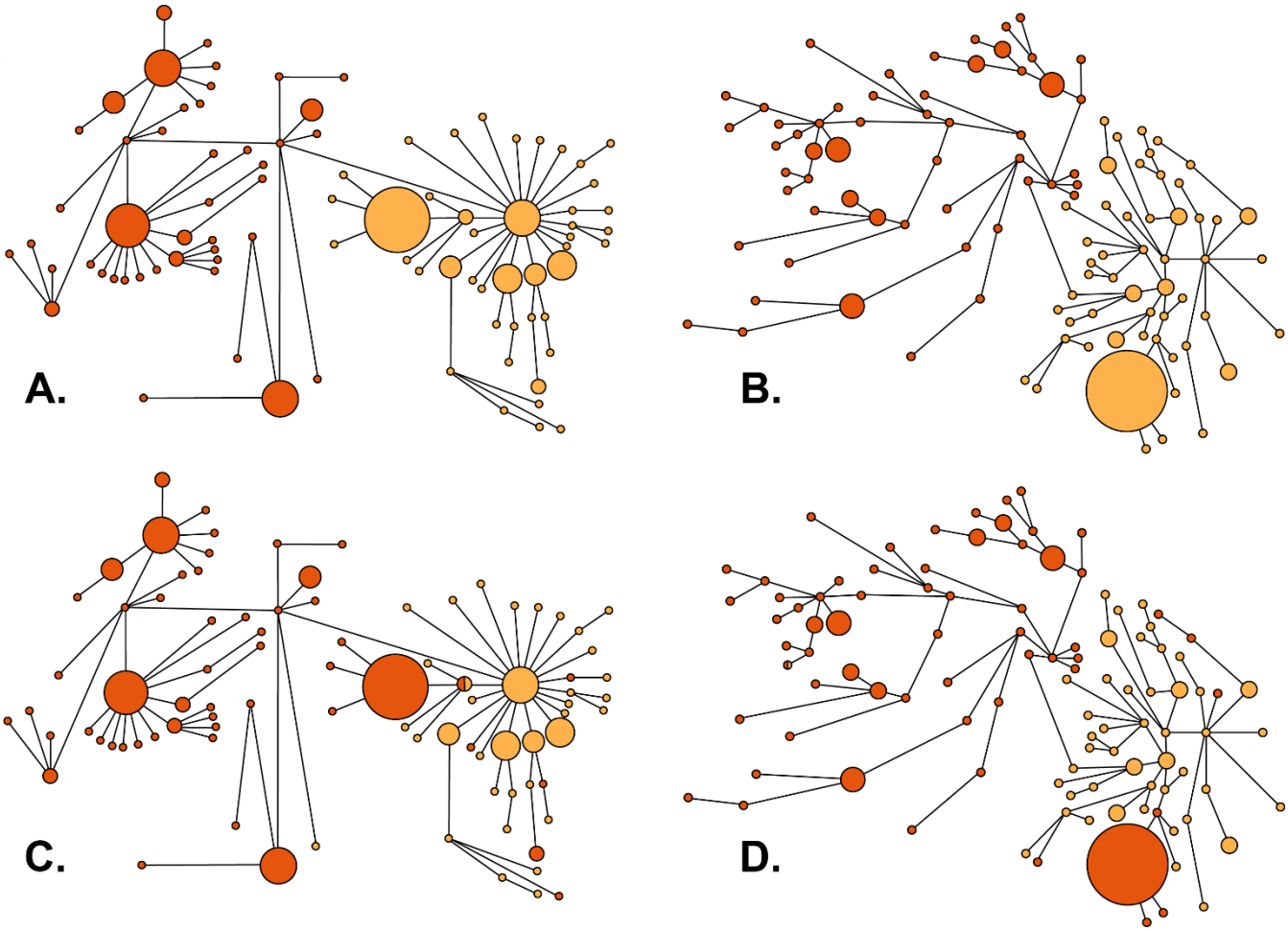

Table 3. AMOVA on microsatellite loci, and general *F*-statistics. All *p*-values of *F*-statistics were significant at the 0.01 level ($p \leq 0.01$).

Source of variation	Percent variation	F-statistics
Among groups	2.05062	F_{CT} = 0.02051
Among populations within groups	3.57435	F_{SC} = 0.03649
Within populations	94.37503	F_{ST} = 0.05625

Figure 4. Genetic and geographic structure in *Sturnira parvidens* using Bayesian posterior probabilities of assignment obtained by GENELAND for *cyt-b* (A), *D-loop* (B), *RAG1* (C), and microsatellite loci (D). The maps show the distribution of each genetic group: the orange colour shows West (A, B) or West-nu (C, D) groups, and yellow colour shows East (A, B) or East-nu (C, D) groups; the bar size is proportional to the number of samples per locality. An assignment probability >50% determined the colour (orange or yellow) of each individual on the map. Light grey shaded area represents the geographical range of West (A, B) or West-nu (C, D) groups, and dark grey shaded area represents the geographical range of East (A, B) or East-nu (C, D) groups. Bar plots of assignment probabilities are at the bottom left of each box; each vertical line represents an individual, and the populations are ordered from left to right according to their geographic location from north to south. The population to which individuals with a mixed membership belongs is indicated below each bar plot.

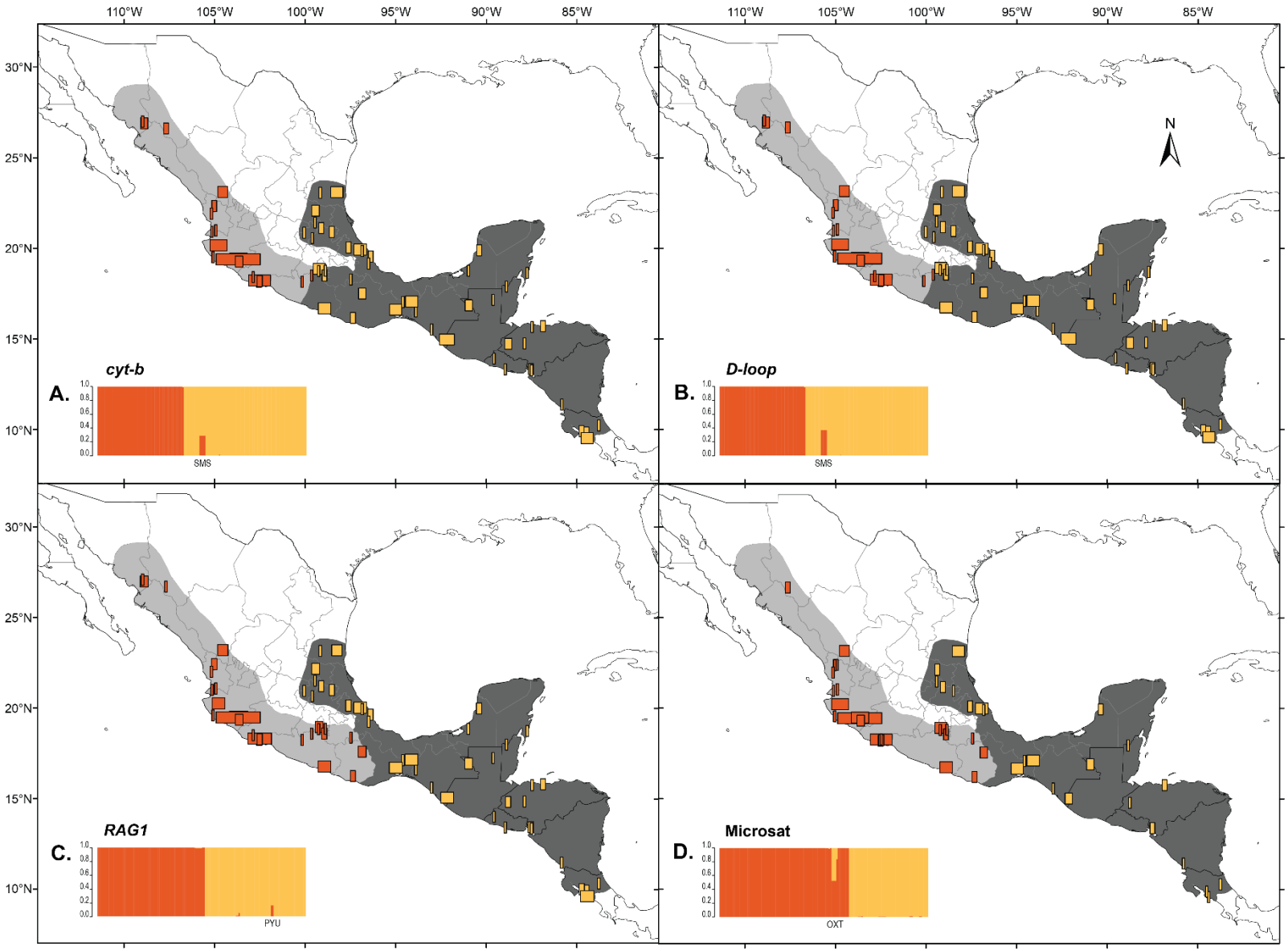

Figure 5. Genetic structure in *Sturnira parvidens* using Bayesian posterior probabilities of membership obtained by STRUCTURE for microsatellite loci. Bars on the map show the probabilities of membership of each analysed individual to the West-nu group in orange, and to the East-nu group in yellow. Light grey and dark grey shaded areas indicate the geographical ranges of the West-nu and East-nu groups, respectively. Haplotype networks show the mitochondrial topology [*cyt-b* (A), and *D-loop* (B)] but they are coloured according to STRUCTURE results. Each haplotype is represented by a circle. Relative sizes of the circles indicate haplotype frequency, and the length of the branches is proportional to the number of mutations.

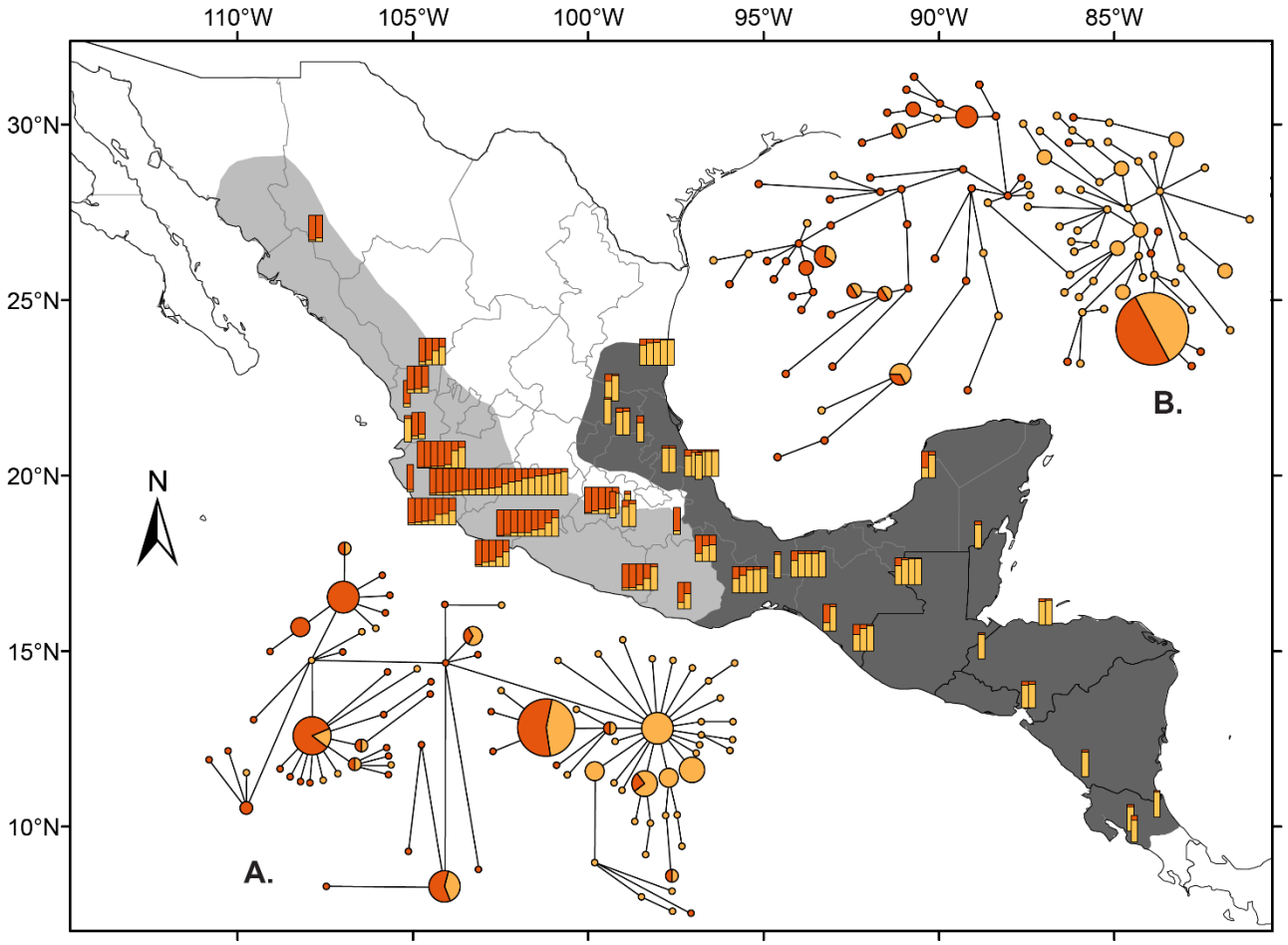

GENELAND Bayesian analysis indicated two well-structured genetic lineages for both mitochondrial and nuclear markers (Figure 4). For *cyt-b* and *D-loop*, the groups obtained correspond with those found previously by Hernández-Canchola & León-Paniagua (2017; West: SMW, NAY, JNP, JAL, JAB, YER, MAG, and MBR; and East: CRN, HND, PYU, YAX, CHI, ISN, NIZ, SMS, OXT, BAL, VEP, SME, and TAM). In contrast, for the *RAG1* and microsatellite loci, two new groups were obtained, which corresponded to the groups found with STRUCTURE (West-nu: SMW, NAY, JNP, JAL, JAB, YER, MAG, MBR, OXT, BAL, and SMS; and East-nu:

CRN, HND, PYU, YAX, CHI, ISN, NIZ, VEP, SME, and TAM). The values of probability assignment were high, but the geographic boundaries between groups for each kind of marker were located in different geographic areas (Figures 1 and 4). For mitochondrial loci, the boundary between the groups was shown in the northern Sierra Madre del Sur mountain range, particularly in the Balsas River Basin (Figure 4A-B). For nuclear markers, it was around the dry lowland region of the Tehuacán-Cuicatlán and Oaxacan Central Valleys, in the southern Sierra Madre del Sur mountain range, on the Pacific Slope of Mexico (Figure 4C-D).

The discrimination between populations using DAPC was low to moderate, with an average of 41.5% in the assignment per population percentage. The first two PC's included 35.08% of the variance. PC-1 shows the trend of separating western and eastern populations from geographic distribution, but some overlaps can be observed (Supplementary Figure S5).

The STRUCTURE v2.3.4 Bayesian assignment identified two groups based on Pr (K=2) and the largest mean value of log-likelihood observed for K = 2 (Ln[X | K=2] = -4836.540 vs. Ln[X | K=1] = -4865.493, Ln[X | K=3] = -4930.500, Ln[X | K=4] = -5661.046, Ln[X | K=5] = -5435.540). Evanno et al.'s (2005) approach also indicated two groups, with $\Delta K(2)$ much larger than all other ΔK-values (Figure 5).

In AMOVA, however, the division into two groups was not evident using microsatellite loci (Table 3). The percent variation was higher within populations (94.37%) than between groups (i.e., West-nu vs. East-nu, 2.051%; Table 3).

Relatively low levels of genetic differentiation between populations of *S. parvidens* were observed by F_{ST} pairwise estimates (Figure 6; Supplementary Figure S6; Supplementary Tables S2-S3). The average value of the F_{ST} comparisons between populations that constitute the West-nu group was 0.042, and between populations that belong to the East-nu group was 0.032. The average value of the F_{ST} comparisons between populations from different groups was 0.059. The overall F_{ST} was 0.05625 (Table 3).

Figure 6. Pairwise F_{ST} values for 21 populations in the geographic distribution of *Sturnira parvidens*. The populations are ordered from top to bottom and from left to right according to their geographic location from south to north. The significance for these F_{ST} comparisons can be found in Supplementary Figure S6 and Supplementary Table S3.

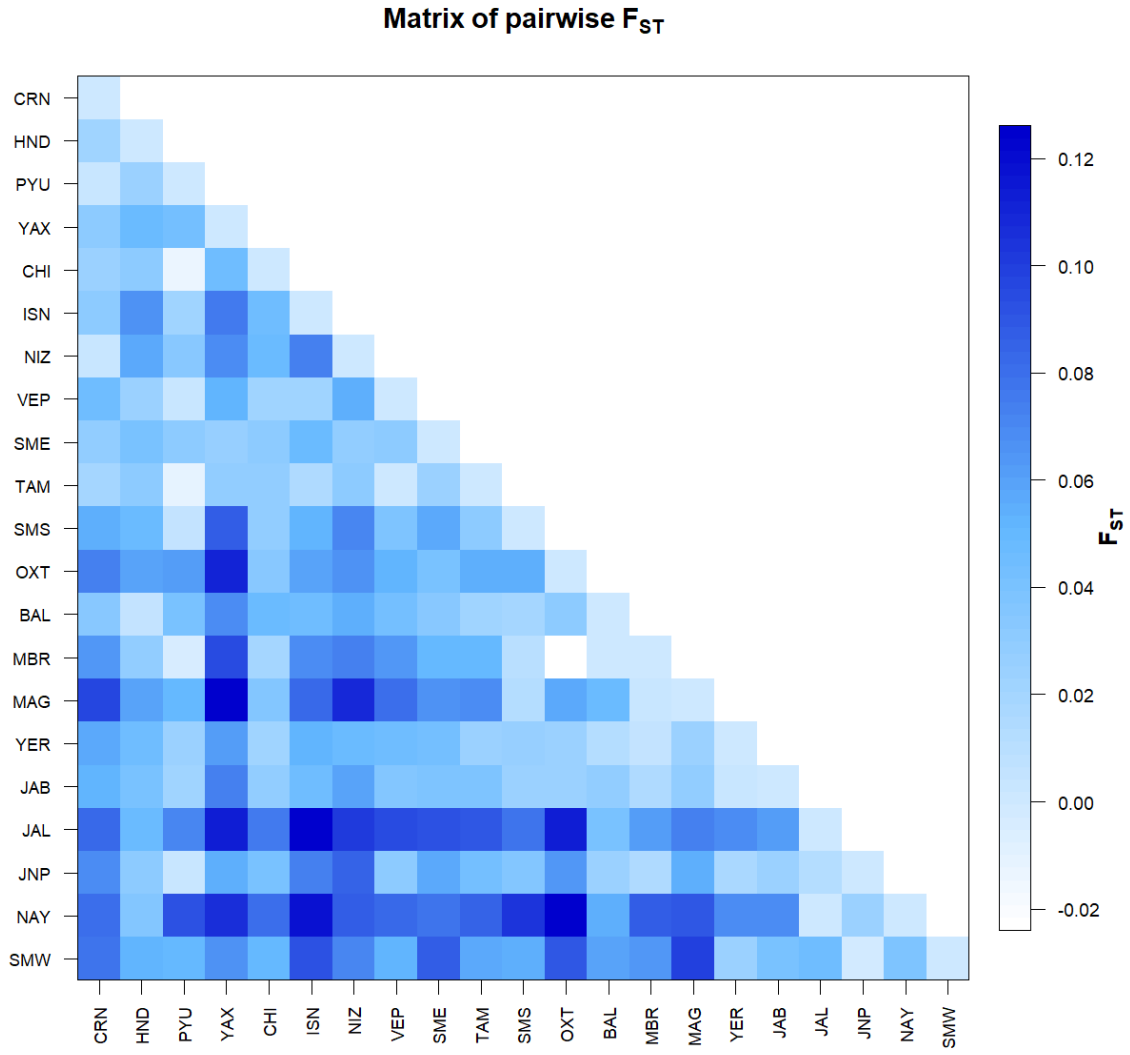

In Mantel tests, all R^2 values were low, but all *p*-values were significant, indicating correlation between the geographic and genetic distances for all molecular markers: *cyt-b* (R^2= 0.1781, *P*= 0.001), *D-loop* (R^2= 0.1515, *P*= 0.001), *RAG1* (R^2= 0.1458, *P*= 0.001), microsatellite loci (R^2= 0.0555, *P*= 0.028). Thus, Mantel tests indicated an isolation by distance pattern among the populations of *S. parvidens*, being more evident and with higher values of $F_{ST} / (1-F_{ST})$ for mitochondrial loci than nuclear loci (Supplementary Figure S7).

Gene flow. The IMA2 analysis showed that the West-nu group of *S. parvidens* diverged from the East-nu group *c.* 172,740 years ago (95% HPD [highest posterior density interval]: 240,225 – 135,809 years). We detected recent migration in both directions: from the West-nu to East-nu group at a rate of 6.847 (95% HPD: 4.581 – 8.602) migrants per generation, and from the East-nu to West-nu at a rate of 4.961 (95% HPD: 4.074 – 6.113) migrants per generation. These two rates were not statistically different.

DISCUSSION

Genetic studies based on more than one type of molecular marker have shown that by combining the genetic information of both nuDNA and mtDNA it is possible to recover accurate inferences, with more reliable and complete evidence about the evolutionary history of taxa than when a single marker type is used (Castellanos-Morales et al. 2014, Chen et al. 2010, Martins et al. 2009). Here, we recovered the clear mitochondrial haplogroups previously reported (Hernández-Canchola & León-Paniagua 2017), but we detected a less evident genetic structure based on nuclear loci, and a pattern of biogeographic mito-nuclear discordance between *S. parvidens* groups. Furthermore, our results support the idea that females are philopatric, and that a male-biased dispersal pattern is responsible for long-distance gene flow in this species.

Genetic variation within *S. parvidens*

Levels of genetic variation for both microsatellite and sequence markers in *S. parvidens* (Tables 1 and 2; Figure 2; Supplementary Table S1) were high and within the range reported for other tropical bat species (for mtDNA: *Hd*= 0.86-1.0 and π= 0.0073-0.027, Meyer et al. 2009, Ruiz et al. 2013, Ripperger et al. 2013, Ripperger et al. 2014, Llaven-Macías et al. 2017, Cruz-Salazar et al. 2018; for nuclear microsatellite loci: H_o= 0.78-0.89 and H_e= 0.78-0.87, Chen et al. 2010, Korstian et al. 2015).

Since genetic variation is basically the result of effective population size and mutation (Hedrick 2011), the Pleistocene interglacial periods, with their associated demographic expansions and contractions of vegetation and *S. parvidens* populations (Hernández-Canchola & León-Paniagua 2017) likely played a crucial role in the effective population sizes and genetic diversity of *S. parvidens* over time. We also recovered higher values of genetic diversity in *S. parvidens* East-nu (H_e= 0.901 for nuclear microsatellite loci, *Hd*= 0.976 for nuDNA, *Hd*= 0.985 for mtDNA; Table 2) than West-nu (H_e= 0.865 for nuclear microsatellite loci, *Hd*= 0.938 for nuDNA, *Hd*= 0.982 for mtDNA; Table 2), which is consistent with a stronger demographic expansion in the eastern than the western populations (Hernández-Canchola & León-Paniagua 2017).

The high genetic variability in *S. parvidens* could also be influenced by ecological traits, such as its mating system, social structure, and dispersal patterns. For example, several studies support the idea that bats of the genus *Sturnira* have a great ability to colonize new areas and environmental spaces, but due to their small dispersal renges they form well-structured genetic groups after geographic isolation (Iudica 2000, Hernández-Canchola & León-Paniagua 2017, Velazco & Patterson 2013).

Tracking the history of contemporary mito-nuclear discordance

Our genetic structure analyses of *S. parvidens* across Mexico and Central America revealed strong and significant population genetic structure based on mitochondrial loci (*cyt-b* and *D-loop*), recovering two well-defined groups (West and East; Figures 3 and 4), as previously reported by Hernández-Canchola & León-Paniagua (2017). We also obtained some population genetic structure based on nuclear loci (microsatellites and *RAG1*), recovering two different groups (West-nu and East-nu; Figures 3 and 4). The time of the split between the West-nu and East-nu groups found by incorporating the microsatellite data in coalescent analysis (*c.* 172,740 years ago [95% HPD: 240,225 – 135,809]) was consistent with the termination of the glacial MIS-8 *c*. 0.243 Ma (Lisiecki & Raymo 2005), one of the most intense cycles of the Middle Pleistocene (EPICA Community

Members 2004). The splitting time obtained by Hernández-Canchola & León-Paniagua (2017; *c.* 0.423Ma [95% CI: 0.586–0.268]) did not match the one we found exactly, though it was also during the Middle Pleistocene. These time variations could be related to methodological differences, as Hernández-Canchola & León-Paniagua (2017) used a Bayesian approach, and we used a coalescent approximation. Also, the rapid mutation rate of microsatellites may have reduced the estimated divergence time, as has been previously reported (Harrison et al. 2003, Martins et al. 2009, Castellanos-Morales et al. 2016). However, the divergence time we obtained agrees with the time of demographic expansions experienced by this bat species according to Hernández-Canchola & León-Paniagua (2017), which could indicate that population expansion and differentiation could have occurred simultaneously. Given the body of evidence, we conclude that the differentiation between western and eastern populations of *S. parvidens* occurred during the period of intense glacial-interglacial cycles of the Middle Pleistocene.

There also was a discrepancy in the geographic limits between the West-East and West-nu–East-nu groups when comparing the mtDNA and nuDNA ranges of each group (Figure 4), evidence of biogeographic mito-nuclear discordance in *S. parvidens*, as has been reported in other bats (Castella et al. 2001, Martins et al. 2009, Naidoo et al. 2016).

One of the most common explanations for this pattern is the isolation of taxa for long periods of time in the past, followed by secondary contact in the present (Toews & Brelsford 2012). This hypothesis has been reported in many studies on mammals (Roca et al. 2005, Berthier et al. 2006, Bryja et al. 2010, Hulva et al. 2010, Cabria et al. 2011). During the isolation period, the divergent groups accumulated mutations in both nuDNA and mtDNA, which increased in frequency due to selection, genetic drift or a combination of the two; then, during secondary contact, these groups formed hybrid zones and interbred, giving rise to mito-nuclear discordance due to divergent patterns of gene flow between the two genomes (Toews & Brelsford 2012). In *S. parvidens*, the isolation periods may correspond to strong glacial cycles that promoted their genetic differentiation,

and we may be currently documenting a posterior contact between the two lineages in the absence of geographic barriers (Hernández-Canchola & León-Paniagua 2017).

In most previous studies, it has been suggested that the geographic discordance does not extend far beyond the current area of taxa sympatry, and foreign DNA does not usually extend beyond 50% of the range of the native taxon (Ruegg 2008, Gligor et al. 2009, Bryson et al. 2010, Ng & Glor 2011).

Our results show that the geographic limit between the nuDNA groups (West-nu and East-nu) is situated in the dry lowland region of Tehuacán-Cuicatlán and Oaxacan Central Valleys (OXT and SMS populations; Figures 1 and 4), while the boundary between mtDNA groups is located in the western Balsas River Basin (BAL population; Figures 1 and 4). It seems that the nuDNA of the western lineage (foreign DNA) is within the range of the eastern lineage (native taxon) in the Mexican states of Morelos, Guerrero, southern Puebla, and eastern Oaxaca (Figures 1 and 4), demonstrating the geographic extent of discordance. Also, we can observe that this overlapping area is <50% of the range of eastern lineage, which corresponds with the pattern reported in the aforementioned studies.

In summary, we can infer that although the genetic lineages of *S. parvidens* may have completely separated and formed two well-structured genetic groups during the climatic oscillations of the second half of the Pleistocene, they likely came back into contact more recently, generating the pattern of biogeographic discordance between the mtDNA and nuDNA that we observe today.

Current patterns of dispersion and gene flow that influence genetic structure

We detected migrants between the two groups in both directions ($m_{West\text{-}nu \rightarrow East\text{-}nu} = 6.9$, and $m_{East\text{-}nu \rightarrow West\text{-}nu} = 5.0$ per generation). Wright (1969) mentioned that a migration rate > 1 per generation is usually enough to inhibit any genetic differentiation due to genetic drift; however, the migration rates we detected were not statistically different and more studies are necessary. On the other hand, the low F_{ST} value (0.056; Table 3), the pairwise estimates of F_{ST} (Figure 6; Supplementary Figure

S6; Supplementary Tables S2-S3), and the lower percentage of variation among groups (2.051%; Table 3) detected in microsatellite data suggest a nearly panmictic pattern of genetic variation in *S. parvidens*. However, using mtDNA, Hernández-Canchola & León-Paniagua (2017) found a contrasting and strong mitochondrial genetic structure (*cyt-b*: Φ_{ST}= 0.586, and 58.64% of variation among groups; *D-loop*: Φ_{ST}= 0.406, and 40.64% of variation among groups). Differences in the genetic structuration between nuclear and mitochondrial loci are consistent with those reported in several bat species (Kerth et al. 2002, Ruedi & Castella 2003, Chen et al. 2008, Piaggio et al. 2009), in which the F_{ST} values among groups were very low, but Φ_{ST} values varied considerably from one species to another and were always higher than F_{ST}, suggesting that sex-biased asymmetries are responsible for these differences. Thus, we consider that the low values of F_{ST} and relatively high values of Φ_{ST} in *S. parvidens* are related to the dispersal and mating system of this species.

For other *Sturnira* species, Pacheco & Patterson (1992) assumed philopatry in *S. erythromos*, and Saldaña-Vázquez et al. (2013) indicated female philopatry in *S. hondurensis*: females have a preference for forest sites with high availability of food resources due to their increased metabolic costs associated with pregnancy and lactation, whereas males disperse to other areas to avoid competition for resources with females. It is possible that similar patterns of female philopatry and male-biased dispersal, that homogenize the genetic variability among populations, are also be present in *S. parvidens*, as has been also reported for other bat species (Chen et al. 2008, Kerth & Van Schaik 2012, Gürün et al. 2019).

On the other hand, the isolation by distance patterns we detected (Supplementary Figure S7) could be the consequence of ecological attributes of *S. parvidens*: the wing morphology of *S. parvidens* and the relatively short travel distances reported for individuals of this species (García-García et al. 2014, Fleming et al. 1972, Estrada et al. 1993), have been interpreted as indicators that this species is incapable of long-distance movements. Besides, it has been reported that this species is roost-faithful (Evelyn & Stiles 2003), mainly using day roosts in standing tree cavities and

roosting alone or in small groups in the wild (1-3 or more individuals of *S. parvidens* in few cases; Fenton et al. 2000; Hernández-Canchola & León-Paniagua *in press*).

In summary, our findings support that *S. parvidens* females are philopatric and contribute little to large-geographic scale gene flow. Because divergent patterns of gene flow between the mtDNA and nuDNA can promote mito-nuclear discordance (Toews & Brelsford 2012), we hypothesize that males, although they do not migrate or perform large geographic movements, have a greater dispersal capacity than females. Furthermore, the status of *S. parvidens* as a relatively common and locally abundant species suggests that even relatively small movements by males (represented in this work by nuclear loci) could maintain the connections between populations by gene flow throughout their geographical distribution, as has been reported in other Neotropical fruit bats (Morrison 1979, Morrison & Hagen-Morrison 1981, Brooke 1990, Altringham 2011).

Finally, we consider that future works should concentrate their study efforts on the individuals of the Balsas River Basin and the Valley of Tehuacán-Cuicatlán and Central Valleys of Oaxaca, using different approaches (such as other molecular genetic tools, like Y chromosome markers; geometric morphometric; and ecological and behavioural observations) with the aim of obtaining additional evidence of their current and historical population dynamics.

Funding

Consejo Nacional de Ciencia y Tecnología and Universidad Nacional Autónoma de México (Master fellowship 778388 to M.Y.C.G); Consejo Nacional de Ciencia y Tecnología (239482 to L.L.P.; postdoctoral fellowship 549963 to G.H.C.); U.S. National Science Foundation (NSF DEB-1754393 and DEB-1441634 to G.H.C.).

Acknowledgements

This paper constitutes the master's degree research of M.Y.C.G., who thanks the graduate program Maestría en Ciencias Biológicas, UNAM. Thanks to Gabriela Castellanos, Edgar Gutiérrez, and

Susette Castañeda for early advice, support, comments and critiques. Thanks to Celia López, Diego García, Frederick H. Sheldon, Donna L. Dittmann, Mark Hafner, Jesús Fernández, Francisco Durán, Robert Baker, Cibele Sotero, Burton Lim, and Jaqueline Miller, for providing samples; and to all the people who collected the samples in each scientific collection. Thanks to the Laboratorio de Evolución Molecular y Experimental, Instituto de Ecología, UNAM, in particular the technicians, Erika Aguirre-Planter and Laura Espinosa Asuar, for their help in the initial lab work. Our special thanks to the whole great team of Mastozoología of Museo de Zoología "Alfonso L. Herrera", Facultad de Ciencias, UNAM, for their assistance, guidance and support throughout this project. We especially thank H. Dawn Marshall and her students Alexander Flynn and Thaneah Alanazi for the help and advice provided in a research visit made by M.Y.C.G to the Memorial University of Newfoundland, St. John's, Canada.

Data Availability

The primary data underlying these analyses is deposited in Dryad. Primary data includes sampling locations and microsatellite genotypes.

References

Altringham, J. D. (2011). *Bats: From Evolution to Conservation* (2nd ed.). New York: Oxford University Press.

Arif, I. A., Khan, H. A., Shobrak, M., Al Homaidan, A. A., Al Sadoon, M., Al Farhan, A. H., & Bahkali, A. H. (2010). Interpretation of electrophoretograms of seven microsatellite loci to determine the genetic diversity of the Arabian Oryx. *Genetics and Molecular Research*, *9*(1), 259–265. https://doi.org/10.4238/vol9-1gmr714

Avise, J. C. (2004). *Molecular Markers, Natural History and Evolution* (2nd ed.). Sunderland, Massachusetts: Sinauer Associates, Inc. Publishers.

Berthier, P., Excoffier, L., & Ruedi, M. (2006). Recurrent replacement of mtDNA and cryptic hybridization between two sibling bat species *Myotis myotis* and *Myotis blythii*. *Proceedings of the Royal Society B: Biological Sciences*, *273*(1605), 3101–3109. https://doi.org/10.1098/rspb.2006.3680

Bilgin, R., Çoraman, E., Karataş, A., & Morales, J. C. (2009). Phylogeography of the Greater Horseshoe Bat, *Rhinolophus ferrumequinum* (Chiroptera: Rhinolophidae), in Southeastern Europe and Anatolia, with a Specific Focus on Whether the Sea of Marmara is a Barrier to Gene Flow . *Acta Chiropterologica*, *11*(1), 53–60. https://doi.org/10.3161/150811009x465686

Brooke, A. P. (1990). Tent selection, roosting ecology and social organization of the tent-making bat, *Ectophylla alba*, in Costa Rica. *Journal of Zoology*, *221*(1), 11–19. https://doi.org/10.1111/j.1469-7998.1990.tb03771.x

Brown, A. H., Feldman, M. W., & Nevo, E. (1980). Multilocus structure of natural populations of *Hordeum spontaneum*. *Genetics*, *96*(2), 523–536.

Bryja, J., Granjon, L., Dobigny, G., Patzenhauerová, H., Konečný, A., Duplantier, J. M., … Nicolas, V. (2010). Plio-Pleistocene history of West African Sudanian savanna and the phylogeography of the *Praomys daltoni* complex (Rodentia): The environment/geography/genetic interplay. *Molecular Ecology*, *19*(21), 4783–4799. https://doi.org/10.1111/j.1365-294X.2010.04847.x

Bryja, Josef, Kaňuch, P., Fornůsková, A., Bartonička, T., & Řehák, Z. (2009). Low population genetic structuring of two cryptic bat species suggests their migratory behaviour in continental Europe. *Biological Journal of the Linnean Society*, *96*(1), 103–114. https://doi.org/10.1111/j.1095-8312.2008.01093.x

Bryson, R. W., Nieto-Montes de Oca, A., Jaeger, J. R., & Riddle, B. R. (2010). Elucidation of cryptic diversity in a widespread nearctic treefrog reveals episodes of mitochondrial gene capture as frogs diversified across a dynamic landscape. *Evolution*, *64*(8), 2315–2330. https://doi.org/10.1111/j.1558-5646.2010.01014.x

Cabria, M. T., Michaux, J. R., Gómez-Moliner, B. J., Skumatov, D., Maran, T., Fournier, P., … Zardoya, R. (2011). Bayesian analysis of hybridization and introgression between the endangered european mink (*Mustela lutreola*) and the polecat (*Mustela putorius*). *Molecular Ecology*, *20*(6), 1176–1190. https://doi.org/10.1111/j.1365-294X.2010.04988.x

Castañeda-Rico, S., León-Paniagua, L., Ruedas, L. A., & Vázquez-Domínguez, E. (2011). High genetic diversity and extreme differentiation in the two remaining populations of *Habromys simulatus*. *Journal of Mammalogy*, *92*(5), 963–973. https://doi.org/10.1644/10-mamm-a-171.1

Castella, V., Ruedi, M., & Excoffier, L. (2001). Contrasted patterns of mitochondrial and nuclear structure among nursery colonies of the bat *Myotis myotis*. *Journal of Evolutionary Biology*, *14*(5), 708–720. https://doi.org/10.1046/j.1420-9101.2001.00331.x

Castellanos-Morales, G., Gámez, N., Castillo-Gámez, R. A., & Eguiarte, L. E. (2016). Peripatric speciation of an endemic species driven by Pleistocene climate change: The case of the Mexican prairie dog (*Cynomys mexicanus*). *Molecular Phylogenetics and Evolution*, *94*, 171–181. https://doi.org/10.1016/j.ympev.2015.08.027

Castellanos-Morales, G., Gasca-Pineda, J., Ceballos, G., & Ortega, J. (2014). Genetic variation in a peripheral and declining population of black-tailed prairie dogs (*Cynomys ludovicianus*) from Mexico. *Journal of Mammalogy*, *95*(3), 467–479. https://doi.org/10.1644/12-mamm-a-099

Castellanos-Morales, G., Ortega, J., Castillo-Gámez, R. A., Sackett, L. C., & Eguiarte, L. E. (2015). Genetic Variation and Structure in Contrasting Geographic Distributions: Widespread Versus Restricted Black-Tailed Prairie Dogs (Subgenus *Cynomys*). *Journal of Heredity*, *106*(S1), 478–490. https://doi.org/10.1093/jhered/esv021

Cegelski, C. C., Waits, L. P., & Anderson, N. J. (2003). Assessing population structure and gene flow in Montana wolverines (*Gulo gulo*) using assignment-based approaches. *Molecular Ecology*, *12*(11), 2907–2918. https://doi.org/10.1046/j.1365-294X.2003.01969.x

Chen, J., Rossiter, S. J., Flanders, J. R., Sun, Y., Hua, P., Miller-Butterworth, C., … Zhang, S. (2010). Contrasting genetic structure in two co-distributed species of Old World fruit bat. *PLoS ONE*, *5*(11), e13903. https://doi.org/10.1371/journal.pone.0013903

Chen, S. F., Jones, G., & Rossiter, S. J. (2008). Sex-biased gene flow and colonization in the Formosan lesser horseshoe bat: Inference from nuclear and mitochondrial markers. *Journal of Zoology*, *274*(3), 207–215. https://doi.org/10.1111/j.1469-7998.2007.00391.x

Contreras Vega, M., & Cadena, A. (2000). Una nueva especie del género *Sturnira* (Chiroptera: Phyllostomidae) de los Andes colombianos. *Revista de La Academia Colombiana de Ciencias Exactas, Físicas y Naturales*, *24*(91), 285–287.

Cruz-Salazar, B., Ruiz-Montoya, L., Mendoza-Sáenz, V. H., Riechers-Pérez, A., & García-Bautista, M. (2018). Genetic diversity of tropical bats and its relationship with ecological role in a tropical semievergreen rain forest in El Ocote Biosphere Reserve, Chiapas, Mexico. *Tropical Conservation Science*, *11*, 1–21. https://doi.org/10.1177/1940082917752473

Currat, M., Ruedi, M., Petit, R. J., & Excoffier, L. (2008). The hidden side of invasions: massive introgression by local genes. *Evolution*, *62*(8), 1908–1920. https://doi.org/10.1111/j.1558-5646.2008.00413.x

Earl, D. A., & VonHoldt, B. M. (2012). STRUCTURE HARVESTER: A website and program for visualizing STRUCTURE output and implementing the Evanno method. *Conservation Genetics Resources*, *4*(2), 359–361. https://doi.org/10.1007/s12686-011-9548-7

Eguiarte, L. E., Aguirre-Liguori, J. A., Jardón-Barbolla, L., Aguirre-Planter, E., & Souza, V. (2013). Genómica de poblaciones: Nada en evolución va a tener sentido si no es a la luz de la genómica, y nada en genómica tendrá sentido si no es a la luz de la evolución. *TIP Revista Especializada En Ciencias Químico-Biológicas*, *16*(1), 42–56. https://doi.org/10.1016/s1405-888x(13)72077-1

Eizirik, E., Kim, J.-H., Menotti-Raymond, M., Crawshaw Jr., P. G., O´Brien, S. J., & Johnson, W. E. (2001). Phylogeography, population history and conservation genetics of jaguars (*Panthera onca*, Mammalia, Felidae). *Molecular Ecology*, *10*, 65–79.

Endler, J. A. (1977). *Geographic Variation, Speciation, and Clines*. Princeton, NJ: Princeton University Press.

EPICA, C. M. (2004). Eight glacial cycles from an Antarctic ice core. *Nature*, *429*, 623–628. https://doi.org/10.1038/nature02599

Estrada, A., Coates-Estrada, R., & Meritt, D. (1993). Bat species richness and abundance in tropical rain forest fragments and in agricultural habitats at Los Tuxtlas, Mexico. *Ecography*, *16*(4), 309–318.

https://doi.org/10.1111/j.1600-0587.1993.tb00220.x

Evanno, G., Regnaut, S., & Goudet, J. (2005). Detecting the number of clusters of individuals using the software STRUCTURE: A simulation study. *Molecular Ecology*, *14*(8), 2611–2620. https://doi.org/10.1111/j.1365-294X.2005.02553.x

Evelyn, M. J., & Stiles, D. A. (2003). Roosting requirements of two frugivorous bats (*Sturnira lilium* and *Arbiteus intermedius*) in fragmented Neotropical Forest. *Biotropica*, *35*(3), 405–418. https://doi.org/10.1646/02063

Excoffier, L. and Lischer, H. E. L. (2010). Arlequin 3.5.2 Manual. *Molecular Ecology Resources*, *10*, 564–567. https://doi.org/10.1111/j.1755-0998.2010.02847.x

Excoffier, L., Smouse, P. E., & Quattro, J. M. (1992). Analysis of molecular variance inferred from metric distances among DNA haplotypes: Application to human mitochondrial DNA restriction data. *Genetics*, *131*(2), 479–491.

Fabiani, A., Hoelzel, A. R., Galimberti, F., & Muelbert, M. M. C. (2003). Long-range paternal gene flow in the southern elephant seal. *Science*, *299*(5607), 676. https://doi.org/10.1126/science.299.5607.676

Fenton, M. B., Vonhof, M. J., Bouchard, S., Gill, S. A., Johnston, D. S., Reid, F. A., … Wagner, R. (2000). Roosts Used by *Sturnira lilium* (Chiroptera: Phyllostomidae) in Belize. *BIOTROPICA*, *32*(4), 729–733. https://doi.org/10.1646/0006-3606(2000)032[0729:rubslc]2.0.co;2

Fleming, T. H., Hooper, E. T., & Wilson, D. E. (1972). Three Central American bat communitis: structure, reproductive cycles, and movement patterns. *Ecology*, *53*(4), 555–569. https://doi.org/10.2307/1934771

Funk, D. J., & Omland, K. E. (2003). Species-Level paraphyly and polyphyly: frequency, causes, and consequences, with insights from animal mitochondrial DNA. *Annual Review of Ecology, Evolution, and Systematics*, *34*, 397–423.

García-García, J. L., Santos-Moreno, A., & Kraker-Castañeda, C. (2014). Ecological traits of phyllostomid bats associated with sensitivity to tropical forest fragmentation in Los Chimalapas, Mexico. *Tropical Conservation Science*, *7*(3), 457–474. https://doi.org/10.1177/194008291400700307

García-Mudarra, J. L., Ibáñez, C., & Juste, J. (2009). The Straits of Gibraltar: barrier or bridge to Ibero-Moroccan bat diversity? *Biological Journal of the Linnean Society*, *96*(2), 434–450. https://doi.org/10.1111/j.1095-8312.2008.01128.x

Gariboldi, M. C., Túnez, J. I., Failla, M., Hevia, M., Panebianco, M. V., Paso Viola, M. N., … Cappozzo, H. L. (2016). Patterns of population structure at microsatellite and mitochondrial DNA markers in the franciscana dolphin (*Pontoporia blainvillei*). *Ecology and Evolution*, *6*(24), 8764–8776. https://doi.org/10.1002/ece3.2596

Gligor, M., Ganzhorn, J. U., Rakotondravony, D., Ramilijaona, O. R., Razafimahatratra, E., Zischler, H., & Hapke, A. (2009). Hybridization between mouse lemurs in an ecological transition zone in southern Madagascar. *Molecular Ecology*, *18*(3), 520–533. https://doi.org/10.1111/j.1365-294X.2008.04040.x

González-Suárez, M., Flatz, R., Aurioles-Gamboa, D., Hedrick, P. W., & Gerber, L. R. (2009). Isolation by distance among California sea lion populations in Mexico: Redefining management stocks. *Molecular Ecology*, *18*(6), 1088–1099. https://doi.org/10.1111/j.1365-294X.2009.04093.x

Greenwood, P. J. (1980). Mating systems, philopatry and dispersal in birds and mammals. *Animal Behaviour*, *28*(4), 1140–1162. https://doi.org/10.1016/S0003-3472(80)80103-5

Guillot, G., Mortier, F., & Estoup, A. (2005). GENELAND: A computer package for landscape genetics. *Molecular Ecology Notes*, *5*(3), 712–715. https://doi.org/10.1111/j.1471-8286.2005.01031.x

Guillot, G., Renaud, S., Ledevin, R., Michaux, J., & Claude, J. (2012). A unifying model for the analysis of phenotypic, genetic, and geographic data. *Systematic Biology*, *61*, 897–911. https://doi.org/10.1093/sysbio/sys038

Gürün, K., Furman, A., Juste, J., Pereira, M. J. R., Palmeirim, J. M., Puechmaille, S. J., … Bilgin, R. (2019). A continent-scale study of the social structure and phylogeography of the bent-wing bat, *Miniopterus schreibersii* (Mammalia: Chiroptera), using new microsatellite data. *Journal of Mammalogy*, *100*(6), 1865–1878. https://doi.org/10.1093/jmammal/gyz153

Gutiérrez, E. G., Hernández Canchola, G., León Paniagua, L. S., Martínez Méndez, N., & Ortega, J. (2017). Isolation and characterization of microsatellite markers for *Sturnira parvidens* and cross-species amplification in *Sturnira* species . *PeerJ*, *5*, e3367. https://doi.org/10.7717/peerj.3367

Harrison, R. G., Bogdanowicz, S. M., Hoffmann, R. S., Yensen, E., & Sherman, P. W. (2003). Phylogeny and evolutionary history of the ground squirrels (Rodentia: Marmotinae). *Journal of Mammalian Evolution*, *10*(3), 249–276. https://doi.org/10.1023/B:JOMM.0000015105.96065.f0

Hedrick, P. W. (2011). *Genetics of populations* (4th ed.). Sudbury, Massachusetts: Jones and Bartlett Publishers.

Hernández-Canchola, G., & León-Paniagua, L. (2017). Genetic and ecological processes promoting early diversification in the lowland Mesoamerican bat *Sturnira parvidens* (Chiroptera: Phyllostomidae). *Molecular Phylogenetics and Evolution*, *114*, 334–345. https://doi.org/10.1016/j.ympev.2017.06.015

Hernández-Canchola, G., & León-Paniagua, L. S. (n.d.). *Sturnira parvidens* (Chiroptera: Phyllostomidae). *Mammalian Species*.

Hey, J. (2005). On the number of new world founders: A population genetic portrait of the peopling of the Americas. *PLoS Biology*, *3*(6), 0965–0975. https://doi.org/10.1371/journal.pbio.0030193

Hey, J. (2010a). Isolation with migration models for more than two populations. *Molecular Biology and Evolution*, *27*(4), 905–920. https://doi.org/10.1093/molbev/msp296

Hey, J. (2010b). The divergence of chimpanzee species and subspecies as revealed in multipopulation isolation-with-migration analyses. *Molecular Biology and Evolution*, *27*(4), 921–933. https://doi.org/10.1093/molbev/msp298

Hey, J. (2011). *IMa2 Documentation*. 1–60.

Hey, J., & Nielsen, R. (2007). Integration within the Felsenstein equation for improved Markov chain Monte Carlo methods in population genetics. *Proceedings of the National Academy of Sciences of the United States of America*, *104*(8), 2785–2790. https://doi.org/10.1073/pnas.0611164104

Hudson, R. R., & Turelli, M. (2003). Stochasticity overrules the "three-times rule": genetics drift, genetic draft, and coalescence times for nuclear loci versus mitochondrial DNA. *Evolution*, *57*(1), 182–190. https://doi.org/10.1554/0014-3820(2003)057[0182:sotttr]2.0.co;2

Hulva, P., Fornůsková, A., Chudárková, A., Evin, A., Allegrini, B., Benda, P., & Bryja, J. (2010). Mechanisms of radiation in a bat group from the genus *Pipistrellus* inferred by phylogeography, demography and population genetics. *Molecular Ecology*, *19*(24), 5417–5431. https://doi.org/10.1111/j.1365-294X.2010.04899.x

Iudica, C. A. (2000). Systematic revision of the neotropical fruit bats of the genus *Sturnira*: A molecular and morphological approach. University of Florida, Gainesville.

Jarrín-V, P., & Kunz, T. H. (2011). A new species of *Sturnira* (Chiroptera: Phyllostomidae) from the Chocó forest of Ecuador. *Zootaxa*, *2755*, 1–35. https://doi.org/10.11646/zootaxa.2755.1.1

Jarrín, P. V., & Clare, E. L. (2013). Systematics of *Sturnira* (Chiroptera: Phyllostomidae) in Ecuador, with comments on species boundaries. *Zootaxa*, *3630*, 165–183. https://doi.org/10.11646/zootaxa.3630.1.7

Jombart, T., Pontier, D., & Dufour, A. B. (2009). Genetic markers in the playground of multivariate analysis. *Heredity*, *102*(4), 330–341. https://doi.org/10.1038/hdy.2008.130

Jombart, Thibaut. (2008). Adegenet: A R package for the multivariate analysis of genetic markers. *Bioinformatics*, *24*(11), 1403–1405. https://doi.org/10.1093/bioinformatics/btn129

Jombart, Thibaut, Devillard, S., & Balloux, F. (2010). Discriminant analysis of principal components: A new method for the analysis of genetically structured populations. *BMC Genetics*, *11*(1), 94. https://doi.org/10.1186/1471-2156-11-94

Kalinowski, S. T. (2004). Counting alleles with rarefaction: Private alleles and hierarchical sampling designs. *Conservation Genetics*, *5*(4), 539–543. https://doi.org/10.1023/B:COGE.0000041021.91777.1a

Kalinowski, S. T. (2005). HP-RARE 1.0: A computer program for performing rarefaction on measures of allelic richness. *Molecular Ecology Notes*, *5*(1), 187–189. https://doi.org/10.1111/j.1471-8286.2004.00845.x

Kamvar, Z. N., Tabima, J. F., & Grünwald, N. J. (2014). Poppr : an R package for genetic analysis of populations with clonal, partially clonal, and/or sexual reproduction . *PeerJ*, *2*, e281. https://doi.org/10.7717/peerj.281

Kerr, K. C. R., Stoeckle, M. Y., Dove, C. J., Weigt, L. A., Francis, C. M., & Hebert, P. D. N. (2007). Comprehensive DNA barcode coverage of North American birds. *Molecular Ecology Notes*, *7*(4), 535–543. https://doi.org/10.1111/j.1471-8286.2007.01670.x

Kerth, G., Mayer, F., & Petit, E. (2002). Extreme sex-biased dispersal in the communally breeding, nonmigratory Bechstein's bat (*Myotis bechsteinii*). *Molecular Ecology*, *11*(8), 1491–1498. https://doi.org/10.1046/j.1365-294X.2002.01528.x

Kerth, G., & Van Schaik, J. (2012). Causes and consequences of living in closed societies: Lessons from a long-term socio-genetic study on Bechstein's bats. *Molecular Ecology*, *21*(3), 633–646. https://doi.org/10.1111/j.1365-294X.2011.05233.x

Korstian, J. M., Hale, A. M., & Williams, D. A. (2015). Genetic diversity, historic population size, and population structure in 2 North American tree bats. *Journal of Mammalogy*, *96*(5), 972–980. https://doi.org/10.1093/jmammal/gyv101

Lawson Handley, L. J., & Perrin, N. (2007). Advances in our understanding of mammalian sex-biased

dispersal. *Molecular Ecology*, *16*(8), 1559–1578. https://doi.org/10.1111/j.1365-294X.2006.03152.x

Librado, P., & Rozas, J. (2009). DnaSP v5: a software for comprehensive analysis of DNA polymorphism data. *Bioinformatics*, *25*(11), 1451–1452. https://doi.org/10.1093/bioinformatics/btp187

Lisiecki, L. E., & Raymo, M. E. (2005). A Pliocene-Pleistocene stack of 57 globally distributed benthic δ18O records. *Paleoceanography*, *20*(1), 1–17. https://doi.org/10.1029/2004PA001071

Llaven-Macías, V., Ruiz Montoya, L., García Bautista, M., Lesher Gordillo, J., & Machkour M'rabet, S. (2017). Diversidad y estructura genética de *Artibeus jamaicensis* (Chiroptera: Phyllostomidae) en Chiapas, México. *Acta Zoológica Mexicana (n.S.)*, *33*(1), 55–66. https://doi.org/10.21829/azm.2017.3311013

Loew, S. S., Williams, D. F., Ralls, K., Pilgrim, K., & Fleischer, R. C. (2005). Population structure and genetic variation in the endangered giant kangaroo rat (*Dipodomys ingens*). *Conservation Genetics*, *6*(4), 495–510. https://doi.org/10.1007/s10592-005-9005-9

Lyrholm, T., Leimar, O., Johanneson, B., & Gyllensten, U. (1999). Sex-biased dispersal in sperm whales: contrasting mitochondrial and nuclear genetic structure of global populations. *Proceedings of the Royal Society B: Biological Sciences*, *266*(1417), 347–354. https://doi.org/10.1098/rspb.1999.0644

Marshall, H. D., Yaskowiak, E. S., Dyke, C., & Perry, E. A. (2011). Microsatellite population structure of Newfoundland black bears (*Ursus americanus hamiltoni*). *Canadian Journal of Zoology*, *89*(9), 831–839. https://doi.org/10.1139/z11-056

Martins, F. M., Templeton, A. R., Pavan, A. C., Kohlbach, B. C., & Morgante, J. S. (2009). Phylogeography of the common vampire bat (*Desmodus rotundus*): Marked population structure, Neotropical Pleistocene vicariance and incongruence between nuclear and mtDNA markers. *BMC Evolutionary Biology*, *9*(1), 1–13. https://doi.org/10.1186/1471-2148-9-294

McCarthy, T. J., Albuja V, L., & Alberico, M. S. (2006). A new species of Chocoan *Sturnira* (Chiroptera: Phyllostomidae: Stenodermatinae) from Western Ecuador and Colombia. *Annals of Carnegie Museum*, *75*(2), 97–110. https://doi.org/10.2992/0097-4463(2006)75[97:ansocs]2.0.co;2

Meyer, C. F. J., Kalko, E. K. V., & Kerth, G. (2009). Small-scale fragmentation effects on local genetic diversity in two phyllostomid bats with different dispersal abilities in Panama. *Biotropica*, *41*(1), 95–102. https://doi.org/10.1111/j.1744-7429.2008.00443.x

Molinari, J., Bustos, X. E., Burneo, S. F., Camacho, M. A., Moreno, S. A., & Fermín, G. (2017). A new polytypic species of yellow-shouldered bats, genus *Sturnira* (Mammalia: Chiroptera: Phyllostomidae), from the Andean and coastal mountain systems of Venezuela and Colombia. *Zootaxa*, *4243*(1), 75–96. https://doi.org/10.11646/zootaxa.4243.1.3

Morrison, D.W. (1979). Apparent male defense of tree hollows in the fruit bat, *Artibeus jamaicensis*. *Journal of Mammalogy*, *60*(1), 11–15. https://doi.org/10.2307/1379753

Morrison, Douglas W., & Hagen-Morrison, S. (1981). Economics of harem maintenance by a neotropical bat. *Ecology*, *62*(2), 864–866. https://doi.org/10.2307/1937751

Moussy, C., Atterby, H., Griffiths, A. G. F., Allnutt, T. R., Mathews, F., Smith, G. C., … Hosken, D. J. (2015). Population genetic structure of serotine bats (*Eptesicus serotinus*) across Europe and

implications for the potential spread of bat rabies (European bat lyssavirus EBLV-1). *Heredity*, *115*(1), 83–92. https://doi.org/10.1038/hdy.2015.20

Mullenbach, R., Lagoda, P. L. J., & Welter, C. (1989). An efficient salt-chloroform extraction of DNA from blood and tissues. *Trends in Genetics*, *5*(12), 391.

Naidoo, T., Schoeman, M. C., Goodman, S. M., Taylor, P. J., & Lamb, J. M. (2016). Discordance between mitochondrial and nuclear genetic structure in the bat *Chaerephon pumilus* (Chiroptera: Molossidae) from southern Africa. *Mammalian Biology*, *81*(2), 115–122. https://doi.org/10.1016/j.mambio.2015.11.002

Neubaum, M. A., Douglas, M. R., Douglas, M. E., & O'Shea, T. J. (2007). Molecular Ecology of the Big Brown Bat (*Eptesicus fuscus*): Genetic and Natural History Variation in a Hybrid Zone. *Journal of Mammalogy*, *88*(5), 1230–1238. https://doi.org/10.1644/06-mamm-a-228r1.1

Ng, J., & Glor, R. E. (2011). Genetic differentiation among populations of a Hispaniolan trunk anole that exhibit geographical variation in dewlap colour. *Molecular Ecology*, *20*(20), 4302–4317. https://doi.org/10.1111/j.1365-294X.2011.05267.x

Pacheco, V., & Patterson, B. D. (1992). Systematics and biogeographic analysis of four species of *Sturnira* (Chiroptera: Phyllostomidae), with emphasis on Peruvian forms. In K. R. Young & N. Valencia (Eds.), *Biogeografía, ecología y conservación del bosque montano en el Perú* (pp. 57–81). Universidad Nacional Mayor de San Marcos, Lima.

Peakall, R., & Smouse, P. E. (2006). GenAlEx 6: Genetic analysis in Excel. Population genetic software for teaching and research. *Molecular Ecology Notes*, *6*, 288–295.

Peakall, R., & Smouse, P. E. (2012). GenALEx 6.5: Genetic analysis in Excel. Population genetic software for teaching and research-an update. *Bioinformatics*, *28*, 2537–2539. https://doi.org/10.1093/bioinformatics/bts460

Perry, W. L., Feder, J. L., Dwyer, G., & Lodge, D. M. (2001). Hybrid zone dynamics and species replacement between *Orconectes* crayfishes in a northern Wisconsin lake. *Evolution*, *55*(6), 1153–1166. https://doi.org/10.1111/j.0014-3820.2001.tb00635.x

Piaggio, A. J., Navo, K. W., & Stihler, C. W. (2009). Intraspecific comparison of population structure, genetic diversity, and dispersal among three subspecies of Townsend's big-eared bats, *Corynorhinus townsendii townsendii*, *C. t. pallescens*, and the endangered *C. t. virginianus*. *Conservation Genetics*, *10*(1), 143–159. https://doi.org/10.1007/s10592-008-9542-0

Pritchard, J. K., Stephens, M., & Donnelly, P. (2000). Inference of population structure using multilocus genotype data. *Genetics*, *155*, 945–959.

Proctor, M. F., McLellan, B. N., Strobeck, C., & Barclay, R. M. R. (2004). Gender-specific dispersal distances of grizzly bears estimated by genetic analysis. *Canadian Journal of Zoology*, *82*(7), 1108–1118. https://doi.org/10.1139/Z04-077

R Core Team. (2016). R: A Language and Environment for Statistical Computing. *R Foundation for Statistical Computing*. https://doi.org/http://www.R-project.org/

Ramírez-Pulido, J., & Castro-Campillo, A. (1990). Regiones y Provincias Mastogeográficas. In

Regionalización Mastofaunística, IV.8.8 Atlas Nacional de México Vol. III. Ciudad de México: Instituto de Geografía, UNAM.

Ripperger, S. P., Tschapka, M., Kalko, E. K. V, Rodriguez-Herrera, B., & Mayer, F. (2013). Life in a mosaic landscape: Anthropogenic habitat fragmentation affects genetic population structure in a frugivorous bat species. *Conservation Genetics*, *14*(5), 925–934. https://doi.org/10.1007/s10592-012-0434-y

Ripperger, S. P., Tschapka, M., Kalko, E. K. V, Rodríguez-Herrera, B., & Mayer, F. (2014). Resisting habitat fragmentation: High genetic connectivity among populations of the frugivorous bat *Carollia castanea* in an agricultural landscape. *Agriculture, Ecosystems and Environment*, *185*, 9–15. https://doi.org/10.1016/j.agee.2013.12.006

Ritland, K., Newton, C., & Marshall, H. D. (2001). Inheritance and population structure of the white-phased "Kermode" black bear. *Current Biology*, *11*(18), 1468–1472. https://doi.org/10.1016/S0960-9822(01)00448-1

Roca, A. L., Georgiadis, N., & O'Brien, S. J. (2005). Cytonuclear genomic dissociation in African elephant species. *Nature Genetics*, *37*(1), 96–100. https://doi.org/10.1038/ng1485

Rohwer, S., Bermingham, E., & Wood, C. (2001). Plumage and mitochondrial DNA haplotype variation across a moving hybrid zone. *Evolution*, *55*(2), 405–422.

Rojas, D., Warsi, O. M., & Dávalos, L. M. (2016). Bats (Chiroptera: Noctilionoidea) challenge a recent origin of extant Neotropical diversity. *Systematic Biology*, *65*(3), 432–448. https://doi.org/10.1093/sysbio/syw011

Rousset, F. (1997). Genetic differentiation and estimation of gene flow from F-statistics under isolation by distance. *Genetics*, *145*(4), 1219–1228.

Ruedi, M., & Castella, V. (2003). Genetic consequences of the ice ages on nurseries of the bat *Myotis myotis*: A mitochondrial and nuclear survey. *Molecular Ecology*, *12*(6), 1527–1540. https://doi.org/10.1046/j.1365-294X.2003.01828.x

Ruegg, K. (2008). Genetic, morphological, and ecological characterization of a hybrid zone that spans a migratory divide. *Evolution*, *62*(2), 452–466. https://doi.org/10.1111/j.1558-5646.2007.00263.x

Ruiz, E. A., Vargas-Miranda, B., & Zúñiga, G. (2013). Late-Pleistocene phylogeography and demographic history of two evolutionary lineages of *Artibeus jamaicensis* (Chiroptera: Phyllostomidae) in Mexico. *Acta Chiropterologica*, *15*(1), 19–33. https://doi.org/10.3161/150811013x667830

Saldaña-Vázquez, R. A., Castro-Luna, A. A., Sandoval-Ruiz, C. A., Hernández-Montero, J. R., & Stoner, K. E. (2013). Population composition and ectoparasite prevalence on bats (*Sturnira ludovici*; Phyllostomidae) in forest fragments and coffee plantations of Central Veracruz, Mexico. *Biotropica*, *45*(3), 351–356. https://doi.org/10.1111/btp.12007

Sánchez-Hernández, C., Romero-Almaraz, M. L., & Schnell, G. D. (2005). New species of *Sturnira* (Chiroptera: Phyllostomidae) from northern South America. *Journal of Mammalogy*, *86*(5), 866–872. https://doi.org/10.1644/1545-1542(2005)86[866:nsoscp]2.0.co;2

Schlötterer, C. (2000). Evolutionary dynamics of microsatellite DNA. *Chromosoma*, *109*(6), 365–371. https://doi.org/10.1007/s004120000089

Sun, J. T., Wang, M. M., Zhang, Y. K., Chapuis, M. P., Jiang, X. Y., Hu, G., … Hong, X. Y. (2015). Evidence for high dispersal ability and mito-nuclear discordance in the small brown planthopper, *Laodelphax striatellus*. *Scientific Reports*, *5*(January), 8045. https://doi.org/10.1038/srep08045

Toews, D. P. L., & Brelsford, A. (2012). The biogeography of mitochondrial and nuclear discordance in animals. *Molecular Ecology*, *21*(16), 3907–3930. https://doi.org/10.1111/j.1365-294X.2012.05664.x

Uphyrkina, O., Johnson, W. E., Quigley, H., Miquelle, D., Marker, L., Bush, M., & O'Brien, S. J. (2001). Phylogenetics, genome diversity and origin of modern leopard, *Panthera pardus*. *Molecular Ecology*, *10*(11), 2617–2633. https://doi.org/10.1046/j.0962-1083.2001.01350.x

Van Oosterhout, C., Hutchinson, W. F., Wills, D. P. M., & Shipley, P. (2004). MICRO-CHECKER: Software for identifying and correcting genotyping errors in microsatellite data. *Molecular Ecology Notes*, *4*(3), 535–538. https://doi.org/10.1111/j.1471-8286.2004.00684.x

Velazco, P. M., & Patterson, B. D. (2013). Diversification of the Yellow-shouldered bats, Genus *Sturnira* (Chiroptera, Phyllostomidae), in the New World tropics. *Molecular Phylogenetics and Evolution*, *68*(3), 683–698. https://doi.org/10.1016/j.ympev.2013.04.016

Velazco, P. M., & Patterson, B. D. (2014). Two new species of yellow-shouldered bats, genus *Sturnira* Gray, 1842 (Chiroptera, Phyllostomidae) from Costa Rica, Panama and western Ecuador. *ZooKeys*, *402*, 43–66. https://doi.org/10.3897/zookeys.402.7228

Velazco, P. M., & Patterson, B. D. (2019). Small mammals of the Mayo River Basin in northern Peru, with the description of a new species of *Sturnira* (Chiroptera: Phyllostomidae). *Bulletin of the American Museum of Natural History*, *2019*(429), 1–67. https://doi.org/10.1206/0003-0090.429.1.1

Weir, B. S., & Cockerham, C. C. (1984). Estimating F-Statistics for the Analysis of Population Structure. *Evolution*, *38*(6), 1358–1370. https://doi.org/10.2307/2408641

Wright, S. (1969). *Evolution and Genetics of Populations. Vol. 2: The theory of gene frequencies*. Chicago, USA: University of Chicago Press.

Zink, R. M., & Barrowclough, G. F. (2008). Mitochondrial DNA under siege in avian phylogeography. *Molecular Ecology*, *17*(9), 2107–2121. https://doi.org/10.1111/j.1365-294X.2008.03737.x

Discusión general

En comparación con estudios basados en un solo tipo de marcador molecular, los estudios genéticos basados en más de un tipo de marcador han demostrado que es posible realizar inferencias más precisas al combinar la información genética proveniente de nuADN y mtADN, lo cual provee evidencia más completa y confiable sobre la historia evolutiva de los taxa (Castellanos-Morales *et al.* 2014, Chen *et al.* 2010, Martins *et al.* 2009).

Así, en este trabajo basado en loci nucleares y mitocondriales, detectamos los haplogrupos mitocondriales previamente reportados en *S. parvidens* (Hernández-Canchola & León-Paniagua 2017) pero además pudimos detectar estructura genética menos evidente usando loci nucleares, encontrando discordancia biogeográfica mito-nuclear entre los grupos genéticos de *S. parvidens.* Nuestros resultados apoyan la idea de que las hembras de esta especie son filopátricas, y que el flujo génico a grandes distancias es dependiente de los machos.

Variación genética en *Sturnira parvidens*

Los niveles de variación genética para microsatélites (H_e= 0.893) y para los genes (*Hd* = 0.976 para *RAG1*; *Hd* = 0.989 para *cyt-b*; *Hd*= 0.995 para *D-loop*) en *S. parvidens* fueron altos y se encuentran dentro del rango reportado para otras especies de murciélagos tropicales: para mtDNA: *Hd*= 0.86-1.0 y π= 0.0073-0.027 (Meyer *et al.* 2009, Ruiz *et al.* 2013, Ripperger *et al.* 2013, 2014, Llaven-Macías *et al.* 2017, Cruz-Salazar *et al.* 2018); para microsatélites nucleares: H_o= 0.78-0.89 y H_e= 0.78-0.87 (Chen *et al.* 2010, Korstian *et al.* 2015).

Dado que la variación genética es básicamente el resultado del tamaño efectivo poblacional y la tasa de mutación (Hedrick 2011), los períodos interglaciales del Pleistoceno junto con los eventos de expansión de la vegetación asociados a estos, probablemente jugaron un papel crucial en la expansión demográfica de *S. parvidens* (Hernández-Canchola & León-Paniagua 2017) y en el incremento de sus tamaños efectivos poblacionales y diversidad genética. De igual forma, encontramos mayores valores de diversidad genética en el grupo Este-nu (H_e= 0.901 para microsatélites; *Hd*= 0.976 y π= 0.006 para nuADN; *Hd*= 0.985 y π= 0.083 para mtADN; Tabla 2) que en el grupo Oeste-nu (H_e= 0.865 para microsatélites; *Hd*= 0.938 y π= 0.003 para nuADN; *Hd*= 0.982 y π= 0.019 para mtADN; Tabla 2), lo cual es consistente con una expansión demográfica más fuerte en las poblaciones orientales que en las occidentales

(Hernández-Canchola & León-Paniagua 2017).

Las condiciones de alta variabilidad genética en *S. parvidens* podrían también ser resultado de una combinación de factores asociados a su historia evolutiva y/o su propia biología, como su sistema de apareamiento, estructura social y patrones de dispersión. Por ejemplo, diversos estudios apoyan la idea de que los murciélagos del género *Sturnira* tienen una gran capacidad para colonizar áreas y espacios ambientales nuevos, al igual que para formar grupos genéticos bien diferenciados después de experimentar eventos de aislamiento geográfico (Hernández-Canchola & León-Paniagua 2017, Iudica 2000, Velazco & Patterson 2013).

Discordancia mito-nuclear contemporánea

Evidencia genética sobre la historia evolutiva de *S. parvidens* indica que divergió de su especie hermana hace cerca de 1.84 millones de años (Ma; ± 2.553 – 1.179) durante uno de los pulsos del Gran Intercambio Biótico Americano (GABI-2; Hernández-Canchola & León-Paniagua 2017, Rojas et al. 2016). En el contexto de los ciclos glaciales-interglaciales subsecuentes que variaron en frecuencia y magnitud, podemos asumir que después de su divergencia, cada grupo de *S. parvidens* experimentó procesos continuos de aislamiento y expansión que promovieron su diferenciación siguiendo las oscilaciones climáticas de la época.

Nuestros análisis de estructura genética basados en loci mitocondriales (*cyt-b* y *D-loop*) en *S. parvidens* a lo largo de México y Centroamérica revelaron una estructura genética significativa, detectando dos grupos bien definidos (Oeste y Este; Figuras 3 y 4) como lo habían reportado previamente Hernández-Canchola & León-Paniagua (2017). Sin embargo, detectamos estructura genética menos evidente con base en loci nucleares (microsatélites y *RAG1*), recuperando dos grupos distintos (Oeste-nu y Este-nu; Figuras 3 y 4). El tiempo de divergencia que encontramos entre los grupos Oeste-nu y Este-nu al incorporar los datos de microsatélites en los análisis de coalescencia (*c.* 172,740 años [95% HPD: 240,225 – 135,809]) fue consistente con el final del período glacial MIS-8 hace cerca de 0.243 Ma (Lisiecki & Raymo 2005). Este período glacial no fue uno de los ciclos más intensos del Pleistoceno Medio, pero es parte de los últimos ciclos glaciales de la época, cuando se sabe que existió una clara relación entre el clima y los gases de efecto invernadero (EPICA Community Members 2004). No obstante, el tiempo de divergencia que obtuvieron Hernández-Canchola & León-Paniagua (2017; *c.* 0.423 Ma [95% CI: 0.586 – 0.268]) no concuerda con el que encontramos en este trabajo, aunque también está ubicado en el Pleistoceno Medio.

Las diferencias encontradas en los tiempos de divergencia pueden estar relacionadas con diferencias en la metodología, ya que Hernández-Canchola & León-Paniagua (2017) usaron una aproximación bayesiana y nosotros una aproximación de coalescencia. También las características de los marcadores, como la resolución de cada uno y la tasa de mutación rápida de los microsatélites, pudieron haber reducido las estimaciones del tiempo de divergencia, como ha sido previamente reportado (Castellanos-Morales et al. 2016, Harrison et al. 2003). Por otro lado, el tiempo de divergencia obtenido en este trabajo concuerda con el tiempo de las expansiones demográficas experimentadas por *S. parvidens* según lo reportado por Hernández-Canchola & León-Paniagua (2017), lo cual indica que la expansión poblacional y la diferenciación pudieron haber ocurrido simultáneamente. Dado el conjunto de evidencia, concluimos que la diferenciación entre las poblaciones occidentales y orientales de *S. parvidens* ocurrió durante el período de intensos ciclos glaciales-interglaciales del Pleistoceno Medio.

Asimismo, se encontraron diferencias interesantes entre los marcadores nucleares y mitocondriales. Hallamos una discrepancia entre los límites geográficos de los grupos Oeste-Este y Oeste-nu–Este-nu cuando comparamos los rangos geográficos de mtADN y nuADN de cada grupo, confirmando la existencia de un patrón de discordancia biogeográfica mito-nuclear en *S. parvidens*, como ha sido reportado en otras especies de murciélagos (Castella *et al.* 2001, Martins *et al.* 2009, Naidoo *et al.* 2016).

Una de las principales razones reportadas como causa de discordancia mito-nuclear es el aislamiento de los taxa por largos períodos de tiempo en el pasado, seguido de un contacto secundario en el presente (Toews & Brelsford 2012). Esta hipótesis ha sido reportada en diversos estudios en mamíferos (Roca *et al.* 2005, Berthier *et al.* 2006, Bryja *et al.* 2010, Hulva *et al.* 2010, Cabria *et al.* 2011). Durante el período de aislamiento, los grupos divergentes acumulan mutaciones tanto en nuADN como en mtADN, las cuales incrementan su frecuencia debido a la acción simultánea de diversas fuerzas evolutivas, como la selección y la deriva génica. Luego, durante el contacto secundario, estos grupos forman zonas híbridas y se entrecruzan, originando discordancia mito-nuclear debido a patrones divergentes del flujo génico entre los dos genomas (Toews & Brelsford 2012). En *S. parvidens*, los períodos de aislamiento pueden corresponder con los fuertes ciclos glaciales que promovieron su diferenciación genética, y es posible que ahora estemos documentando el contacto secundario entre los dos linajes, llevado a cabo en un tiempo relativamente reciente y en ausencia de

barreras geográficas (Hernández-Canchola & León-Paniagua 2017).

En la mayoría de los estudios previos se ha sugerido que la discordancia geográfica no se extiende más allá del área actual de simpatría de los taxa, y que usualmente el ADN "extranjero" no se extiende más del 50% del área del taxón nativo (Bryson *et al.* 2010, Gligor *et al.* 2009, Ng & Glor 2011, Ruegg 2008).

Nuestros resultados muestran que el límite geográfico entre los grupos de nuADN (Oeste-nu y Este-nu) está situado en la región seca del Valle de Tehuacán-Cuicatlán y los Valles Centrales de Oaxaca (poblaciones OXT y SMS; Figuras 1 y 4), mientras que el límite entre los grupos de mtADN (Oeste y Este) está ubicado en el oeste de la depresión del río Balsas (población BAL; Figuras 1 y 4). Por tanto, podemos señalar que el nuADN del linaje occidental (ADN extranjero) está dentro del área del linaje oriental (taxón nativo) en los estados de Morelos, Guerrero, el sur de Puebla y el este de Oaxaca (Figuras 1 y 4), demostrando la extensión geográfica de la discordancia. También podemos observar que esta área de traslape es menor al 50% del área de distribución del linaje oriental, lo cual corresponde con el patrón reportado en los estudios mencionados anteriormente.

En resumen, podemos inferir que aunque los linajes genéticos de *S. parvidens* pudieron haberse separado completamente y formado dos grupos genéticamente bien estructurados durante las oscilaciones climáticas de la segunda mitad del Pleistoceno, probablemente volvieron a entraron en contacto en un tiempo más reciente, generando el patrón de discordancia biogeográfica entre mtADN y nuADN que hoy observamos.

Patrones actuales de dispersión y flujo génico que influyen en la estructura genética

Detectamos migrantes entre los dos grupos nucleares de *S. parvidens* en ambas direcciones ($m_{\text{Oeste-nu}\rightarrow\text{Este-nu}} = 6.9$, y $m_{\text{Este-nu}\rightarrow\text{Oeste-nu}} = 5.0$ por generación). Wright (1969) menciona que una tasa de migración mayor a 1 por generación es usualmente suficiente para inhibir diferenciación genética debido a la deriva génica. Las tasas estimadas son mayores que 1, sin embargo, no fueron estadísticamente diferentes entre sí y más estudios son necesarios. Adicionalmente, el bajo valor de F_{ST} (0.056; Tabla 3), lo mismo que las estimaciones pareadas de F_{ST} (Figura 6; Figura Suplementaria S6; Tablas Suplementarias S2 y S3) y el bajo porcentaje de variación entre grupos (2.051 %; Tabla 3) obtenidos a partir de los datos de microsatélites, sugieren un patrón casi panmíctico de la variación genética en *S. parvidens*.

En contraste, usando mtADN, Hernández-Canchola & León-Paniagua (2017) encontraron estructura genética (*cyt-b:* $\Phi_{ST} = 0.586$ y 58.64% de variación entre grupos; *D-loop*: $\Phi_{ST} = 0.406$ y 40.64% de variación entre grupos). Estos patrones de diferenciación

en la estructura genética entre loci nucleares y mitocondriales son consistentes con los reportados en diferentes especies de murciélagos (Ruedi & Castella 2003, Chen *et al.* 2008, Kerth *et al.* 2002, Piaggio *et al.* 2009) en los cuales los valores de F_{ST} nucleares entre grupos fueron muy bajos, pero los valores de Φ_{ST} mitocondriales variaron considerablemente de una especie a otra y fueron siempre mayores que los de F_{ST} nucleares, sugiriendo que las asimetrías sesgadas por el sexo son responsables de tales diferencias. Por tanto, consideramos que los bajos valores de F_{ST} nucleares y los relativamente altos valores de Φ_{ST} mitocondriales en *S. parvidens* son resultado de los sistemas de dispersión y apareamiento de esta especie.

En otras especies del género *Sturnira*, Pacheco & Patterson (1992) supusieron un patrón de filopatría general en *S. erythromos*, y Saldaña-Vázquez *et al.* (2013) indicaron filopatría materna en *S. hondurensis*: las hembras tienen preferencia por sitios de bosque con una alta disponibilidad de recursos alimenticios debido al incremento de los costos metabólicos asociados con la preñez y la lactancia, mientras que los machos se dispersan a otras áreas para evitar la competencia de recursos con las hembras. Es posible que patrones similares de filopatría materna y dispersión sesgada por los machos esté presente también en *S. parvidens*, como ha sido reportado en otras especies de murciélagos (Chen *et al.* 2008, Kerth & Van Schaik 2012, Gürün *et al.* 2019).

Por otro lado, los patrones de aislamiento por distancia que detectamos (Figura Suplementaria S7), podrían ser consecuencia de rasgos ecológicos de *S. parvidens*: la morfología alar y las distancias de viaje relativamente cortas reportadas para los individuos de esta especie (García-García *et al.* 2014, Fleming *et al.* 1972, Estrada *et al.* 1993) han sido interpretados como indicadores de la incapacidad de *S. parvidens* para realizar desplazamientos a grandes distancias. Además, se ha reportado que esta especie es fiel a sus sitios de percha (Evelyn & Stiles 2003), que sus refugios diurnos son principalmente cavidades en árboles maduros y que los individuos perchan solos o en pequeños grupos en vida silvestre (1-3 o más individuos en pocos casos; Fenton *et al.* 2000, Hernández-Canchola & León-Paniagua *en prensa*).

En resumen, nuestros hallazgos apoyan la idea de que las hembras de *S. parvidens* son filopátricas y que contribuyen poco al flujo génico de larga distancia. Debido a que patrones divergentes de flujo génico entre mtADN y nuADN pueden promover discordancia mito-nuclear (Toews & Brelsford 2012) hipotetizamos que los machos, aunque no migran ni desarrollan desplazamientos a grandes distancias geográficas, tienen una mayor capacidad de dispersión que las hembras. Además, el estado de *S. parvidens* como una especie común y localmente abundante, sugiere que

incluso movimientos relativamente pequeños realizados por los machos (representados en este trabajo por loci nucleares) podrían mantener conectadas a las poblaciones a lo largo de su distribución geográfica mediante flujo génico, como ha sido reportado en otros murciélagos frugívoros neotropicales (Altringham 2011, Brooke 1990, Morrison 1979, Morrison & Hagen-Morrison 1981).

Finalmente, consideramos que trabajos futuros deberán concentrar los esfuerzos de estudio en los individuos de la Cuenca del Río Balsas, el Valle de Tehuacán-Cuicatlán y los Valles Centrales de Oaxaca, usando diferentes aproximaciones (p. ej., otras herramientas genéticas, como marcadores moleculares del cromosoma Y; morfometría geométrica; observaciones ecológicas y de comportamiento) con el objetivo de obtener evidencia adicional de la dinámica poblacional actual e histórica.

Conclusiones

- *Sturnira parvidens* posee una alta variabilidad genética, la cual podría ser resultado de su historia evolutiva y diferentes factores asociados a su propia biología.
- Se detectaron dos grupos genéticos bien definidos con base en loci mitocondriales (Oeste y Este). Sin embargo, se detectaron dos grupos diferentes con base en loci nucleares (Oeste-un y Este-nu), los cuales mostraron estructura genética menos evidente.
- El límite geográfico entre los grupos Oeste y Este está situado en el occidente ste de la Cuenca del Río Balsas, mientras que el límite entre los grupos Oeste-nu y Este-nu está ubicado en la región del Valle de Tehuacán-Cuicatlán y los Valles Centrales de Oaxaca.
- Es probable que los linajes genéticos de *S. parvidens* se hayan separado completamente en el pasado y formado dos grupos genéticamente bien estructurados durante la segunda mitad del Pleistoceno, y que dichos grupos hayan vuelto a entrar en contacto en un tiempo más reciente, generando un patrón de discordancia biogeográfica mito-nuclear.
- Los patrones de flujo génico y aislamiento por distancia que detectamos apoyan la idea de que las hembras de *S. parvidens* son filopátricas, y que el flujo génico a larga distancia es realizado por los machos.
- Conocer la dinámica evolutiva poblacional de especies comunes como *S. parvidens* en áreas biológicamente diversas como Mesoamérica, nos permite aportar información importante para determinar los patrones biogeográficos de la región.

Bibliografía

Brito, P. H. (2007). Contrasting patterns of mitochondrial and microsatellite genetic structure among Western European populations of tawny owls (*Strix aluco*). *Molecular Ecology*, *16*(16), 3423–3437. https://doi.org/10.1111/j.1365-294X.2007.03401.x

Edwards, S., & Bensch, S. (2009). Looking forwards or looking backwards in avian phylogeography? A comment on Zink and Barrowclough 2008. *Molecular Ecology*, *18*(14), 2930–2933. https://doi.org/10.1111/j.1365-294X.2009.04270.x

Flanders, J., Jones, G., Benda, P., Dietz, C., Zhang, S., Li, G., … Rossiter, S. J. (2009). Phylogeography of the greater horseshoe bat, *Rhinolophus ferrumequinum*: Contrasting results from mitochondrial and microsatellite data. *Molecular Ecology*, *18*(2), 306–318. https://doi.org/10.1111/j.1365- 294X.2008.04021.x

Frankham, R. (2005). Genetics and extinction. *Biological Conservation*, *126*(2), 131–140. https://doi.org/10.1016/j.biocon.2005.05.002

Furmankiewicz, J., & Altringham, J. (2007). Genetic structure in a swarming brown long-eared bat (*Plecotus auritus*) population: evidence for mating at swarming sites. *Conservation Genetics*, *8*(4), 913–923. https://doi.org/10.1007/s10592-006-9246-2

Goodman, S. M., Buccas, W., Naidoo, T., Ratrimomanarivo, F., Taylor, P. J., & Lamb, J. (2010). Patterns of morphological and genetic variation in western Indian Ocean members of the *Chaerephon* "*pumilus*" complex (Chiroptera: Molossidae), with the description of a new species from Madagascar. *Zootaxa*, (2551), 1–36.

Hancock, J. M. (1999). Microsatellites and other simple sequences: genomic context and mutational mechanisms. In D. B. Goldstein & C. Schlötterer (Eds.), *Microsatellites: Evolution and Applications* (pp. 1–10). New York, USA: Oxford University Press.

Jadwiszczak, K. A., Ratkiewicz, M., & Banaszek, A. (2006). Analysis of molecular differentiation in a hybrid zone between chromosomally distinct races of the common shrew *Sorex araneus* (Insectivora: Soricidae) suggests their common ancestry. *Biological Journal of the Linnean Society*, *89*(1), 79–90. https://doi.org/10.1111/j.1095-8312.2006.00659.x

Jiggins, F. M. (2003). Male-killing *Wolbachia* and mitochondrial DNA: Selective sweeps, hybrid introgression and parasite population dynamics. *Genetics*, *164*(1), 5–12.

McKay, B. D., & Zink, R. M. (2010). The causes of mitochondrial DNA gene tree paraphyly in birds. *Molecular Phylogenetics and Evolution*. https://doi.org/10.1016/j.ympev.2009.08.024

Moussy, Caroline, Hosken, D. J., Mathews, F., Smith, G. C., Aegerter, J. N., & Bearhop, S. (2013). Migration and dispersal patterns of bats and their influence on genetic structure. *Mammal Review*, *43*(3), 183–195. https://doi.org/10.1111/j.1365-2907.2012.00218.x

Nielsen, R., & Slatkin, M. (2013). *An Introduction to Population Genetics: Theory and Applications*. Sunderland, Massachusetts: Sinauer Associates, Inc. Publishers.

Racey, P. A., Barratt, E. M., Burland, T. M., Deaville, R., Gotelli, D., Jones, G., & Piertney, S. B.

(2007). Microsatellite DNA polymorphism confirms reproductive isolation and reveals differences in population genetic structure of cryptic pipistrelle bat species. *Biological Journal of the Linnean Society*, *90*(3), 539–550. https://doi.org/10.1111/j.1095-8312.2007.00746.x

Vázquez Lobo, A., & García Morales, A. E. (2014). Microsatélites. In A. Cornejo, A. Serrato, B. Rendón, & M. Rocha (Eds.), *Herramientas moleculares aplicadas en ecología: aspectos teóricos y prácticos* (pp. 75–100). Mexico City, México: INEEC-SEMARNAT, UAM-I.

You, Y., Sun, K., Xu, L., Wang, L., Jiang, T., Liu, S., … Feng, J. (2010). Pleistocene glacial cycle effects on the phylogeography of the Chinese endemic bat species, *Myotis davidii*. *BMC Evolutionary Biology*, *10*(1), 208. https://doi.org/10.1186/1471-2148-10-208

Zane, L., Bargelloni, L., & Patarnello, T. (2002). Strategies for microsatellite isolation: a review. *Molecular Ecology*, *11*(1), 1–16. https://doi.org/10.1046/j.0962-1083.2001.01418.x

Supplementary Material

Supplementary Figure S1. Estimated null alleles of 9 microsatellite loci in 21 *S. parvidens* populations. The loci shown in pink are loci with high levels of null alleles using both 95% and Bonferroni confidence intervals.

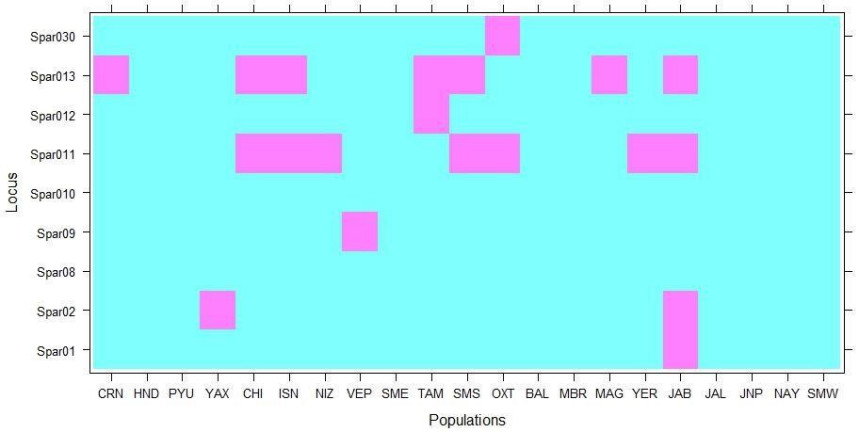

Supplementary Figure S2. Estimated null alleles of 7 microsatellite loci in 21 *S. parvidens* populations. The loci shown in pink are loci with high levels of null alleles using both 95% and Bonferroni confidence intervals.

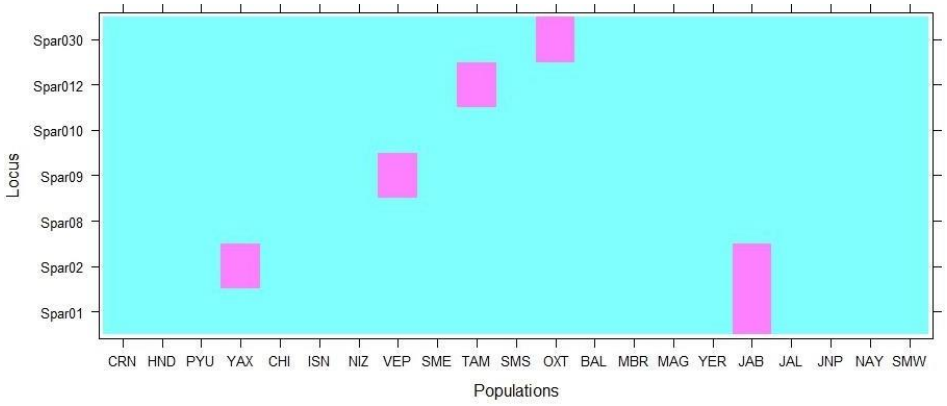

Supplementary Figure S3. Deviations from Hardy-Weinberg equilibrium of 7 microsatellite loci in 21 *S. parvidens* populations. The loci shown in pink are loci suspected of not being in HWE with $p \leq 0.05$ (Spar02 for OXT [$p = 0.046$] and JAB [$p = 4.6e\text{-}06$]; Spar08 for SMS [$p = 0.016$]; and Spar10 for JAB [$p = 0.016$]).

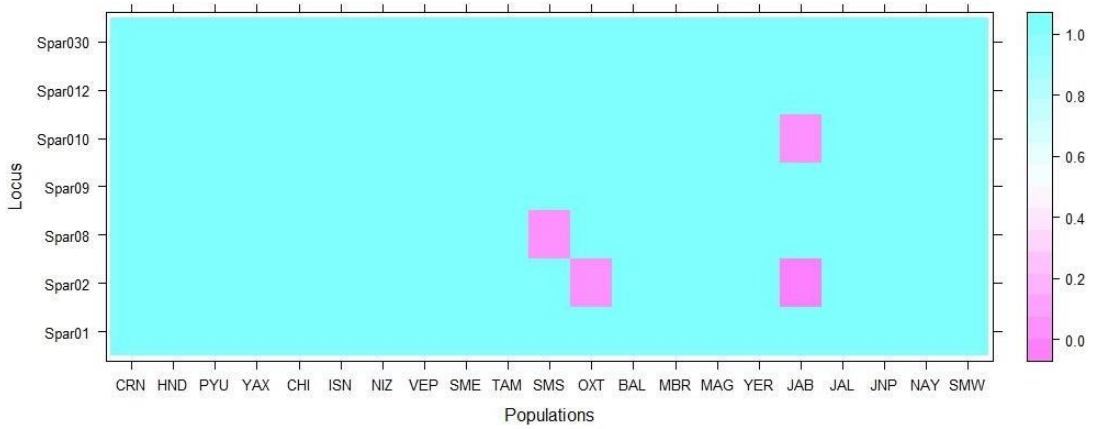

Supplementary Figure S4. Linkage disequilibrium in 21 *S. parvidens* populations. Index $\bar{r}_d$ in plots below is located on left or centrally in the distribution expected from unlinked loci, and the *p* values of each population are represented by colour in the top panel. The locus set of only one population showed a significant $p \leq 0.05$ of I_A and $\bar{r}_d$: BAL ($p\ I_A = 0.041$; $p\ \bar{r}_d = 0.046$). OXT *p* values are not significant ($p\ I_A = 0.064$; $p\ \bar{r}_d = 0.056$).

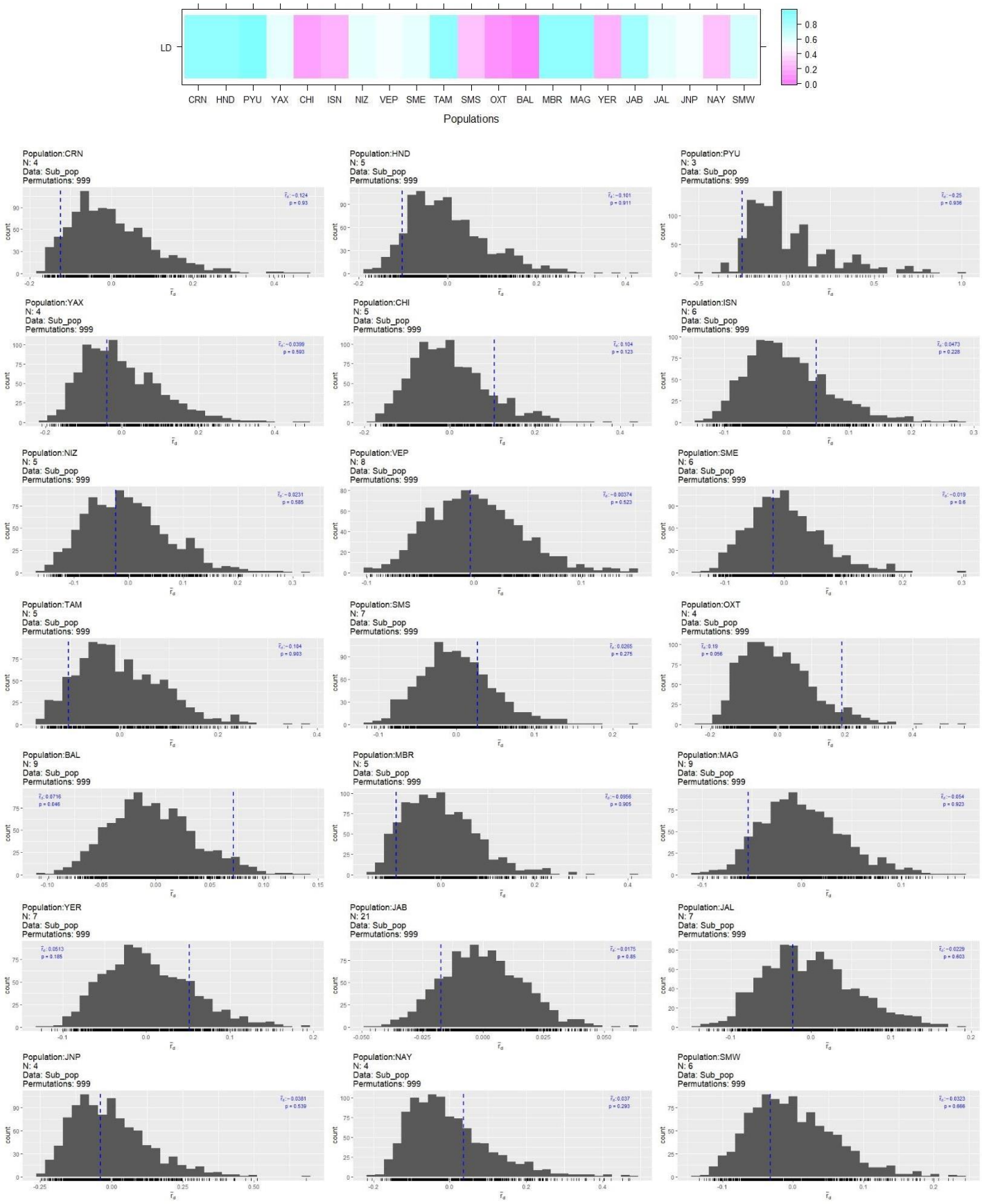

Supplementary Figure S5. Scatterplot of individual principal components on the first two principal component (PC) axes (PC-1: X axis; PC-2: Y axis), obtained using the multivariate assignment method on microsatellite data. Notice that the ellipse centres show a trend of separation according to the membership of the populations to the genetic clusters recovered in this work: those that belong to West-nu are farther left on the Y axis (in orange), and those that belong to East-nu are further right (in yellow).

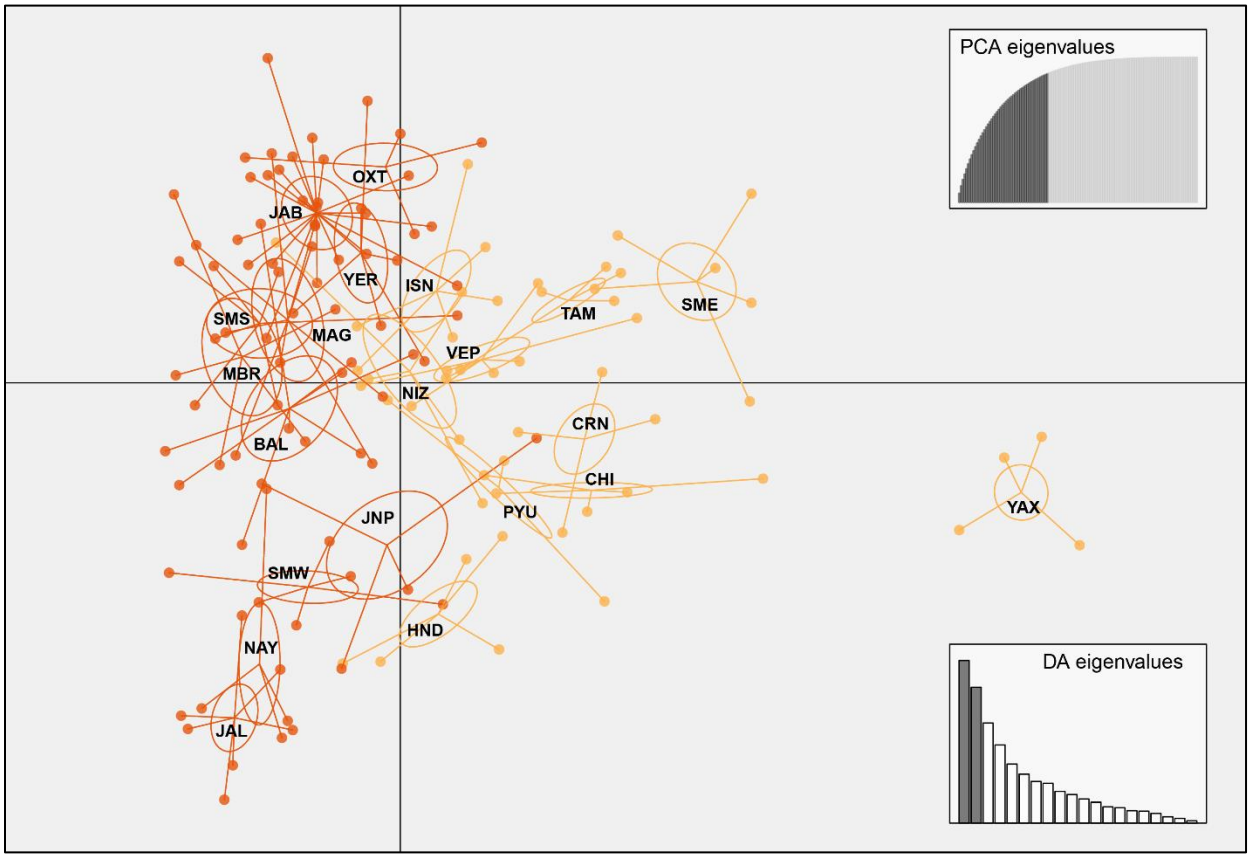

Supplementary Figure S6. F_{ST} significance of microsatellite loci for 21 populations in the geographic distribution of *Sturnira parvidens*. The dark orange squares correspond to F_{ST} *p*-values that are significant at the 0.05 level. The populations are ordered from top to bottom and from left to right according to their geographic location from east to west.

CRN: Nicaragua and Costa Rica lowlands; HND: Honduras; PYU: Yucatan Peninsula; YAX: Yaxchilán, Chiapas; CHI: Chiapas; ISN: North of the Tehuantepec Isthmus; NIZ: Nizanda, Oaxaca; VEP: Puebla-Veracruz; SME: Sierra Madre Oriental; TAM: Tamaulipas; SMS: Sierra Madre del Sur; OXT: Tehuacán-Cuicatlán and Oaxaca Valleys; BAL: Balsas River Basin; MBR: Michoacán lowlands of the Balsas River; MAG: Arteaga, Michoacán; YER: La Yerbabuena, Colima; JAB: El Jabalí, Colima; JAL: Los Naranjitos, Jalisco; JNP: Pacific coasts of Nayarit and Jalisco; NAY: Nayarit; SMW: Sierra Madre Occidental.

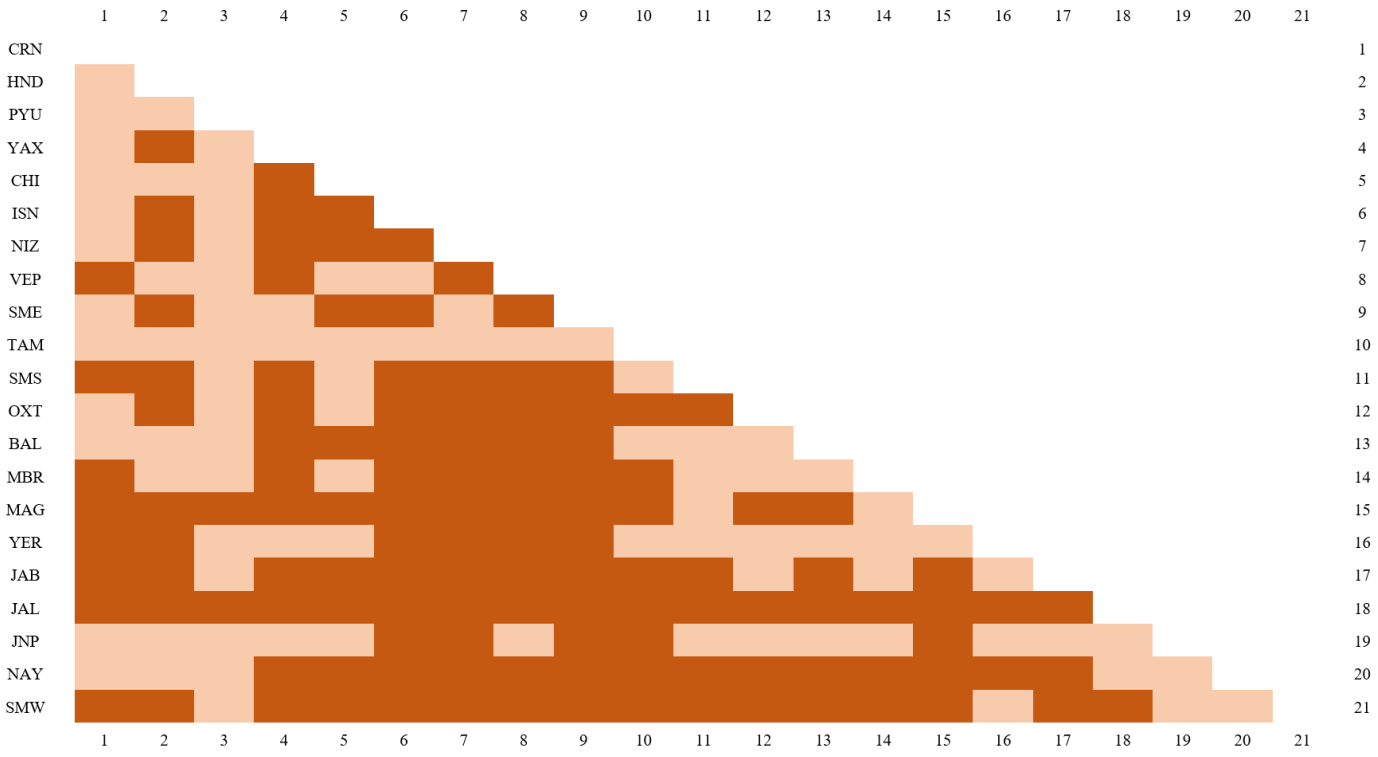

Supplementary Figure S7. Mantel test results for mitochondrial and nuclear genetic markers in *Sturnira parvidens*. $F_{ST} / (1-F_{ST})$ was used as the measure of population distance.

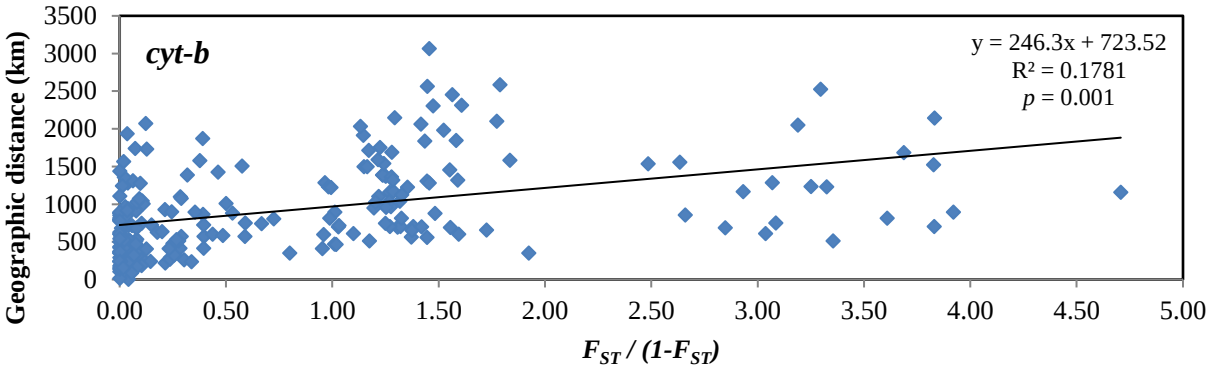

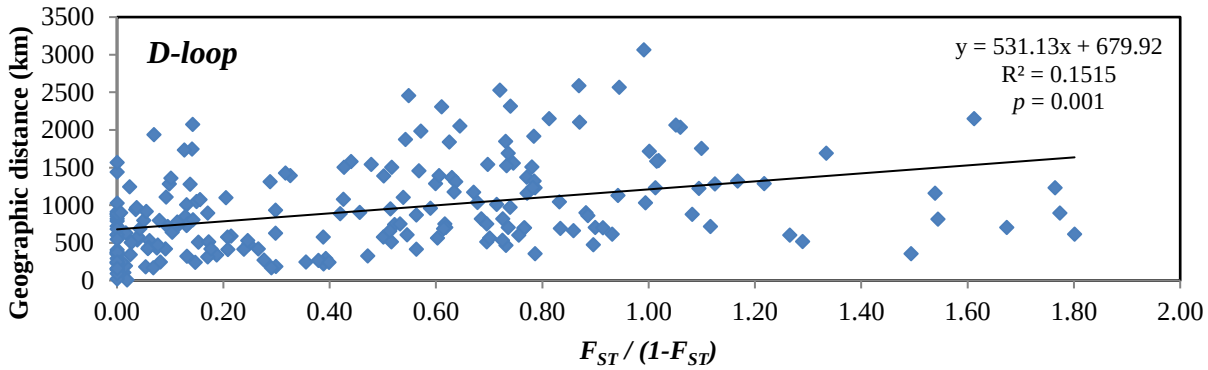

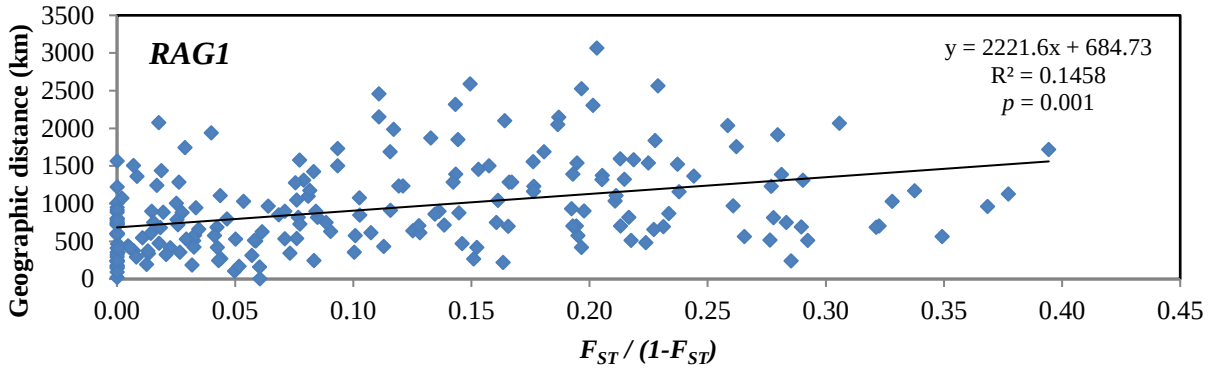

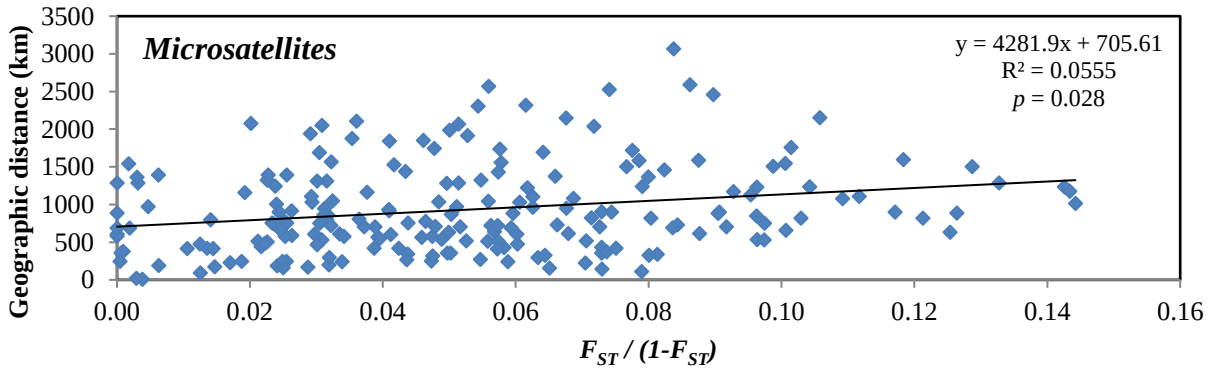

Supplementary Table S1. Genetic diversity obtained from 7 nuclear microsatellite loci and mtDNA and nuDNA sequences for 21 populations of *S. parvidens*. Population, number of individuals genotyped (*n*), number of alleles (N_a), effective number of alleles (N_e), Shannon's information index (*I*), allelic richness (*n* = 6; *R*), private allelic richness (*n* = 6; R_P), observed heterozygosity (H_o), expected heterozygosity (H_e), and heterozygote deficit or excess (fixation index, *F*; Weir & Cockerham 1984) for microsatellite data. Bold numbers indicate the highest *F* values. Number of sequences per population (*n*), number of segregating sites (*S*), number of haplotypes (*h*), haplotype diversity (*Hd*) and their standard deviation [*Hd* (sd)], and nucleotide diversity (π) and their standard deviation [π (sd)] for mtDNA and nuDNA sequences.

		Nuclear Microsatellites									mtDNA and nuDNA sequences		
Population		**Spar01**	**Spar02**	**Spar08**	**Spar09**	**Spar010**	**Spar012**	**Spar030**	**Average**		***cyt-b*** (1140 bp)	***D-loop*** (388 bp)	***RAG1*** (1072 bp)
	N_a	9	4	3	8	7	6	6	6.143	*n*	10	10	18
	N_e	7.200	2.667	2.323	6.545	4.800	4.000	5.143	4.668	S	24	25	12
	I	2.095	1.127	0.960	1.979	1.748	1.583	1.705	1.599	h	9	9	13
SMW	*R*	5.182	2.969	2.682	4.955	4.379	4.038	4.364	4.081	Hd	0.978	0.978	0.961
n = 6	R_P	0.004	0.003	0.000	0.082	0.159	0.000	0.000	0.035	Hd (sd)	0.054	0.054	0.030
	H_o	1.000	0.833	0.333	1.000	1.000	0.833	0.667	0.810	π	0.00750	0.02245	0.00289
	H_e	0.861	0.625	0.569	0.847	0.792	0.750	0.806	0.750	π (sd)	0.00101	0.00224	0.00044
	F	-0.161	-0.333	**0.415**	-0.180	-0.263	-0.111	0.172	-0.066				
	N_a	4	3	5	6	4	4	5	4.429	*n*	4	4	8
	N_e	2.909	1.684	3.200	5.333	3.556	2.909	4.000	3.370	S	19	16	10
	I	1.213	0.736	1.386	1.733	1.321	1.213	1.494	1.299	h	4	4	5
NAY	*R*	3.464	2.500	4.000	4.929	3.679	3.464	4.214	3.750	Hd	1.000	1.000	0.893
n = 4	R_P	0.137	0.008	0.000	0.001	0.000	0.000	0.000	0.021	Hd (sd)	0.177	0.177	0.086
	H_o	0.750	0.500	0.750	1.000	1.000	0.250	1.000	0.750	π	0.00877	0.02234	0.00410
	H_e	0.656	0.406	0.688	0.813	0.719	0.656	0.750	0.670	π (sd)	0.00233	0.00658	0.00096
	F	-0.143	-0.231	-0.091	-0.231	-0.391	**0.619**	-0.333	-0.114				
	N_a	8	4	4	5	4	6	5	5.143	*n*	4	4	8
	N_e	8.000	2.286	2.909	4.000	3.556	5.333	4.571	4.379	S	9	19	9
	I	2.079	1.074	1.213	1.494	1.321	1.733	1.560	1.496	h	4	4	6
JNP	*R*	6.000	3.250	3.464	4.214	3.679	4.929	4.393	4.276	Hd	1.000	1.000	0.929
n = 4	R_P	0.908	0.004	0.000	0.001	0.000	0.000	0.002	0.130	Hd (sd)	0.177	0.177	0.084
	H_o	1.000	0.500	0.750	0.750	1.000	0.750	1.000	0.821	π	0.00395	0.02792	0.00267
	H_e	0.875	0.563	0.656	0.750	0.719	0.813	0.781	0.737	π (sd)	0.00120	0.00759	0.00067
	F	-0.143	0.111	-0.143	0.000	-0.391	0.077	-0.280	-0.110				
	N_a	13	4	5	10	6	6	7	7.286	*n*	7	7	10
	N_e	12.250	1.581	2.579	8.167	4.455	4.455	5.444	5.561	S	23	27	16
	I	2.540	0.755	1.215	2.206	1.631	1.631	1.810	1.684	h	7	7	10
JAL	*R*	5.835	2.286	3.132	5.231	4.060	4.060	4.447	4.150	Hd	1.000	1.000	1.000
n = 7	R_P	0.428	0.005	0.000	0.022	0.000	0.000	0.000	0.065	Hd (sd)	0.076	0.076	0.045
	H_o	1.000	0.429	0.571	1.000	0.714	0.571	0.857	0.735	π	0.00710	0.02823	0.00448
	H_e	0.918	0.367	0.612	0.878	0.776	0.776	0.816	0.735	π (sd)	0.00146	0.00313	0.00077
	F	-0.089	-0.167	0.067	-0.140	0.079	**0.263**	-0.050	-0.005				

Supplementary Table S1. *Continued*.

Population		Nuclear Microsatellites									mtDNA and nuDNA sequences		
		Spar01	**Spar02**	**Spar08**	**Spar09**	**Spar010**	**Spar012**	**Spar030**	**Average**		***cyt-b*** (1140 bp)	***D-loop*** (388 bp)	***RAG1*** (1072 bp)
	N_a	21	12	6	11	10	8	10	11.143	*n*	21	21	40
	N_e	14.226	8.733	4.240	8.400	5.919	6.211	6.000	7.676	S	31	37	18
	I	2.844	2.304	1.582	2.240	1.996	1.921	2.006	2.127	h	16	19	18
JAB	*R*	5.342	4.783	3.630	4.722	4.258	4.260	4.278	4.467	Hd	0.967	0.990	0.927
n = 21	R_P	0.784	0.819	0.000	0.004	0.109	0.190	0.003	0.273	Hd (sd)	0.026	0.018	0.021
	H_o	0.810	0.667	0.667	0.905	0.810	0.810	0.762	0.776	π	0.00628	0.02608	0.00314
	H_e	0.930	0.885	0.764	0.881	0.831	0.839	0.833	0.852	π (sd)	0.00063	0.00197	0.00035
	F	0.129	0.247	0.128	-0.027	0.026	0.035	0.086	0.089				
	N_a	12	7	7	7	7	6	5	7.286	*n*	9	9	14
	N_e	10.889	4.900	5.158	5.765	5.444	4.083	4.455	5.813	*S*	21	27	11
	I	2.441	1.767	1.772	1.847	1.810	1.569	1.537	1.820	*h*	8	9	9
YER	*R*	5.670	4.335	4.337	4.556	4.447	3.880	3.897	4.446	*Hd*	0.972	1.000	0.901
n = 7	R_P	0.699	0.506	0.429	0.009	0.006	0.000	0.043	0.241	*Hd* (sd)	0.064	0.052	0.062
	H_o	0.857	0.714	0.857	0.857	0.857	0.714	0.571	0.776	π	0.00687	0.02491	0.00283
	H_e	0.908	0.796	0.806	0.827	0.816	0.755	0.776	0.812	π (sd)	0.00087	0.00337	0.00059
	F	0.056	0.103	-0.063	-0.037	-0.050	0.054	**0.263**	0.047				
	N_a	12	10	5	10	7	6	5	7.857	*n*	9	9	18
	N_e	9.529	6.000	2.700	8.100	4.500	4.263	2.104	5.314	*S*	27	25	11
	I	2.370	2.062	1.195	2.187	1.692	1.613	1.080	1.743	*h*	7	9	11
MAG	*R*	5.265	4.656	2.946	4.995	3.995	3.907	2.804	4.081	*Hd*	0.917	1.000	0.928
n = 9	R_P	0.066	0.480	0.000	0.002	0.001	0.000	0.010	0.080	*Hd* (sd)	0.092	0.052	0.040
	H_o	1.000	1.000	0.778	0.889	1.000	0.556	0.556	0.825	π	0.00755	0.02370	0.00320
	H_e	0.895	0.833	0.630	0.877	0.778	0.765	0.525	0.757	π (sd)	0.00160	0.00305	0.00043
	F	-0.117	-0.200	-0.235	-0.014	-0.286	**0.274**	-0.059	-0.091				
	N_a	9	5	4	5	6	5	7	5.857	*n*	5	5	10
	N_e	8.333	3.846	2.941	3.846	5.000	3.125	5.556	4.664	*S*	7	15	12
	I	2.164	1.471	1.221	1.471	1.696	1.359	1.834	1.602	*h*	3	4	8
MBR	*R*	5.667	3.929	3.333	3.929	4.500	3.667	4.833	4.265	*Hd*	0.800	0.900	0.956
n = 5	R_P	0.349	0.004	0.000	0.022	0.000	0.000	0.012	0.055	*Hd* (sd)	0.164	0.161	0.059
	H_o	1.000	0.800	0.600	0.800	1.000	0.800	1.000	0.857	π	0.00263	0.01701	0.00371
	H_e	0.880	0.740	0.660	0.740	0.800	0.680	0.820	0.760	π (sd)	0.00124	0.00616	0.00057
	F	-0.136	-0.081	0.091	-0.081	-0.250	-0.176	-0.220	-0.122				
	N_a	14	6	7	10	10	7	6	8.571	*n*	11	11	18
	N_e	11.571	3.375	4.263	7.364	7.714	4.050	4.909	6.178	*S*	19	20	14
	I	2.553	1.442	1.672	2.139	2.168	1.619	1.696	1.898	*h*	6	5	11
BAL	*R*	5.534	3.465	3.951	4.868	4.941	3.802	4.117	4.383	*Hd*	0.727	0.618	0.915
n = 9	R_P	0.886	0.119	0.000	0.002	0.033	0.000	0.000	0.149	*Hd* (sd)	0.144	0.164	0.050
	H_o	1.000	1.000	0.778	1.000	0.889	0.556	0.556	0.825	π	0.00482	0.01378	0.00320
	H_e	0.914	0.704	0.765	0.864	0.870	0.753	0.796	0.810	π (sd)	0.00204	0.00615	0.00053
	F	-0.095	-0.421	-0.016	-0.157	-0.021	**0.262**	**0.302**	-0.021				

Supplementary Table S1. *Continued*.

		Nuclear Microsatellites									mtDNA and nuDNA sequences		
Population		**Spar01**	**Spar02**	**Spar08**	**Spar09**	**Spar010**	**Spar012**	**Spar030**	**Average**		***cyt-b*** (1140 bp)	***D-loop*** (388 bp)	***RAG1*** (1072 bp)
	N_a	7	3	5	5	6	3	6	5.000	*n*	4	4	8
	N_e	6.400	2.909	4.571	4.000	5.333	1.684	5.333	4.319	*S*	14	13	14
	I	1.906	1.082	1.560	1.494	1.733	0.736	1.733	1.463	*h*	2	2	7
OXT	*R*	5.464	2.964	4.393	4.214	4.929	2.500	4.929	4.199	*Hd*	0.500	0.500	0.964
n = 4	R_P	0.860	0.067	0.000	0.010	0.950	0.000	0.000	0.270	*Hd* (sd)	0.265	0.265	0.077
	H_o	1.000	0.750	1.000	0.500	1.000	0.500	0.750	0.786	π	0.00614	0.01675	0.00460
	H_e	0.844	0.656	0.781	0.750	0.813	0.406	0.813	0.723	π (sd)	0.00326	0.00888	0.00106
	F	-0.185	-0.143	-0.280	**0.333**	-0.231	-0.231	0.077	-0.094				
	N_a	9	9	5	5	8	4	6	6.571	*n*	7	7	14
	N_e	7.000	6.533	4.261	3.920	7.000	3.920	3.920	5.222	*S*	30	31	18
	I	2.069	2.045	1.532	1.470	2.008	1.376	1.574	1.725	*h*	6	7	11
SMS	*R*	4.956	4.886	3.895	3.715	4.901	3.552	3.925	4.262	*Hd*	0.952	1.000	0.956
n = 7	R_P	0.745	0.592	0.000	0.000	0.000	0.000	0.000	0.191	*Hd* (sd)	0.096	0.076	0.045
	H_o	1.000	1.000	0.714	0.429	1.000	0.857	0.714	0.816	π	0.00936	0.03191	0.00445
	H_e	0.857	0.847	0.765	0.745	0.857	0.745	0.745	0.794	π (sd)	0.00210	0.00535	0.00079
	F	-0.167	-0.181	0.067	**0.425**	-0.167	-0.151	0.041	-0.019				
	N_a	10	7	8	7	6	5	6	7.000	*n*	6	6	10
	N_e	10.000	4.545	7.143	4.545	5.000	4.545	5.556	5.905	*S*	8	14	17
	I	2.303	1.748	2.025	1.748	1.696	1.557	1.748	1.832	*h*	6	6	8
TAM	*R*	6.000	4.595	5.333	4.595	4.500	4.167	4.667	4.837	*Hd*	1.000	1.000	0.956
n = 5	R_P	1.218	1.067	0.060	0.156	0.425	0.000	0.000	0.418	*Hd* (sd)	0.096	0.096	0.059
	H_o	1.000	1.000	1.000	0.800	0.800	0.600	0.400	0.800	π	0.00269	0.01426	0.00576
	H_e	0.900	0.780	0.860	0.780	0.800	0.780	0.820	0.817	π (sd)	0.00031	0.00169	0.00051
	F	-0.111	-0.282	-0.163	-0.026	0.000	0.231	**0.512**	0.023				
	N_a	10	6	7	8	7	6	5	7.000	*n*	10	10	20
	N_e	9.000	5.538	5.538	5.538	5.538	4.800	4.235	5.741	*S*	16	25	15
	I	2.254	1.748	1.820	1.907	1.820	1.676	1.517	1.820	*h*	10	9	9
SME	*R*	5.546	4.500	4.591	4.742	4.591	4.288	3.924	4.597	*Hd*	1.000	0.978	0.916
n = 6	R_P	1.114	0.183	0.000	0.250	0.003	0.622	0.000	0.310	*Hd* (sd)	0.045	0.054	0.032
	H_o	0.833	0.833	1.000	0.833	1.000	0.500	1.000	0.857	π	0.00331	0.01856	0.00467
	H_e	0.889	0.819	0.819	0.819	0.819	0.792	0.764	0.817	π (sd)	0.00053	0.00263	0.00028
	F	0.062	-0.017	-0.220	-0.017	-0.220	**0.368**	-0.309	-0.050				
	N_a	12	11	6	8	10	10	8	9.286	*n*	11	11	22
	N_e	10.667	7.529	4.571	5.120	8.533	7.529	5.818	7.110	*S*	20	19	24
	I	2.426	2.220	1.630	1.836	2.220	2.166	1.906	2.058	*h*	11	11	15
VEP	*R*	5.500	5.045	3.988	4.327	5.161	5.010	4.519	4.793	*Hd*	1.000	1.000	0.931
n = 8	R_P	0.363	0.296	0.000	0.076	0.179	0.538	0.000	0.207	*Hd* (sd)	0.039	0.039	0.039
	H_o	1.000	0.750	0.750	0.750	0.875	0.625	1.000	0.821	π	0.00357	0.01425	0.00623
	H_e	0.906	0.867	0.781	0.805	0.883	0.867	0.828	0.848	π (sd)	0.00087	0.00201	0.00037
	F	-0.103	0.135	0.040	0.068	0.009	0.279	-0.208	0.031				

Supplementary Table S1. *Continued*.

		Nuclear Microsatellites									mtDNA and nuDNA sequences		
Population		**Spar01**	**Spar02**	**Spar08**	**Spar09**	**Spar010**	**Spar012**	**Spar030**	**Average**		***cyt-b*** (1140 bp)	***D-loop*** (388 bp)	***RAG1*** (1072 bp)
	N_a	9	5	5	6	6	3	6	5.714	*n*	6	6	12
	N_e	8.333	3.125	4.545	5.000	5.000	2.778	4.545	4.761	*S*	10	14	17
	I	2.164	1.359	1.557	1.696	1.696	1.055	1.643	1.596	*h*	5	6	10
NIZ	*R*	5.667	3.667	4.167	4.500	4.500	2.857	4.333	4.242	*Hd*	0.933	1.000	0.970
n = 5	R_P	1.231	1.000	0.000	0.272	0.000	0.000	0.000	0.358	*Hd* (sd)	0.122	0.096	0.044
	H_o	1.000	1.000	1.000	0.600	1.000	0.600	0.600	0.829	π	0.00292	0.01409	0.00522
	H_e	0.880	0.680	0.780	0.800	0.800	0.640	0.780	0.766	π (sd)	0.00080	0.00244	0.00056
	F	-0.136	-0.471	-0.282	0.250	-0.250	0.062	0.231	-0.085				
	N_a	10	6	6	10	7	3	6	6.857	*n*	6	6	12
	N_e	8.000	3.273	4.500	9.000	5.143	2.182	4.500	5.228	*S*	8	12	20
	I	2.210	1.474	1.633	2.254	1.792	0.888	1.633	1.697	*h*	5	5	11
ISN	*R*	5.409	3.772	4.152	5.546	4.515	2.470	4.152	4.288	*Hd*	0.933	0.933	0.985
n = 6	R_P	2.527	0.789	0.000	0.296	0.356	0.000	0.000	0.567	*Hd* (sd)	0.122	0.122	0.040
	H_o	1.000	0.667	0.833	1.000	1.000	0.500	1.000	0.857	π	0.00251	0.01306	0.00628
	H_e	0.875	0.694	0.778	0.889	0.806	0.542	0.778	0.766	π (sd)	0.00072	0.00364	0.00040
	F	-0.143	0.040	-0.071	-0.125	-0.241	0.077	-0.286	-0.107				
	N_a	10	8	5	5	7	8	5	6.857	*n*	8	8	14
	N_e	10.000	7.143	3.846	4.167	5.556	7.143	4.167	6.003	*S*	7	15	21
	I	2.303	2.025	1.471	1.505	1.834	2.025	1.505	1.810	*h*	6	7	12
CHI	*R*	6.000	5.333	3.929	4.000	4.833	5.333	4.000	4.776	*Hd*	0.893	0.964	0.967
n = 5	R_P	2.018	0.208	0.000	0.000	0.017	0.924	0.012	0.454	*Hd* (sd)	0.111	0.077	0.044
	H_o	1.000	0.800	1.000	1.000	1.000	0.800	0.800	0.914	π	0.00210	0.01495	0.00567
	H_e	0.900	0.860	0.740	0.760	0.820	0.860	0.760	0.814	π (sd)	0.00033	0.00246	0.00059
	F	-0.111	0.070	-0.351	-0.316	-0.220	0.070	-0.053	-0.130				
	N_a	5	4	5	6	4	4	7	5.000	*n*	5	5	8
	N_e	4.571	4.000	4.000	5.333	3.556	2.909	6.400	4.396	*S*	10	10	16
	I	1.560	1.386	1.494	1.733	1.321	1.213	1.906	1.516	*h*	5	5	6
YAX	*R*	4.393	3.857	4.214	4.929	3.679	3.464	5.464	4.286	*Hd*	1.000	1.000	0.893
n = 4	R_P	0.859	0.731	0.120	0.534	0.000	0.000	0.000	0.321	*Hd* (sd)	0.126	0.126	0.111
	H_o	0.750	0.000	0.750	1.000	0.750	1.000	0.750	0.714	π	0.00386	0.01237	0.00556
	H_e	0.781	0.750	0.750	0.813	0.719	0.656	0.844	0.759	π (sd)	0.00066	0.00214	0.00081
	F	0.040	**1.000**	0.000	-0.231	-0.043	-0.524	**0.111**	0.050				
	N_a	5	5	5	4	4	4	6	4.714	*n*	6	6	12
	N_e	4.500	4.500	4.500	3.600	3.600	3.600	6.000	4.329	*S*	13	18	21
	I	1.561	1.561	1.561	1.330	1.330	1.330	1.792	1.495	*h*	6	6	8
PYU	*R*	5.000	5.000	5.000	4.000	4.000	4.000	6.000	4.714	*Hd*	1.000	1.000	0.939
n = 3	R_P	0.110	0.066	0.000	0.006	0.000	0.008	0.028	0.031	*Hd* (sd)	0.096	0.096	0.048
	H_o	1.000	1.000	0.667	1.000	0.667	0.333	1.000	0.810	π	0.00380	0.01873	0.00604
	H_e	0.778	0.778	0.778	0.722	0.722	0.722	0.833	0.762	π (sd)	0.00077	0.00281	0.00050
	F	-0.286	-0.286	0.143	-0.385	0.077	**0.538**	-0.200	-0.057				

Supplementary Table S1. *Continued*.

Population		Nuclear Microsatellites									mtDNA and nuDNA sequences		
		Spar01	**Spar02**	**Spar08**	**Spar09**	**Spar010**	**Spar012**	**Spar030**	**Average**		***cyt-b*** (1140 bp)	***D-loop*** (388 bp)	***RAG1*** (1072 bp)
HND *n* = 5	N_a	10	5	6	6	8	7	4	6.571	*n*	12	12	22
	N_e	10.000	3.846	4.167	5.000	7.143	5.556	3.333	5.578	*S*	17	25	26
	I	2.303	1.471	1.609	1.696	2.025	1.834	1.280	1.745	*h*	11	12	17
	R	6.000	3.929	4.262	4.500	5.333	4.833	3.429	4.612	*Hd*	0.985	1.000	0.978
	R_P	2.214	0.660	0.060	0.600	0.739	0.691	0.000	0.709	*Hd* (sd)	0.040	0.034	0.019
	H_o	1.000	1.000	0.800	0.800	1.000	0.800	0.800	0.886	π	0.00284	0.01761	0.00571
	H_e	0.900	0.740	0.760	0.800	0.860	0.820	0.700	0.797	π (sd)	0.00046	0.00173	0.00043
	F	-0.111	-0.351	-0.053	0.000	-0.163	0.024	-0.143	-0.114				
CRN *n* = 4	N_a	5	6	5	4	5	4	5	4.857	*n*	11	12	24
	N_e	4.000	4.571	4.000	3.200	4.571	4.000	4.571	4.131	*S*	10	17	23
	I	1.494	1.667	1.494	1.255	1.560	1.386	1.560	1.488	*h*	7	8	18
	R	4.214	4.750	4.214	3.500	4.393	3.857	4.393	4.189	*Hd*	0.909	0.924	0.978
	R_P	0.711	0.760	0.000	0.000	0.000	0.000	0.000	0.210	*Hd* (sd)	0.066	0.057	0.017
	H_o	0.500	1.000	1.000	0.750	0.500	0.500	1.000	0.750	π	0.00284	0.01582	0.00551
	H_e	0.750	0.781	0.750	0.688	0.781	0.750	0.781	0.754	π (sd)	0.00039	0.00147	0.00048
	F	**0.333**	-0.280	-0.333	-0.091	**0.360**	**0.333**	-0.280	0.006				
Total *n* = 134	N_a	54	31	10	17	17	14	12	22.143	*n*	172	173	322
	N_e	27.991	8.763	6.429	11.339	10.028	7.243	8.313	11.444	*S*	118	72	56
	I	3.580	2.727	2.010	2.545	2.486	2.162	2.268	2.540	*h*	115	135	111
	R	5.544	4.707	4.202	4.876	4.765	4.354	4.541	4.710	*Hd*	0.989	0.995	0.976
	H_o	0.925	0.776	0.769	0.851	0.896	0.664	0.776	0.808	*Hd* (sd)	0.003	0.002	0.003
	H_e	0.964	0.886	0.844	0.912	0.900	0.862	0.880	0.893	π	0.00836	0.02811	0.00496
	F	0.040	0.124	0.090	0.067	0.005	**0.229**	0.118	0.096	π (sd)	0.00026	0.00076	0.00013

Supplementary Table S2. Pairwise F_{ST} values for 21 populations in the geographic distribution of *Sturnira parvidens*. The populations are ordered from top to bottom and from left to right according to their geographic location from east to west.

CRN: Nicaragua and Costa Rica lowlands; HND: Honduras; PYU: Yucatan Peninsula; YAX: Yaxchilán, Chiapas; CHI: Chiapas; ISN: North of the Tehuantepec Isthmus; NIZ: Nizanda, Oaxaca; VEP: Puebla-Veracruz; SME: Sierra Madre Oriental; TAM: Tamaulipas; SMS: Sierra Madre del Sur; OXT: Tehuacán-Cuicatlán and Oaxaca Valleys; BAL: Balsas River Basin; MBR: Michoacán lowlands of the Balsas River; MAG: Arteaga, Michoacán; YER: La Yerbabuena, Colima; JAB: El Jabalí, Colima; JAL: Los Naranjitos, Jalisco; JNP: Pacific coasts of Nayarit and Jalisco; NAY: Nayarit; SMW: Sierra Madre Occidental.

	CRN	**HND**	**PYU**	**YAX**	**CHI**	**ISN**	**NIZ**	**VEP**	**SME**	**TAM**	**SMS**	**OXT**	**BAL**	**MBR**	**MAG**	**YER**	**JAB**	**JAL**	**JNP**	**NAY**	**SMW**
CRN	0																				
HND	0.021	0																			
PYU	0.003	0.024	0																		
YAX	0.031	0.047	0.042	0																	
CHI	0.023	0.030	-0.013	0.045	0																
ISN	0.031	0.067	0.022	0.075	0.045	0															
NIZ	0.003	0.056	0.032	0.068	0.047	0.073	0														
VEP	0.046	0.023	0.002	0.053	0.023	0.021	0.055	0													
SME	0.028	0.042	0.031	0.026	0.030	0.048	0.029	0.031	0												
TAM	0.020	0.031	-0.012	0.028	0.028	0.014	0.031	0.001	0.025	0											
SMS	0.054	0.047	0.005	0.088	0.030	0.053	0.070	0.037	0.057	0.031	0										
OXT	0.073	0.059	0.062	0.111	0.033	0.060	0.066	0.052	0.041	0.054	0.056	0									
BAL	0.034	0.006	0.039	0.068	0.048	0.045	0.054	0.042	0.033	0.022	0.018	0.031	0								
MBR	0.063	0.030	-0.004	0.094	0.019	0.069	0.074	0.064	0.050	0.049	0.010	-0.024	0.001	0							
MAG	0.096	0.060	0.049	0.125	0.036	0.083	0.108	0.081	0.066	0.068	0.013	0.057	0.048	0.004	0						
YER	0.058	0.044	0.025	0.062	0.022	0.053	0.049	0.046	0.044	0.024	0.026	0.025	0.012	0.006	0.024	0					
JAB	0.052	0.039	0.022	0.074	0.029	0.046	0.059	0.036	0.038	0.037	0.025	0.023	0.029	0.014	0.028	0.003	0				
JAL	0.082	0.048	0.071	0.114	0.076	0.125	0.100	0.093	0.091	0.089	0.078	0.112	0.040	0.061	0.074	0.068	0.061	0			
JNP	0.069	0.030	0.002	0.055	0.040	0.073	0.085	0.030	0.056	0.042	0.035	0.063	0.024	0.014	0.054	0.017	0.024	0.012	0		
NAY	0.079	0.035	0.091	0.106	0.080	0.117	0.088	0.083	0.077	0.084	0.105	0.126	0.054	0.088	0.089	0.068	0.069	0.000	0.024	0	
SMW	0.077	0.053	0.050	0.067	0.049	0.092	0.072	0.052	0.087	0.057	0.054	0.090	0.058	0.064	0.098	0.024	0.039	0.044	-0.003	0.038	0

Supplementary Table S3. F_{ST} significance of microsatellite loci for the 21 populations in the geographic distribution of *Sturnira parvidens*. The yellow squares correspond to low F_{ST} values (0.05-0.15). The symbol "+" indicates F_{ST} *p*-values that are significant at the 0.05 level. The populations are ordered from top to bottom and from left to right according to their geographic location from east to west.

CRN: Nicaragua and Costa Rica lowlands; HND: Honduras; PYU: Yucatan Peninsula; YAX: Yaxchilán, Chiapas; CHI: Chiapas; ISN: North of the Tehuantepec Isthmus; NIZ: Nizanda, Oaxaca; VEP: Puebla-Veracruz; SME: Sierra Madre Oriental; TAM: Tamaulipas; SMS: Sierra Madre del Sur; OXT: Tehuacán-Cuicatlán and Oaxaca Valleys; BAL: Balsas River Basin; MBR: Michoacán lowlands of the Balsas River; MAG: Arteaga, Michoacán; YER: La Yerbabuena, Colima; JAB: El Jabalí, Colima; JAL: Los Naranjitos, Jalisco; JNP: Pacific coasts of Nayarit and Jalisco; NAY: Nayarit; SMW: Sierra Madre Occidental.

	CRN	HND	PYU	YAX	CHI	ISN	NIZ	VEP	SME	TAM	SMS	OXT	BAL	MBR	MAG	YER	JAB	JAL	JNP	NAY	SMW
CRN																					
HND																					
PYU																					
YAX		+																			
CHI				+																	
ISN		+		+	+																
NIZ		+		+	+	+															
VEP	+			+			+														
SME		+			+	+		+													
TAM																					
SMS	+	+		+		+	+	+	+												
OXT		+		+		+	+	+	+	+	+										
BAL				+	+	+	+	+	+												
MBR	+			+		+	+	+	+	+											
MAG	+	+	+	+	+	+	+	+	+	+		+	+								
YER	+	+				+	+	+	+												
JAB	+	+		+	+	+	+	+	+	+	+		+		+						
JAL	+	+	+	+	+	+	+	+	+	+	+	+	+	+	+	+	+				
JNP						+	+		+	+					+						
NAY				+	+	+	+	+	+	+	+	+	+	+	+	+	+				
SMW	+	+		+	+	+	+	+	+	+	+	+	+	+	+		+	+			

Supplementary Table S4. Slatkin's distances (F_{ST} / [1-F_{ST}]) for microsatellite loci used as the measure of population distance for the Mantel test for the 21 populations in the geographic distribution of *Sturnira parvidens*. The populations are ordered from top to bottom and from left to right according to their geographic location from east to west.

CRN: Nicaragua and Costa Rica lowlands; HND: Honduras; PYU: Yucatan Peninsula; YAX: Yaxchilán, Chiapas; CHI: Chiapas; ISN: North of the Tehuantepec Isthmus; NIZ: Nizanda, Oaxaca; VEP: Puebla-Veracruz; SME: Sierra Madre Oriental; TAM: Tamaulipas; SMS: Sierra Madre del Sur; OXT: Tehuacán-Cuicatlán and Oaxaca Valleys; BAL: Balsas River Basin; MBR: Michoacán lowlands of the Balsas River; MAG: Arteaga, Michoacán; YER: La Yerbabuena, Colima; JAB: El Jabalí, Colima; JAL: Los Naranjitos, Jalisco; JNP: Pacific coasts of Nayarit and Jalisco; NAY: Nayarit; SMW: Sierra Madre Occidental.

	CRN	HND	PYU	YAX	CHI	ISN	NIZ	VEP	SME	TAM	SMS	OXT	BAL	MBR	MAG	YER	JAB	JAL	JNP	NAY	SMW
CRN	0																				
HND	0.021	0																			
PYU	0.003	0.025	0																		
YAX	0.032	0.049	0.044	0																	
CHI	0.024	0.031	0.000	0.047	0																
ISN	0.032	0.071	0.023	0.081	0.048	0															
NIZ	0.003	0.060	0.033	0.073	0.050	0.079	0														
VEP	0.048	0.024	0.002	0.056	0.023	0.022	0.058	0													
SME	0.029	0.043	0.032	0.026	0.031	0.050	0.030	0.032	0												
TAM	0.020	0.032	0.000	0.029	0.029	0.014	0.032	0.001	0.025	0											
SMS	0.058	0.050	0.005	0.096	0.030	0.056	0.075	0.039	0.060	0.032	0										
OXT	0.079	0.063	0.066	0.125	0.034	0.063	0.070	0.055	0.042	0.057	0.059	0									
BAL	0.035	0.006	0.041	0.073	0.050	0.047	0.057	0.044	0.034	0.022	0.019	0.032	0								
MBR	0.068	0.030	0.000	0.104	0.019	0.074	0.080	0.068	0.053	0.052	0.011	0.000	0.001	0							
MAG	0.106	0.064	0.051	0.143	0.038	0.091	0.121	0.088	0.071	0.073	0.014	0.060	0.050	0.004	0						
YER	0.062	0.046	0.026	0.066	0.023	0.056	0.051	0.048	0.046	0.024	0.026	0.026	0.012	0.006	0.024	0					
JAB	0.054	0.041	0.023	0.080	0.030	0.048	0.063	0.037	0.039	0.039	0.025	0.024	0.030	0.015	0.029	0.003	0				
JAL	0.090	0.050	0.077	0.129	0.082	0.143	0.112	0.103	0.101	0.097	0.084	0.126	0.041	0.064	0.080	0.073	0.065	0			
JNP	0.074	0.031	0.002	0.058	0.042	0.079	0.093	0.031	0.059	0.044	0.036	0.068	0.025	0.014	0.057	0.017	0.025	0.013	0		
NAY	0.086	0.036	0.101	0.118	0.088	0.133	0.096	0.090	0.084	0.092	0.117	0.144	0.057	0.096	0.097	0.073	0.074	0.000	0.025	0	
SMW	0.084	0.056	0.053	0.072	0.051	0.101	0.078	0.055	0.095	0.061	0.057	0.099	0.062	0.069	0.109	0.024	0.041	0.046	0.000	0.039	0